UNIVERSIDADE FEDERAL DE SANTA MARIA
CENTRO DE CIÊNCIAS RURAIS
PROGRAMA DE PÓS-GRADUAÇÃO EM CIÊNCIA DO SOLO

Bruno Chaves

MODELAGEM DA DECOMPOSIÇÃO E EMISSÃO DE N$_2$O DE RESÍDUOS CULTURAIS COM DISTINTA COMPOSIÇÃO QUÍMICA E QUANTIDADE

Santa Maria, RS
2021

Bruno Chaves

MODELAGEM DA DECOMPOSIÇÃO E EMISSÃO DE N$_2$O DE RESÍDUOS CULTURAIS COM DISTINTA COMPOSIÇÃO QUÍMICA E QUANTIDADE

Tese apresentada ao curso de Doutorado do Programa de Pós-Graduação em Ciência do Solo, da Universidade Federal de Santa Maria (UFSM, RS), como requisito parcial para obtenção do título de **Doutor em Ciência do Solo**

Orientador: Dr. Sandro José Giacomini

Santa Maria, RS
2021

Bruno Chaves

MODELAGEM DA DECOMPOSIÇÃO E EMISSÃO DE N$_2$O DE RESÍDUOS CULTURAIS COM DISTINTA COMPOSIÇÃO QUÍMICA E QUANTIDADE

Tese apresentada ao curso de Doutorado do Programa de Pós-Graduação em Ciência do Solo, da Universidade Federal de Santa Maria (UFSM, RS), como requisito parcial para obtenção do título de **Doutor em Ciência do Solo**

Aprovado em 30 de julho de 2021:

Sandro José Giacomini, Dr. (UFSM)
(Presidente/Orientador)

Carlos Gustavo Tornquist, Dr. (UFRGS)

Douglas Adams Weiler, Dr. (UFSC)

Ricardo Bergamo Schenato, Dr. (UFSM)

Getúlio Elias Pilecco, Dr. (UFSM)

Santa Maria, RS
2021

Aos meus pais Dirlei e Roseli,

dedico este trabalho.

AGRADECIMENTOS

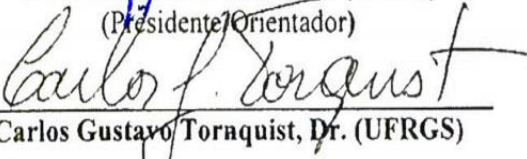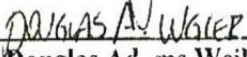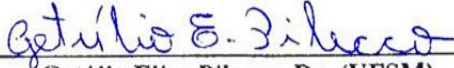# RESUMO

MODELAGEM DA DECOMPOSIÇÃO E EMISSÃO DE N$_2$O DE RESÍDUOS CULTURAIS COM DISTINTA COMPOSIÇÃO QUÍMICA E QUANTIDADE

AUTOR: Bruno Chaves
ORIENTADOR: Sandro José Giacomini

A simulação da dinâmica do carbono (C) e nitrogênio (N) e da emissão de óxido nitroso (N$_2$O) durante a decomposição de resíduos culturais com composição química distinta na superfície do solo (mulch) é essencial para estabelecer estratégias para aumentar os estoques de C no solo e reduzir a emissão de gases do efeito estufa (GEE) em sistemas de cultivo conservacionistas. O objetivo do presente estudo foi utilizar o modelo STICS para: i) interpretar a relação entre a qualidade, localização dos resíduos culturais, e o conteúdo de N no solo sobre a mineralização do C e N (Estudo 1); ii) testar e melhorar a performance do modelo na simulação da dinâmica de decomposição e emissão de N$_2$O com o uso de dois resíduos culturais com distinta composição química e quantidades adicionadas na superfície do solo em sistema plantio direto (Estudo 2). Para atingir estes objetivos, foram utilizados dois conjuntos de dados: i) obtidos em uma incubação de laboratório que avaliou a mineralização do C e do N de dez resíduos culturais (C:N de 13 a 105) mantidos na superfície e incorporados ao solo e com e sem a adição de N (9 e 77 mg N kg^{-1} solo); e ii) oriundos de um experimento de campo que avaliou a dinâmica do C e N e a emissão de N$_2$O durante a decomposição de dois resíduos culturais (ervilhaca e trigo) com distinta composição química e quantidades (3, 6 e 9 Mg MS ha^{-1}). No estudo 1, distintos parâmetros do submodelo de decomposição de STICS foram otimizados para descrever a dinâmica do C e N e compreender o efeito da disponibilidade de N nas características funcionais da biomassa microbiana do solo, permitindo estimar o conteúdo de N disponível para os microrganismos decompositores dos resíduos em superfície. Os parâmetros *CNbio* (relação C:N da biomassa microbiana)*, k* (taxa de decomposição do resíduo)*, h* (taxa de humificação da biomassa microbiana)*, λ* (taxa de decomposição da biomassa microbiana) apresentaram correlação significativa com o conteúdo total de N disponível, definido como a soma do conteúdo de N presente no resíduo (100%) e do solo que foi de 100% para resíduos incorporados e de 24% para os resíduos em superfície. O decréscimo da disponibilidade total de N levou ao aumento da *CNbio* e o decréscimo de *k*, *h* e *λ*. Esses resultados são promissores para descrever os efeitos da disponibilidade de N na mineralização do C e N de resíduos culturais. No estudo 2, os módulos de simulação da decomposição do mulch e emissão de N$_2$O de STICS foram testados e otimizados. STICS com sua parametragem padrão falhou em simular a decomposição e a emissão de N$_2$O. A simulação da decomposição do mulch foi melhorada sem o uso da função contato, estabelecendo todo o mulch decomponível independentemente da quantidade de resíduo adicionada. As emissões de N$_2$O foram otimizadas com a definição de uma nova função para determinar o potencial de desnitrificação em STICS, baseado nas emissões de CO$_2$ para estimar a disponibilidade de C para os desnitrificadores (Dp = a CO2solo + b CO2res N:Cres). As alterações realizadas no modelo STICS melhoraram a descrição da dinâmica de decomposição do mulch e a magnitude e variabilidade temporal das emissões de N$_2$O após adição de resíduos culturais com características químicas e quantidades distintas na superfície do solo.

Palavras-chave: modelo STICS, mulch, óxido nitroso, mineralização do N.

ABSTRACT

MODELING DECOMPOSITION AND N₂O EMISSION FROM CROP RESIDUES WITH DIFFERENT CHEMICAL COMPOSITION AND MASS

AUTHOR: Bruno Chaves
ADVISOR: Sandro José Giacomini

Simulating the dynamics of carbon (C) and nitrogen (N) and nitrous oxide (N_2O) emissions during decomposition of crop residues with distinct chemical composition on the soil surface (mulch) is essential to establish strategies to increase soil C stocks and reduce greenhouse gas (GHG) emissions in conservation tillage systems. The objective of the present study was to use the STICS model to: i) interpret the relationship between crop residue quality, location, and soil N content on C and N mineralization (Study 1); to test and improve the model performance in simulating the decomposition dynamics and N_2O emissions with the use of two crop residues with different chemical composition and mass added to the soil surface in no-tillage system (Study 2). To achieve these objectives, two datasets were used: i) obtained in a laboratory incubation that evaluated the C and N mineralization of ten crop residues (C:N from 13 to 105) kept on the surface and incorporated into the soil and with and without the addition of N (9 and 77 mg N kg^{-1} soil); and ii) from a field experiment that evaluated C and N dynamics and N_2O emission during decomposition of two crop residues (vetch and wheat) with different chemical composition and mass (3, 6 and 9 Mg DM ha^{-1}). In the study 1, distinct parameters of the STICS decomposition submodule were optimized to describe the dynamics of C and N and to comprehend the effect of N availability on the functional characteristics of soil microbial biomass, allowing to estimate the available N content for surface residue decomposing microorganisms. The parameters *CNbio* (C:N ratio of microbial biomass), *k* (decomposition rate of plant residue), *h* (humification rate of microbial biomass), λ (decomposition rate of microbial biomass) showed significant correlation with the total available N content, defined as the sum of the N content present in the residue (100%) and soil which was 100% for incorporated residues and 24% for surface residues. Decreasing total N availability led to increase *CNbio* and decreasing *k*, *h*, and λ. These results are promising for describing the effects of N availability on C and N mineralization of crop residues. In study 2, the simulation modules for mulch decomposition and N_2O emission of STICS were tested and optimized. STICS with its default parameterization failed to simulate decomposition and N_2O emission. The simulation of mulch decomposition was improved without the use of contact function, establishing all mulch decomposable regardless of the mass of residue added. N_2O emissions were optimized by defining a new function to determine denitrification potential in STICS, based on CO_2 emissions to estimate C availability to denitrifiers (Dp = a CO2solo + b CO2res N:Cres). The changes made allowed the STICS model to improve the description of the mulch decomposition dynamics and the magnitude and temporal variability of N_2O emissions after residue addition of crop residues with distinct chemical characteristics and mass on the soil surface.

Key words: STICS model, mulch, nitrous oxide, N mineralization.

LISTA DE FIGURAS

ARTIGO I

ARTIGO II

LISTA DE TABELAS

ARTIGO I

ARTIGO II

SUMÁRIO

1 INTRODUÇÃO GERAL

Os usos de sistemas de cultivo conservacionistas têm se consolidado como uma importante estratégia na redução da erosão, aumento dos estoques de carbono (C) e ciclagem de nutrientes no solo (GALE; CAMBARDELLA, 2000; CHELLAPPA et al., 2021). Dentre estes sistemas, o sistema plantio direto (SPD) é largamente difundido na região sul do Brasil, e caracterizado pela diversidade de espécies utilizadas em rotação e a manutenção dos resíduos em superfície (BERNOUX et al., 2009; TIECHER et al., 2017). Tais condições implicam em modificações na dinâmica de mineralização do C e do nitrogênio (N) pela população microbiana do solo, não apenas pelas características intrínsecas dos resíduos culturais (ABIVEN et al., 2005; REDIN et al., 2014), mas também por alterações indiretas (umidade e temperatura) e acessibilidade dos nutrientes pelos microrganismos do solo na presença de resíduos em superfície (mulch) (COPPENS et al., 2007; FINDELING et al., 2007; TUURE et al., 2021). Logo, a compreensão do processo microbiano de decomposição de resíduos culturais em superfície torna-se importante, pois determina os fluxos de C e N no solo e para a atmosfera, podendo resultar na emissão de gases do efeito estufa (GEE).

A composição química dos resíduos culturais, genericamente denominada "qualidade" é considerada o principal controlador do processo microbiano de decomposição (QUEMADA; CABRERA, 1995; TRINSOUTROT et al., 2000). Resíduos de alta qualidade se caracterizam por elevados teores de N e fração solúvel (baixa relação C:N), enquanto resíduos de baixa qualidade apresentam valores baixos de N e fração solúvel, caracterizando uma elevada relação C:N (JENSEN et al., 2005; REDIN et al., 2014). Estas características implicam na redução das taxas de decomposição com a redução na qualidade dos resíduos, efeito amplamente documentado (TRINSOUTROT et al., 2000; REDIN et al., 2014; STEWART et al., 2015; SCHMATZ et al, 2017). Conjuntamente a qualidade do resíduo, a sua localização exerce importante influência na dinâmica de decomposição, pois a presença do mulch resulta na diminuição do contato solo/resíduo, com menor taxa de decomposição comparada a resíduos incorporados (BREMER; VAN HOUTUM; VAN KESSEL, 1991; HENRIKSEN; BRELAND, 2002; OLIVEIRA et al., 2020). Esta redução é associada ao limitado acesso da população decompositora a nutrientes do solo, principalmente de N (NICOLARDOT et al., 2007). Além disso, para resíduos de alta qualidade o efeito da localização na taxa de decomposição parece ter menor magnitude comparado a resíduos de baixa qualidade (ABIVEN; RECOUS, 2007; CHAVES et al., 2021, no prelo). Esse comportamento sugere que a menor disponibilidade de N para a população decompositora não é limitada apenas pelo contato solo/resíduo, mas

depende também da interação com a qualidade dos resíduos. Neste sentido, as interações que ocorrem no solo em decorrência da localização e composição químico dos resíduos culturais irão afetar não apenas a dinâmica de decomposição, mas também as emissões de oxido nitroso no solo (N_2O), pois as mesmas definem a disponibilidade dos principais precursores dos processos envolvidos na emissão deste importante GEE (GOMES et al., 2009).

O N_2O é um potente GEE com elevado poder radiativo e potencial de aquecimento global, cerca de 265 vezes superior ao do CO_2 (IPCC, 2014). O N_2O resulta principalmente dos processos microbianos de nitrificação e desnitrificação (BUTTERBACH-BAHL et al., 2013; CHEN et al., 2013), dependentes de variáveis ambientais (temperatura e umidade), características do solo (matéria orgânica, amônio, nitrato, pH) e manejo (preparo do solo, fertilização, aporte e qualidade dos resíduos) (BUTTERBACH-BAHL et al., 2013; SIGNOR; CERRI, 2013; CHARLES et al., 2017). As alterações impostas pela qualidade químico e quantidades de resíduo depositadas na superfície do solo influenciam esses processos tanto diretamente, pela disponibilidade de C solúvel e N, quanto indiretamente por alterações na temperatura e umidade do solo (CHEN et al., 2013; SCHMATZ et al., 2020). Devido à grande variabilidade espacial e temporal dos fluxos de N_2O no solo e a necessidade de extensivo monitoramento, a modelagem matemática tem emergido como importante alternativa no estudo da dinâmica de emissão do N_2O no solo (HÉNAULT; GERMON, 2000; HÉNAULT et al., 2005; PLAZZA-BONILLA et al., 2017). A simulação dos fluxos de N_2O por modelos matemáticos ocorre pela representação dos dois principais processos resultantes da sua emissão no solo (nitrificação e desnitrificação). Dentre estes, a desnitrificação ocorre em ambiente anaeróbico e responde pelas maiores emissões de N_2O em sistemas agrícolas (SIGNOR; CERRI, 2013). A maioria dos modelos determinam o potencial de desnitrificação como um valor constante ou dependente da disponibilidade de C (HEINEN, 2006). Contudo, a correlação entre os fluxos de N_2O e CO_2 observada em alguns estudos sugere que as emissões de N_2O podem estar relacionadas ao aumento da atividade microbiana após a adição de resíduos no solo. Além disso, para a correta representação dos fluxos de N_2O pelos modelos empregados, se faz necessário a simulação das dinâmicas do C e N de forma correta.

A dinâmica de decomposição do mulch é simulada por vários modelos como STICS (BRISSON et al., 2003), PASTIS (FINDELING et al., 2007), APSIM (THORBURN; PROBERT; ROBERTSON, 2001), os quais apresentam um submodelo de decomposição do mulch desenvolvido com base em estudos que observaram uma diminuição na decomposição do mulch com o incremento da quantidade de resíduos na superfície do solo (STOTT et al., 1990; STEINER et al., 1999). Nesses submodelos o mulch é representado por duas camadas,

uma decomponível em contato com o solo, e uma camada não decomponível localizada acima, que abastece a primeira camada. Neste caso, o fator contato solo/resíduo é reduzido e diminui a taxa de decomposição do mulch com o aumento na quantidade depositada na superfície do solo. Contudo, estudos recentes têm relatado uma dinâmica de decomposição semelhante para distintas quantidades de resíduo adicionadas (ACOSTA et al., 2014; HALDE; ENTZ, 2016; DIETRICH et al., 2017; WILLIAMS et al., 2018). Dietrich et al. (2019) demonstraram que existe um gradiente de decomposição no interior do mulch, onde as melhores condições de umidade e temperatura na interface solo/resíduo levam a uma compensação das menores taxas de decomposição nas camadas superiores do mulch. Logo, a dinâmica de decomposição do mulch baseado nestes estudos necessita ser avaliada e integrada nos modelos de decomposição, visando a reprodução dos processos relacionados a decomposição do mulch e emissão de N_2O no solo. Dentre estes, STICS (Simulateur mulTIdisciplinaire pour les Cultures Standard) é um modelo genérico caracterizado pela sua robustez, generalidade e adaptação a uma elevada gama de culturas (BRISSON, et al., 2003). STICS foi desenvolvido em condições de clima temperado por pesquisadores do INRA a partir de 1996, o modelo simula o comportamento do sistema solo-planta-atmosfera, integra e descreve a decomposição de resíduos em superfície (NICOLARDOT; RECOUS; MARY, 2001) e os fluxos de N_2O do solo em escala diária.

Dentro deste contexto, o modelo STICS foi utilizado para a interpretação dos resultados obtidos em uma incubação que avaliou a interação da composição química e localização (superfície vs. incorporado) na decomposição de resíduos culturais e na avaliação e melhoria das simulações da decomposição e emissão de N_2O em condições de campo de dois resíduos culturais (ervilhaca e trigo) com distinta composição química e quantidades (3, 6 e 9 Mg MS ha^{-1}).

1.1 Hipóteses

1) A interação entre os conteúdos de N mineral do solo, conteúdo de N e localização do resíduo (superfície vs incorporado) determina a disponibilidade de N para a população decompositora do solo e controla as dinâmicas de mineralização do C e N dos resíduos culturais adicionados, representada pela disponibilidade total de N.

2) O modelo de decomposição de dupla camada não simula adequadamente a dinâmica de decomposição do mulch de resíduos culturais com composição química e quantidades distintas.

3) O uso dos fluxos de CO_2 como uma estimativa dos conteúdos de C lábil disponível para a desnitrificação pode melhorar as simulações do N_2O pelo modelo STICS.

1.2 Objetivo geral

Utilizar o modelo STICS para interpretar a relação entre a qualidade e localização dos resíduos culturais no solo, testar e melhorar a simulação da dinâmica de decomposição e emissão de N_2O de dois resíduos culturais com distinta composição química e quantidades adicionadas na superfície do solo.

1.3 Objetivos específicos

1) Utilizar o modelo STICS para interpretar e descrever a relação entre o conteúdo de N mineral do solo, N no resíduo e localização do resíduo (superfície vs incorporado) na dinâmica de mineralização do C e N no solo.

2) Testar o modelo STICS na simulação da decomposição de dois resíduos culturais em superfície com composição química e quantidades distintas.

3) Avaliar a performance do modelo STICS na simulação das emissões de N_2O em condições de adição de resíduos culturais com características químicas e quantidades distintas.

4) Sugerir melhorias nas sub-rotinas de simulação da decomposição do mulch e emissão de N_2O do modelo STICS.

2 ARTIGO I – THE COMBINATION OF RESIDUE QUALITY, RESIDUE PLACEMENT AND SOIL MINERAL N CONTENT DRIVES C AND N DYNAMICS BY MODIFYING N AVAILABILITY TO MICROBIAL DECOMPOSERS[1]

2.1 Abstract

Crop residues are the main source of carbon inputs to soils in cropping systems, and their subsequent decomposition is crucial for nutrient recycling. The interactive effects of residue chemical quality, residue placement and soil mineral nitrogen (N) availability on carbon (C) and N mineralization dynamics were experimentally examined and interpreted using a modelling approach with the deterministic-functional, dynamic decomposition module of the Simulateur mulTIdisciplinaire pour les Cultures Standard (STICS) model. We performed a 120-day incubation at 25°C to evaluate how the mineralization of C and N from residues would respond to residue type (residues of 10 crop species with C:N ratios varying from 13 to 105), placement (surface or incorporated) and initial soil mineral N content (9 or 77 mg N kg^{-1} dry soil). A reduced C mineralization rate was associated with N limitation, as observed for high-C:N ratio residues, and shaped by residue placement and initial soil mineral N content. This was not observed for low-C:N ratio residues. Overall, increased net N mineralization corresponded with reduced N availability. Using the optimization procedure in the STICS decomposition module to explain the C and N dynamics of surface-decomposing residues, we estimated that 24% of the total soil mineral N would be accessible to decomposers. The STICS decomposition module reproduced the C and N dynamics for each treatment well after five parameters were optimized. The optimized values of the biomass C:N (*CNbio*), residue decomposition rate (*k*), humification coefficient of microbial C (*h*), and microbial decomposition rate (*λ*) were significantly correlated with total N availability across all 40 treatments. Under low total N availability, *CNbio* increased, while *k*, *h* and *λ* decreased compared to their values under high N availability, suggesting functional changes in the microbial community of decomposers. Our results show that an N availability approach could be used to estimate residue C dynamics and net N mineralization in the field in response to crop residue quality and placement and demonstrate the potential to improve decomposition models by considering the effects of N availability on C dynamics.

[1]Artigo submetido a Revista Soil Biology and Biochemistry

2.2 Introduction

The objectives of reducing reliance on mineral fertilizers as well as reactive nitrogen (N) losses in agrosystems and diversifying cropping systems (diversification of crops in rotation, double cropping, mixed cropping, reduction or suppression of soil tillage) have increased the need for an accurate method of predicting the decomposition dynamics of crop residues and their effect on carbon (C) fluxes and mineral N availability. C and N cycles are closely coupled during the microbial degradation of plant residues and litter in soils (Trinsoutrot et al., 2000; Li et al., 2013; Redin et al., 2014b). The intensity of C and N fluxes and the resulting net availability of mineral N in soils are controlled by the chemical characteristics of these substrates (Trinsoutrot et al., 2000; Liang et al., 2017) and the conditions of their decomposition, particularly the location of the residues in the soil and the environmental conditions (Coppens et al., 2006; Aita et al., 2012; Mulvaney et al., 2017).

Regarding residue placement, many studies have found that crop residues left on the soil surface decompose more slowly than incorporated residues (Curtin et al., 1998; Coppens et al., 2006; Mulvaney et al., 2017; Oliveira et al., 2020); this effect was attributed mainly to changes in conditions such as soil-residue contact and soil water content, which control decomposition (Coppens et al., 2007). The effect of the placement of crop residues on their decomposition rate has also been shown to depend on the nature of these residues; the decomposition of labile, N-rich residues (from immature plants) is little influenced by their initial placement (Bremer et al., 1991; Bending and Turner, 1999; Abiven and Recous, 2007). This finding suggests that N availability to decomposers, as influenced by soil-residue contact, is involved in the interaction between crop residue quality and placement (Giacomini et al., 2007; Li et al., 2013): N-rich residues contain and release N in sufficient amounts to sustain decomposition even if little N is available in the soil; in contrast, decomposition of N-poor residues is dependent on soil N, which, if not available (for example, when surface placement limits contact with the soil), becomes a limiting factor for decomposition. Studies examining the role of mineral N availability in C and N dynamics during decomposition showed that low N availability to decomposers not only slowed the rate of decomposition of N-poor (or high C:N) residues but also modified the amount of N assimilated per unit of decomposed C, suggesting the adaptation of microbial communities of decomposers to N richness in their environment (Zechmeister-Boltenstern et al., 2015). This could be due to a shift in the dominant microbial decomposer community (Nicolardot et al., 2007) and/or the stoichiometric flexibility of the microorganisms (Agumas et al., 2021; Bai et al., 2021). The effects of N availability on organic matter turnover

have been more completely described for soil humus than for plant residue decomposition, particularly in forest ecosystems subjected to nitrogen enrichment (Chen et al., 2020; Geng et al., 2021). Few models have formalized the relationships between crop residue decomposition and N availability during decomposition (Molina et al., 1983; Li et al., 1992; Henriksen and Brelan, 1999a; Brisson et al., 2003). It can therefore be seen that the overall availability of N to microbial decomposers, which impacts C dynamics and the net mineralization of N, culminates in a given situation from three factors: the soil and its mineral N content, the crop residue and its N content (organic and sometimes mineral), and the colocation of the two sources of N (soil and residue) determined by residue placement, which affects the greater or lesser accessibility of soil N to decomposers.

In this context, the objective of this work was to investigate the effect of the interaction between the chemical quality of crop residues and their placement on residue decomposition, with a focus on the role of N availability. To address this topic, we used an incubation approach to control all experimental conditions, and we explored the responses obtained from 10 crop residues of different N richness and biochemical composition that were left on the soil surface or incorporated into the soil; the experimental soils had two initial levels of mineral N (abundant or limited). Manipulating the initial mineral N content allowed us to disentangle the chemical quality and N richness of the residues and to explore a wide range of N availability levels during decomposition. We hypothesized that the placement of crop residues would first influence access to soil mineral N for decomposers and interact with residue quality. We also tested the hypothesis that the soil mineral N, residue N and residue placement as drivers of decomposition could be translated into a single variable, i.e., the overall N availability to decomposers, across the wide range of residue types investigated. We used the decomposition module of the Simulateur mulTIdisciplinaire pour les Cultures Standard (STICS) model (Nicolardot et al., 2001) to interpret our experimental data, i.e., to estimate the functional adaptations of the soil microbial biomass.

2.3 Materials and methods

2.3.1 Collection of plant material

Ten representative plant species grown as main crops or cover crops from agricultural systems in Brazil were studied (Table 1). The plants selected included four *Poaceae* (Gramineae), four *Fabaceae* (legumes), one *Brassicaceae*, and one *Asteraceae* species. The

plants were cultivated in Typic Hapludalf soil under a no-till system in the experimental area (29°41′ S, 53°48′ W; approximately 90 m elevation) of the Soil Department of the Federal University of Santa Maria in the state of Rio Grande do Sul, Brazil. The region has a subtropical climate, with a mean annual precipitation of 1686 mm and a mean air temperature of 19.3°C. For the previous 12 years, the experimental site had been cultivated using a no-till system. All the crops were managed appropriately according to the technical recommendations for the area. The shoots of the plants were collected at flowering and harvest for the cover crop species and main crop species, respectively, and 3 replicates were obtained per species. The leaves that senesced before harvest were collected gradually until harvest, stored in paper bags and kept at room temperature. Subsequently, the plant shoots were separated into leaves and stems to determine their biomass proportion for each plant species (Table 1). The residues were first dried at 40°C, and the leaves and stems were then cut into pieces 1 cm in length. Subsequently, the residues were cut lengthwise into pieces with a thickness of approximately 0.5 and 0.3 cm for leaves and stems, respectively. A mixture of leaves and stems with a leaf:stem ratio similar to the ratio of dry biomass between leaves and stems determined under field conditions was also prepared (Table 1). One subsample of residue per species was dried at 40°C and ground to a size of 1 mm; a second subsample of each type of residue was dried at 65°C and finely ground (<1 mm) for chemical analyses.

2.3.2 Chemical characterization of plant residues

The total organic C and total N contents of the mixtures of leaves + stems were determined from three finely ground subsamples dried at 65°C using an elemental autoanalyser (FlashEA 1112, Thermo Finnigan, Milan, Italy). A proximate analysis using the Van Soest method was performed using the subsamples of ground residues predried at 40°C. The soluble (SOL), cellulose (CEL), hemicellulose (HEM), and lignin (LIG) fractions of the residues were determined by proximate analysis (Van Soest, 1963) according to Redin et al. (2014a). The residues were placed in a 60-ml snap cap vial with distilled water (20°C) and mechanically stirred for 30 min. After mixing, the material was filtered (Whatman n° 5), and the contents of water-soluble organic C (Csw) and water-soluble total N (Nsw) in the filtrate were determined. All analyses were performed with 3 replicates, and the results are shown in Table 1.

2.3.3 Soil, treatments, and experimental conditions

The soil used was a Typic Hapludalf (USDA classification) collected from the 0–10-cm layer in the no-till system. The soil contained 120 g kg^{-1} clay, 280 g kg^{-1} silt, 600 g kg^{-1} sand, 8.7 g kg^{-1} organic C, and 0.9 g kg^{-1} total N and had a pH (H$_2$O) of 5.4. After visible organic residues had been removed, the soil was sieved to 4 mm. Two initial mineral soil N levels were established for the incubations: 1) 9 mg N kg^{-1} dry soil (low N availability; 9 N) and 2) 77 mg N kg^{-1} dry soil (high N availability; 77 N). These levels were obtained by adding KNO$_3$-N prior to incubation to prevent N limitation during decomposition (Recous et al., 1995). In the two treatments, the amount of water added was calculated to achieve a soil moisture content of 80% of field capacity, i.e., 13.8 g H$_2$O 100 g^{-1} dry soil. The soils were preincubated in plastic bags at 25°C for 5 days.

The experiment consisted of incubation conducted for 120 days in the dark at 25 ± 1°C to measure the C and N mineralization of the residue-amended soils. The experimental design consisted of two sets of incubation jars prepared and monitored in parallel. One set of jars was used to evaluate C-CO$_2$ emissions, and the second was used to measure the evolution of inorganic N in soils. The treatments were arranged in a completely randomized design, and each treatment was replicated three times. The residues, added at a rate of 0.56 g dry matter (DM) pot^{-1} (equivalent to 4.76 g DM per kg dry soil), were either applied to the soil surface (S) or incorporated into the soil (I). This was equivalent to the addition of 1952 (oilseed rape) to 2155 (maize) mg C kg^{-1} of dry soil and 20 (maize) to 170 (vetch) mg N kg^{-1} of dry soil. To set up the pots for the experiment, a subsample of 134 g of moist soil was taken from each replicate. A subsample of 67 g of moist soil (S treatments) or soil mixed with half of the residues (I treatments) was then placed in a 110-ml cylindrical acrylic pot (5.0 cm in diameter and 5.0 cm in height) and compressed to a height of 2.5 cm. Then, a second subsample of 67 g of moist soil (S treatments) or soil mixed with half of the residues (I treatments) was placed in the same acrylic pot and packed to a total height of 5 cm. Thus, the soil in each pot reached a final bulk density of 1.2 g cm^{-3}. In the S treatments, the residues were homogeneously applied to the top of the soil in the pot. Treatments with soil and no residues were set up as controls. Each acrylic pot was placed in a 1000-ml glass jar prior to incubation.

2.3.4 Analytical procedures

C mineralization was assessed by quantifying continuous CO$_2$ release using NaOH trapping for samples taken at 2, 4, 7, 10, 14, 21, 28, 35, 50, 70, 90, and 120 days after the start of the incubation. The CO$_2$ produced in the soil was trapped in 10 ml of 1 M NaOH in a beaker

placed inside each glass jar. The carbonate trapped in the NaOH was precipitated with a $BaCl_2$ solution in excess of 2 M, and the remaining NaOH was back-titrated with 1 M HCl. At all sampling times, the jars were aerated for 10 min to refresh the internal atmosphere, and the soil water content was checked by weighing and adjusted as necessary with a micropipette.

The soil mineral N content ($NH_4^+ + NO_2^- + NO_3^-$) was measured destructively on day 0 and at 7, 14, 21, 35, 63, 90 and 120 days of incubation. At each sampling time, the visible residual particles were removed. Mineral N was extracted from fresh soil samples with 1 M KCl (30 min shaking, soil-to-solution ratio 1:4). The soil KCl suspension was settled for 30 min until the supernatant liquid was clear, and the mineral N in an aliquot of the soil extracts was then measured by steam distillation (Keeney and Nelson, 1982). The jars were opened periodically, aerated and adjusted for humidity when necessary.

2.3.5 Data and statistical analyses

The apparent mineralization of C from the crop residues was calculated by subtracting the amount of $C-CO_2$ released with the control treatment from the amount of $C-CO_2$ released with the amended treatments. The apparent mineralization assumes that crop residue addition has no effect on soil C mineralization (no priming effect) or that this effect is similar regardless of the type of crop residue mixture added. Net N mineralization was calculated by subtracting the mineral N measured in the control from the amount of mineral N that accumulated with each amended treatment (the same control used to calculate the apparent C mineralization). The data on N mineralization and cumulative C mineralization measured over 120 days were analysed by analysis of variance (ANOVA), and the mean values were compared by the Tukey test ($p < 0.05$).

To obtain a quantitative measure of the relative importance of the initial chemical characteristics of the residues for determining residue mineralization, we first calculated C mineralization using an exponential equation according to Jung et al. (2011):

$$Cmin = C_0 \, (1 - e^{-b\,t}) \qquad\qquad (1)$$

where *Cmin* is the amount of mineralized carbon, C_0 is the potentially mineralizable C pool, *b* is the total mineralization constant (crop residue and microbial biomass), and *t* is the incubation period. Stepwise multiple regression analysis was then used to determine which combinations of chemical variables best explained the variations in C_0 and *b*. Only those variables that were found to be significant at $p < 0.05$ were retained in the regressions. Regressions were performed with all available chemical variables of the residues.

2.3.6 Modelling

The decomposition module developed by Nicolardot et al. (2001) was used to analyse the observed dynamics of C and N mineralization as affected by residue type, residue placement and initial soil mineral N content. This decomposition module is part of the crop-soil model STICS (Brisson et al., 2003), which is a dynamic, simple and robust model. The module was previously parametrized under non-nitrogen-limited conditions from a dataset with a large range of crop residues that were finely ground and homogeneously incorporated into the soil (Nicolardot et al., 2001; Justes et al., 2009).

The module has three organic compartments: crop residue (*R*), decomposer microbial biomass (*B*) and humified organic matter (*H*). The crop residues and microbial biomass are assumed to decompose according to first-order kinetics with rate constants of *k* and λ (day^{-1}), respectively. The decomposed C is either mineralized as CO_2 or assimilated by the microbial biomass with yield efficiency *Y* (g g^{-1}). Microbial decay is assumed to result in C humification and secondary C mineralization at proportions of *h* and 1 – *h*, respectively (g g^{-1}). The N dynamics are governed by the C transformation rates and the C:N ratios of the pools. The C and N fluxes are thus governed by seven parameters: two rate parameters (*k* and λ), two partitioning coefficients (*Y* and *h*) and three C:N ratios (those of the crop residue, the microbial biomass and the newly formed humified organic matter).

In the standard parameterization proposed by Nicolardot et al. (2001) and improved by Justes et al. (2009), the residue decomposition rate (*k*), the biomass C:N ratio (*CNbio*) and the humification coefficient of microbial C (*h*) are obtained using hyperbolic functions according to the residue C:N ratio (which is directly measured), while the rate of decomposition of microbial biomass (λ), the assimilation of residue C by the microbial biomass (*Y*) and the newly formed humified organic matter C:N (*CNhum*) are fixed and are therefore not related to the C:N ratio of the residue. This standard parameterization was obtained by nonlinear fitting and by minimizing the differences between observed and simulated apparent C and N mineralization from an incubation dataset including 43 different residues (Justes et al., 2009).

Although this module was originally parameterized and evaluated under non-nitrogen-limited conditions, Giacomini et al. (2007) found that it was able to reproduce observed data obtained under N limitation caused either by insufficient soil mineral N or by poor contact between soil and residues if certain decomposition parameters were modified. These authors

proposed that three parameters (k, λ and *CNbio*) should be reoptimized and found that when N availability decreased, k and λ decreased, while *CNbio* increased. These principles were then incorporated into the STICS crop-soil model (v8 and later) by that addition of a cascade of effects under N-limited conditions: a reduction in the decomposition rates (k, λ), an increase in the C:N of the microbial biomass and, if the availability of the mineral N is still insufficient, an increase in the C:N of the newly formed humified organic matter.

2.3.7 Model testing, parameter optimization and relationship with total N availability

The 40 sets of apparent C and net N mineralization data obtained from the 10 crop residues decomposing under 4 different conditions of residue placement and initial soil N content (I-77N, I-9N, S-77N and S-9N) were compared with the simulations generated by the decomposition module. The simulation process was organized into two steps: simulation with default values (standard parameterization) and simulation after parameter optimization.

Simulations were first performed with the default parameter set established for incorporated residues (Justes et al., 2009) to verify the ability of the STICS decomposition module to simulate the present dataset.

Regarding the optimization process, we chose to limit the number of optimized parameters. Our strategy was to build on the standard parameterization, only optimizing a small number of parameters chosen according to previous works (Giacomini et al., 2007) and to literature describing the relationship between N availability and the decomposition process (e.g., Mooshamer et al., 2014; Manzoni et al., 2021). Indeed, we aimed not only to improve the model prediction of C and N mineralization but also to express relationships between microbial traits and total N available to decomposers. To do so, we tested three different scenarios with an increasing number of optimized parameters. In each scenario, different model parameters were optimized simultaneously but independently for each incubation treatment:

Scenario 1: k, λ, *CNbio*, *CNhum*. In *scenario 1*, we selected the parameters that were already considered in the STICS soil-crop model to take into account the effect of low N availability on the decomposition of crop residues. Indeed, the work by Giacomini et al. (2007) suggested that k and λ are reduced with low N availability, while *CNbio* may increase. This was then incorporated into the STICS soil-crop model, with the additional hypothesis that *CNhum* is ultimately affected if N availability remains low. This first scenario therefore corresponds to how STICS manages the effect of N availability on decomposition.

Scenario 2: *k*, *λ*, *CNbio*, *CNhum*, *h*. For *scenario 2*, we added to the four parameters selected in *scenario 1* the humification rate of microbial biomass (*h*). In the standard parameterization, *h* varies according to the C:N ratio of the residue, which implies that residue quality affects the humification efficiency. In this scenario, we hypothesized that this parameter was affected not only by the C:N ratio of the residue but also more globally by the N availability (resulting from the C:N ratio of residue and from residue placement and soil N status).

Scenario 3: *k*, *λ*, *CNbio*, CNhum, *h*, *Y*. *Scenario 3* added the assimilation yield of residue C by microbial biomass (*Y*) to the five parameters optimized in *scenario 2*. Indeed, previous experimental works have shown that microbial carbon use efficiency can be affected by N availability (Manzoni et al., 2012): it tends to decrease when N availability is limited. Changes in *Y* according to N availability are considered in other decomposition models (e.g., Manzoni et al., 2021). The variation in *Y* during residue decomposition is associated with the higher energy investment and adaptation of microbial communities, which decrease under conditions of reduced N availability.

The optimization algorithm (Newton's method) available in Excel was used to minimize the deviations between the simulated and observed values. The minimization criterion was the RR (relative residual):

$$RR = \frac{RRMSE\ (C) + RRMSE\ (N)}{2}$$

with

$$RRMSE\ (A) = \sqrt{\frac{1}{n} \sum_{i=1}^{n} \left(\frac{A_i - \hat{A}_i}{max\ (A_i) - min\ (A_i)} \right)^2}$$

where RRMSE (*A*) represents the relative root mean square error for variable *A* (carbon or nitrogen mineralization from plant residues).

The maximum and minimum limits for each parameter except for *CNbio* and *CNhum* were those proposed by Nicolardot et al. (2001) ($0.05 \leq h \leq 1$; $0 \leq Y \leq 0.65$). *CNbio* had its upper limits increased to 30 ($6 \leq CNbio \leq 30$) to take into account the possibility of stoichiometric flexibility of the fungal community (Cleveland and Liptzin, 2007; Camenzind et al., 2021). We considered that *CNhum* could vary between 8 and 12 ($8 \leq CNhum \leq 12$), which is consistent with the observed range of C:N of soil organic matter measured in cropped soils (e.g., Clivot et al., 2017). These parameters were assumed to be constant throughout the

duration of the incubations. In all scenarios, the values of nonoptimized parameters were fixed or calculated according to their hyperbolic relationships with the C:N ratio of the residue (Justes et al., 2009).

The relationships between the observed and simulated data for C and N mineralization were evaluated using the root mean square error (RMSE):

$$RMSE \ (A) = \sqrt{\frac{1}{n}\sum_{i=1}^{n}(A_i - \hat{A}_i)^2}$$

The subsequent selection of the optimization scenario to interpret the effect of reduction of N availability on the decomposition process was made combining three criteria: i) the available knowledge of model parameters that are assumed to be dependent on the total N availability; ii) the resulting quality of prediction (RMSE), globally and for individual treatments; iii) and the quality of the relationship between optimized parameters and total N availability, to interpret the response of microbial traits to N availability.

2.3.7.1 Use of simulation results to estimate total N availabilty for decomposers

The main hypothesis of this work is that the interactive effects of residue type, residue placement, and soil initial mineral N content on the C and N mineralization of residues result from the overall N availability to decomposers. The total N availability was assumed to be the sum of the initial soil mineral N content plus the initial residue total N content. For the residue incorporation treatments, the soil mineral N in the soil core and the residue total N were assumed to be totally available to decomposers. For the surface residue application treatments, we assumed that only a fraction of the initial soil mineral N content would be available to decomposers due to limited soil-residue contact, while all the residue N was considered potentially available. Therefore, the following calculations were aimed at estimating the plausible size of the soil mineral N fraction available to decomposers of surface-applied residues.

To estimate the size of this soil mineral N pool, the parameters k, λ, h and *CNbio* obtained in the optimization step (*scenario 2*) were plotted against the pool of N available to decomposers (total N availability), which was calculated separately for the incorporated and surface-applied residues. The plausible proportion of soil mineral N available for the

decomposition of surface residues was determined using the Excel solver tool as the proportion allowing the best fit of the optimized parameters and the total N availability calculated for all treatments (incorporation and surface application).

2.4 Results

2.4.1 Crop residues characteristics

The residue C concentration varied slightly, from 421 g kg^{-1} DM (oilseed rape) to 453 g kg^{-1} (vetch), while the N concentration varied greatly, from 4.3 g kg^{-1} DM (maize) to 35.2 g kg^{-1} (vetch); therefore, the C:N ratios of the residues ranged from 13 to 105 (Table 1), with the C:N ratios of the cover crop residues in the low C:N range compared to the main crop residues. The LIG contents of the crop residues ranged from 61 g kg^{-1} DM (wheat) to 143 g kg^{-1} (soybean). In this dataset, the residue soluble DM concentration and total N concentration were strongly linearly correlated (r^2= 0.831), resulting from the crop maturity stage at which crop residues were harvested. Plants destroyed at the green stage, such as cover crops (black oat, showy rattlebox, gray mucuna and vetch), have cell vacuoles with both high soluble content and high N concentration, with the reverse when plants are mature (six other residues), due to the remobilization of carbon and nutrient reserves during grain-filling periods. Increased plant maturity is generally related to the deposition of lignocellulosic tissues (cellulose, hemicellulose and lignin) and governs the ratio of cytosoluble to cell wall fractions in plants (Bertrand et al., 2019), as observed here for the residues of the crops harvested at maturity.

2.4.2 Global C and N mineralization patterns

The cumulative C-CO_2 and net N mineralization from crop residues varied widely (Fig. 1). The soil N availability, residue type and residue placement significantly affected the cumulative C mineralization (P<0.05). The cumulative C mineralization (expressed as % added C) after 120 days ranged from 39% (maize, S-9N) to 67% (black oat, S-77N) of the added C from surface residues and from 43% (soybean, I-77N) to 66% (black oat and vetch, I-9N) of the added C from incorporated residues (Fig. 1a,b). The mineral N dynamics indicated net immobilization or net mineralization in the different treatments, and the values ranged from -26 mg N kg^{-1} soil (maize, S-9N) to +84 mg N kg^{-1} soil (vetch, S-77N) with surface residues and

from -30 mg N kg^{-1} soil (wheat, I-77N) to +100 mg N kg^{-1} soil (vetch, I-9N) with incorporated residues (Fig. 1c,d).

The potentially mineralizable C pool (C_0) was calculated with a simple exponential decay function and ranged from 40.7% added C (soybean; I-77N) to 66.6% added C (black oat; S-77N); these values were close to the measured cumulative C mineralized over 120 days (Supplementary Table S1). The mineralization constant (*b*) of C_0 differed among residues (Supplementary Table S1) and ranged from 0.017 for maize (S-77N) to 0.126 for vetch (I-77N). A correlation analysis showed that *b* was positively correlated with the residue N content (surface residues, r = 0.96; incorporated residues, r = 0.97) and negatively correlated with CEL and HEM (surface residues, r = -0.84; incorporated residues, r = -0.95). The potential mineralization pool (C_0) was correlated with the CEL, HEM, and LIG contents, negatively correlated with surface residues (r = -0.35) and positively correlated with incorporated residues (r = 0.55).

The C and N mineralization for the three crop residues (wheat, vetch, and oilseed rape) are shown in Fig. 2 to illustrate the three main responses observed in the dataset (the values for the other residues are presented in the supplementary material, Figs. S1 and S2). For wheat, the rate of C mineralization was modified by the placement and availability of soil mineral N, with I77>I9>S77>S9. This was not the case for vetch, for which the treatment had no effect on the initial C mineralization; as the experiment continued, the C mineralization in the treatments slightly diverged, with I9> I77 and S9 and S77 having intermediate values. For oilseed rape residue, there was no difference in the kinetics of C mineralization regardless of the soil N availability or the initial residue placement. The response typologies were very different for the net N mineralization in the soil. For wheat, as expected from a residue with C:N=89, strong net N immobilization was observed throughout the decomposition period (peaking at approximately -35 mg N kg^{-1} soil); N immobilization was more pronounced and faster when the residues were incorporated and had a high initial mineral N content (I77>I9>S77>S9). For the oilseed rape residue (C:N=22), N immobilization was more limited (peaking at approximately -10 mg N kg^{-1} soil) and more transient in treatments I77 and I9, while only positive net mineralization was observed in the S77 and S9 treatments, which had less mineral N in the soil (S9>S77). For the vetch residues with a C:N ratio of 13, only net N mineralization was observed, and there were no significant differences between treatments. On average, for all treatments, greater net N immobilization was observed in the treatments with high initial soil mineral N (S-77N and I-77N) than in the treatments with low initial soil mineral N (S-9N and I-9N).

To express the relationship between N and C dynamics and to compare treatments at similar stages of decomposition, net N immobilization was expressed as a function of the cumulative C mineralization for each treatment (Fig. 2g, h, i). The greatest net N immobilization was observed from the incorporated residues of the *Poaceae* species, sunflower and soybean (mainly in the I-77N treatment), when approximately 35% of the added residue C was mineralized (Fig. 2g and Supplementary Figs. S1, S2). The residues decomposing at the soil surface immobilized less N than the same residues incorporated into the soil at the same stage of decomposition (35% of the cumulative residue C mineralized). The net N mineralization of residues with low initial C:N ratios (vetch, grey mucuna) was not affected by the different treatments.

2.4.3 Simulations with the standard parameters and with optimization scenarios

Overall, C and N mineralization was not well simulated using the standard parameters of the decomposition module developed under optimal conditions (finely ground residues and no N limitation). As expected, the best simulation results were obtained for the residue incorporation treatment with a high soil mineral N content (I-77N) (Figs. 3 and 4; Supplementary Figs. S1 and S2). In this treatment, the lowest values of RMSE (C) and RMSE (N) were found for residues with low C:N ratios (vetch, I-77N and oilseed rape, I-77N). The same was observed for the surface-applied residues, and the lowest RMSE (C) and RMSE (N) were observed for the showy rattlebox residue in the treatment with high soil mineral N (S-77N) (Supplementary Fig. S1). In general, for the low soil N treatments (I-9N and S-9N), the model tended to overestimate C mineralization and underestimate net N mineralization, resulting in average RMSE values of 13.5% added C and 18.8 mg N kg^{-1} soil.

The parameter optimization performed in the three scenarios resulted in significant improvements in the simulations of C and N mineralization dynamics (Table 2). The RMSE (C) and RMSE (N) values decreased to averages of 2.48% added C and 2.04 mg N kg^{-1} for the three scenarios. The similar RMSE values obtained after optimization suggest that distinct decomposition model parameters lead to improved C and N mineralization predictions. However, *scenario 2* showed the most significant correlations between parameters and total N availability and therefore was selected to interpret the results (Fig. 5). Under *scenario 3,* no relationship was observed between *Y* and total N availability (Supplementary Fig. S3). In this scenario, the relationship between *k*, λ, and *CNbio* and the total N availability was slightly weakened compared to that with *scenario 2* (Supplementary Fig. S3), while *CNbio* values

varied within the same range and were not markedly different between *scenario 2* and *scenario 3* (Supplementary Fig. S4).

2.4.4 Estimation of total N availability

For the residue incorporation treatments, the total N availability varied from 113.6 kg N (vetch, I-77) to 15.8 kg N (maize, I-9) per ton of residue C added (Supplementary Table S2). For the surface residue application treatments, using the parameter values generated through the optimization of *scenario 2*, the best fit between k, λ, h, and *CNbio* and the total N availability was obtained when 24% of the mineral N present in the soil was considered available to decomposers. This relationship resulted in significant correlations for k, λ, h and *CNbio* with total N available (Fig. 5). The calculated N availability ranged from 10.5 (maize, S-9N) to 86.3 (vetch, S-77N) kg N per ton of residue C added (Supplementary Table S2).

2.4.5 Model optimization and effect of N availability

The value of the parameter k optimized in *scenario 2* varied widely across the 10 residues × 4 treatments, from 0.02 to 0.23 day^{-1}, and increased with increasing total N availability (Fig. 5a) regardless of the cause of the variation in total N availability (residue type or placement or initial soil mineral N). The highest k values were observed for vetch residues; these varied little among the different treatments (from 0.21 to 0.23 day^{-1} for I-77N and S-9N) because the main source of available N for vetch was the residue N itself (Supplementary Table S2). For the mature residues with intermediate to low N contents, k increased more drastically with increasing N availability, reflecting the role of initial soil N and placement in the rate of C mineralization (Fig. 5). For example, for the residues of barley and sunflower, k varied from 0.02–0.03 day^{-1} (S-9N) to 0.10–0.13 day^{-1} (I-77N) (Supplementary Table S2).

The optimized parameter λ, which represents the decomposition rate of microbial biomass, also increased with increasing total N availability (Fig 5). Higher values of λ were observed with higher N residues (e.g., λ=0.038 and 0.030 day^{-1} for showy rattlebox and oilseed rape, respectively, under I-77N) (Supplementary Table S2). Conversely, the lowest values of λ were observed for the most mature residues with the lower N content, e.g., 0.003 and 0.002 day^{-1} for the maize and wheat S-9N treatments, respectively (Fig. 5). However, the quality of fit obtained for these relationships was much poorer than that for k (r = 0.48 vs. 0.86).

The optimized *CNbio* parameter showed a negative correlation with N availability and decreased when the total N availability increased, with I-77N<I-9N<S-77N<S-9N (Fig. 5). *CNbio* decreased from a maximal value of C:N=30 (wheat, barley, maize, sunflower in the S-9 treatments) at low N availability to a minimum value of C:N= 8–11 at high N availability (grey mucuna, vetch, showy rattlebox, oilseed rape in the I-77N & I-9N treatments). The parameter *h* decreased with decreasing N availability, varying from 0.76 (showy rattlebox, I-77N) to 0.05 (residues with high C:N ratios) (Supplementary Table S2). For immature residues with high N content, the *h* values remained highly independent of residue placement and soil mineral N status (Fig. 5). The parameter *CNhum* was also optimized in *scenario 2*; its values did not vary consistently and could not be correlated with the change in total N availability (data not shown). However, it was often higher in the I treatments than in the S treatments.

2.5. Discussion

2.5.1 Drivers of crop residue decomposition

The chemical characteristics and placement of crop residues and the soil mineral N content were shown in this study to be important drivers of residue decomposition. Considerable work has been done on these topics in the past, particularly on the relationship between crop residue quality and potential biodegradability (Trinsoutrot et al., 2000; Abiven et al., 2005; Harguindeguy et al., 2008; Redin et al., 2014b; Cyle et al., 2016). However, much less work has been done to unravel the effects of crop residue placement and its interaction with crop residue quality (Coppens et al., 2006; Li et al., 2013; Datta et al., 2019). Under field conditions, residue placement characterizes different agricultural management practices (tilled vs. no-tilled agroecosystems) that can affect the decomposition process by changing soil-residue contact, soil N availability and soil water dynamics (Arcand et al., 2016; Iqbal et al., 2015). Our study does not allow us to evaluate the effect of soil water dynamics on residue C and N mineralization. However, it is important to mention that in experimental situations with the potential for large water evaporation, dry conditions could also be a factor slowing down the decomposition of surface-applied residues compared to that of incorporated residues (Iqbal et al., 2015; Dietrich et al., 2019). It was previously shown that the chemical features of plant tissues (their proportions of various carbohydrate pools and their tissue architecture) and their N concentrations should be considered separately (Sall et al., 2007; Sukitprapanon et al., 2020).

The former determines the intrinsic accessibility of plant cells to microorganisms and their enzymes and therefore drives the kinetics of degradation (Almagro et al., 2021). The latter, residue N, which is essential for microbial growth and metabolism, determines which of the two elements, C or N, is limiting; moreover, in soil, residue N determines the balance between N immobilization and N mineralization (Yansheng et al., 2020).

As observed in this study, the crop residue characteristics are mostly related to the maturation stage of the plants, as crops used as cover crops (i.e., hairy vetch, grey mucuna, showy rattlebox and oilseed rape in this study) were harvested in the vegetative stage, when they had low LIG contents and high soluble DM and N concentrations. Therefore, the soluble DM pool and the total N concentration were strongly and linearly correlated across the 10 plant residues, and the effects of these two residue characteristics on C and N dynamics cannot be easily disentangled. The best treatments for examining how the residue composition affects the dynamics of C mineralization were therefore those that provided optimal conditions for decomposition, i.e., those in which the residues were incorporated into soils with high initial mineral N levels (the I-77N treatments). The high mineral N availability (corresponding on average to 37.0 ± 0.9 mg N g^{-1} added C) allowed the N-poor residues to overcome N limitation, as the threshold for N limitation has been estimated to be approximately 30 mg N g^{-1} added C according to Recous et al. (1995) and Mary et al. (1996). Under these non-N-limited conditions, the kinetics of C mineralization exhibited biochemical differences between crop residues (Trinsoutrot et al., 2000; Sall et al., 2007). Across the ten treatments, our results confirm a previously noted pattern in which the degradation rate (*b*) is negatively correlated with the CEL and HEM contents and positively correlated with the N and soluble DM contents (Redin et al., 2014b). Conversely, the main driver of net N mineralization was the residue N content and the associated C:N ratio. As expected (Abiven and Recous, 2007; Li et al., 2013; Yansheng et al., 2020), net N mineralization was observed for residues with low C:N ratios, and N immobilization predominated for residues with high C:N ratios.

One major finding of this study is the interaction of residue placement with residue quality and how this interaction influences C and N dynamics. The placement of crop residues at the soil surface has often been found to significantly decrease the rate of residue decomposition; for example, this was observed by Coppens et al. (2006) with oilseed rape residue and by Datta et al. (2019) with rice and wheat residues. However, it has also been shown (Schomberg et al., 1994) that this effect of residue placement is dependent on the residue characteristics. Under laboratory conditions with controlled temperature and moisture, this effect was attributed to poor soil-residue contact, which reduced the availability of soil mineral

N for microbial biomass during decomposition of crop residues (Coppens et al. 2007). Our results confirm these findings, as the effect of residue placement was not observed for the residues with low C:N ratios in this study (vetch and oilseed rape residues). Conversely, surface placement drastically decreased the rates of mineralization of mature residues such as maize, wheat, sunflower, and barley to the extent that, at the end of the incubation, the dynamics of decomposition for surface maize residues with low mineral N (S-9N) was not advanced enough (maximal cumulative $C-CO_2$ = 39.4% C added) to initiate the phase of net N remineralization, which was observed fairly rapidly in all the other treatments.

In addition to modifying C mineralization kinetics, residue placement strongly influenced the intensity of N immobilization during decomposition and the net mineral N balance. Immobilization increased when residues were incorporated (incorporated > surface) for both soil mineral N levels, with 77N > 9N, e.g., for wheat and oilseed rape residues. The fact that incorporated residues promote N immobilization more than surface application was previously described by several authors (Giacomini et al., 2007; Aita et al., 2012; Mulvaney et al., 2017; Yansheng et al., 2020); the difference was more pronounced with high-C:N ratio residues, confirming our results. With intermediate-C:N ratio residues (e.g., oilseed rape and showy rattlebox), despite the lack of an effect of placement on C mineralization, net N immobilization was observed when the residues were incorporated, while only net N mineralization was observed when the residues were left on the soil surface. This pattern suggests differences in microbial N consumption during decomposition, even in treatments with no N limitation on C degradation (i.e., the vetch and grey mucuna treatments). This reduction in N consumption by decomposers for a given amount of decomposed C was previously highlighted by Recous et al. (1995) and Mary et al. (1996), who demonstrated with maize and wheat residues a threshold of N availability below which microbial N consumption per unit of mineralized C was lower but the straw C mineralization rate was unchanged. In their work, the microbial N immobilization rate varied from 30 mg N g^{-1} C mineralized under high N availability conditions to 11–15 mg N g^{-1} C mineralized under N-limited conditions (Mary et al., 1996). Therefore, our results, which were obtained with a large range of residue qualities, confirm the important role of N availability in the dynamics of residue C mineralization and N mineralization; N availability is modulated by the interaction between crop residue composition, crop residue placement and initial soil mineral N, which are drivers that interact to determine the overall N availability to decomposers. We believe that the conditions that control the degradation of crop residues by the availability of mineral N are very common in field conditions, especially in cereal systems, where large amounts of straw may be left in the

field, either on the soil surface as mulch (no-till systems) or incorporated into the topsoil layer by reduced-tillage techniques, while the soil layer concerned does not contain the amounts of mineral N corresponding to the microbial needs created by straw incorporation. Limited soil-residue contact and access to mineral N are also affected by the size of the residue particles, and larger particles (decimetre size range, such in that observed the field) induce heterogeneity of distribution in the soil and potentially slow decomposition (e.g., Iqbal et al., 2014). To unravel the response of microbial biomass to N limitation in terms of metabolic traits, this assumption was further tested using a modelling approach.

2.5.2 Conceptual approach of overall N availability to decomposers

Few studies have proposed a conceptual approach for determining the accessibility of soil mineral N from a crop residue layer left on the soil surface. Some models that take into account the possible N control of decomposition introduced a parameter that defines the thickness of the underlying soil that "feeds" the decaying mulch (Findeling et al., 2007; Balwinder-Singh et al., 2011). Some work has also demonstrated the biological realities of these processes by observing either nutrient translocation by fungal hyphae (George et al., 1992) or the N diffusion gradient in the soil, e.g., in the detritusphere (Gaillard et al., 1999). The observed differences between the S77 and S9 treatments indicate that the amount of mineral N under the residue layer influenced their decomposition, revealing the contribution of soil N to decomposition. Here, we adopted an empirical approach using the STICS decomposition module (Nicolardot et al., 2001) that was based on optimization of the microbial parameters k, λ, h, $CNbio$ and $CNhum$ to determine the plausible size of the soil N pool that is accessible to decomposers under surface decomposition conditions. Across the ten crop residues and the two initial levels of mineral N (9 and 77 mg N kg^{-1} dry soil), the best fit between the observed and simulated C and N dynamics was obtained by considering that 24% of the soil mineral N was accessible to decomposers during surface residue decomposition; this corresponded to an approximately 1.25-cm soil depth in the soil pots used in the present work. Such an estimation allowed us to calculate the total N availability for the 40 treatments tested.

2.5.3 Effects of N availability on microbial biomass modelled parameters

The independent optimization of the STICS module parameters for each residue × treatment combination indicated a reduction in the residue decomposition rate (k), an increase

in the C:N ratio of microbial biomass *(CNbio)*, a decrease in decomposer microbial biomass decay *(λ)* and a reduction in humification *(h)* when N availability was reduced; optimizing the assimilation yield parameter (*Y*) did not improve the simulations and did not significantly change the range of *CNbio* values. The most notable result was that each of these four parameters exhibited a relationship with the total available N, regardless of crop residue, residue placement or initial soil mineral N content; this confirms our initial hypothesis of the relevance of the conceptual approach based on total N availability. This relationship to N availability was particularly strong for *k* and *CNbio*.

Evidence of a reduction in the residue decomposition rate under conditions of low N availability was observed by other authors (Henriksen and Breland, 1999b; Hadas et al., 2004; Wang et al., 2004; Delgado-Baquerizo et al., 2015). The lower the C:N ratio of the residues was, the lower the reduction in the decomposition rate. These results show the same substantial effect of reduced N availability on high-C:N ratio residues, as observed by Schomberg et al. (1994), who found greater changes in the decomposition rate between incorporated and surface-applied grain sorghum and wheat residues than between incorporated and surface-applied alfalfa residues. The decomposer microbial biomass decay *(λ)* was also reduced under conditions of low total N availability. In the Henriksen and Breland (1999a) model, the decay rate constant of the microbial biomass changed for different organic pools (plant decomposable, plant structural and humus pools) and decreased with the increase in the N-deficient structural material.

We also noted an increase in humification (*h*) with increasing N availability, which is in agreement with the initial soil mineral N-limitation formalism of the model (Justes et al., 2009) but also takes into account the N limitation linked to residue placement. These results reinforce the importance of microbial biomass as a precursor to stable soil organic matter (Alvarez and Alvarez, 2000; Liang et al., 2019; Wang et al., 2020). The higher humification rate observed for low-C:N ratio residues is related to their large soluble DM fractions, which are rapidly assimilated by microbial biomass but are also available for the stabilization and formation of soil mineral-associated organic matter (MAOM) (Cyle et al., 2016). Residues with a high C:N ratio contain a higher percentage of complex polymers (e.g., cellulose and hemicellulose), resulting in fewer compounds that can be stabilized as MAOM (Almagro et al., 2021).

An increase in the C:N ratio of microbial biomass when N availability is reduced has been included in other models (Blagodatsky and Richter, 1998; Henriksen and Brelan, 1999a; Manzoni et al. 2021). This increase implicitly reflects a change in the microbial community

structure of decomposers that is probably related to the higher contribution of fungi to decomposition. The maximal C:N value of the microbial biomass (here, *CNbio* ≤ 30) is an optimized parameter of a simple model and does not necessarily reflect a biological reality; however, variations in microbial biomass C:N ratios appear on average rather constrained, at 8.6 ± 0.3 according to Cleveland and Liptzin (2007), but ranged between 3 and 24 in their study. Evidence for some stoichiometric flexibility of microbial communities was also shown by Li et al. (2012) and Fanin et al. (2013). Fungi exhibit lower metabolic activity than bacteria as well as highly efficient N use (Zechmeister-Boltenstern et al., 2015). Their filamentous hyphae can provide access to soil resources through the remobilization and transfer of N, allowing surface residues to decompose under conditions of low N availability (Frey et al., 2000). Camenzind et al. (2021) demonstrated the high flexibility of the C:N ratio of soil fungal mycelia in conditions of varied N availability, varying their C:N ratio from 8–18 (high N supply) to 84 (low N supply). Another possible explanation for the change in C:N ratios is that the C-use efficiency or assimilation yield (*Y*) decreases with decreased N availability, consequently decreasing the N requirements of the microbial community by modifying their cellular composition according to the external nutrient availability (Sinsabaugh et al., 2013; Manzoni et al., 2021;). In this study, optimization *scenario 3*, which had varying *Y* values, did not result in a good overall correlation with N availability and could not explain the lower N immobilization observed in the low N availability treatments. Although the closest correlation to N availability was found using a fixed value of *Y* with STICS (0.62), Sinsabaugh et al. (2013) recommended using a value of 0.30 for C-use efficiency in large-scale models and a variable *Y* value for small-scale models. The literature shows evidence of changes in *Y* with decreasing N availability (Agumas et al., 2021; Bai et al., 2021), which can also be linked to changes in the microbial community (Bölscher et al., 2016); however, as a result of the simplicity of the model and the optimization procedure, the model could compensate for the variation in *Y* by increasing *CNbio*, which still indicates a modification in the soil microbial decomposer community. Manzoni et al. (2021) showed that the response of microbial adaptation to N limitation should be done by different mechanisms: flexible C-use efficiency, selective enzymes, the plastic microbial biomass C:N ratio, and nutrient retention in the microbial biomass. The authors conclude that all four mechanisms could be used during microbial adaptation to low N availability.

2.6 Conclusion

A combination of incubation experiments and modelling showed for the first time, across a large range of crop residue types, how the combination of residue chemical quality, residue placement and soil mineral N content drives C and N dynamics by modifying N access for microbial decomposers, defined in this work as the total N availability. The placement of residues on the soil surface imposes a limitation on soil N resources for microbial decomposer biomass. This limitation is critical for high-C:N ratio residues but less important or negligible for low-C:N ratio residues. The use of a modelling approach allowed the possibility of exploring the effects of these interactions on microbial biomass functional traits and understanding the unique C and N mineralization patterns observed. The reduction in total N availability led to a reduction in residue decomposition, microbial biomass decay and humification rates and to an increase in the C:N ratio of microbial biomass. These parameter changes were more notable for high-C:N ratio residues than for low-C:N ratio residues, for which the high residue N content was the main source of N for microorganism metabolism, independent of residue placement and soil mineral N status. The N availability approach appears to be appropriate for predicting the dynamics of N mineralization after crop residue recycling under management conditions where available N can often be a driver of organic matter decomposition, such as under reduced- or no-tillage field conditions with, e.g., cereal straw. However, this approach needs to be further tested at the field level under different N-limitation conditions. Further work should be done first by implementing or improving N-limitation functions in C-N decomposition models and then combining experiments and modelling under field conditions.

Acknowledgements

2.7 References

Abiven, S., Recous, S., 2007. Mineralisation of crop residues on the soil surface or incorporated in the soil under controlled conditions. Biology and Fertility of Soils 43, 849–852. doi:10.1007/s00374-007-0165-2

Abiven, S., Recous, S., Reyes, V., Oliver, R., 2005. Mineralisation of C and N from root, stem and leaf residues in soil and role of their biochemical quality. Biology and Fertility of Soils 42, 119–128. doi:10.1007/s00374-005-0006-0

Agumas, B., Blagodatsky, S., Balume, I., Musyoki, M.K., Marhan, S., Rasche, F., 2021. Microbial carbon use efficiency during plant residue decomposition: Integrating multi-enzyme stoichiometry and C balance approach. Applied Soil Ecology 159, 103820. doi:10.1016/j.apsoil.2020.103820

Aita, C., Recous, S., Cargnin, R.H.O., da Luz, L.P., Giacomini, S.J., 2012. Impact on C and N dynamics of simultaneous application of pig slurry and wheat straw, as affected by their initial locations in soil. Biology and Fertility of Soils 48, 633–642. doi:10.1007/s00374-011-0658-x

Almagro, M., Ruiz-navarro, A., Díaz-pereira, E., Albaladejo, J., Martínez-Mena, M., 2021. Plant residue chemical quality modulates the soil microbial response related to decomposition and soil organic carbon and nitrogen stabilization in a rainfed Mediterranean agroecosystem. Soil Biology and Biochemistry 156, 108198. doi:10.1016/j.soilbio.2021.108198

Alvarez, R., Alvarez, C.R., 2000. Soil Organic Matter Pools and Their Associations with Carbon Mineralization Kinetics. Soil Science Society of America Journal 64, 184–189.

Arcand, M.M., Helgason, B.L., Lemke, R.L., 2016. Microbial crop residue decomposition dynamics in organic and conventionally managed soils. Applied Soil Ecology 107, 347–359. doi:10.1016/j.apsoil.2016.07.001

Bai, X., Dippold, M.A., An, S., Wang, B., Zhang, H., Loeppmann, S., 2021. Extracellular enzyme activity and stoichiometry: The effect of soil microbial element limitation during leaf litter decomposition. Ecological Indicators 121, 107200. doi:10.1016/j.ecolind.2020.107200

Balwinder-Singh, Gaydon, D.S., Humphreys, E., Eberbach, P.L., 2011. The effects of mulch and irrigation management on wheat in Punjab, India-Evaluation of the APSIM model. Field Crops Research 124, 1–13. doi:10.1016/j.fcr.2011.04.016

Bending, G.D., Turner, M.K., 1999. Interaction of biochemical quality and particle size of crop residues and its effect on the microbial biomass and nitrogen dynamics following incorporation into soil. Biology and Fertility of Soils 29, 319–327. doi:10.1007/s003740050559

Bertrand, I., Viaud, V., Daufresne, T., Pellerin, S., Recous, S., 2019. Stoichiometry constraints challenge the potential of agroecological practices for the soil C storage. A review. Agronomy for Sustainable Developtment 39, 1–16.

Blagodatsky, S.A., Richter, O., 1998. Microbial growth in soil and nitrogen turnover: a theoretical model considering the activity state of microorganisms. Soil Biology and Biochemistry 30, 1743–1755. doi:10.1016/S0038-0717(98)00028-5

Bölscher, T., Wadsö, L., Börjesson, G., Herrmann, A.M., 2016. Differences in substrate use efficiency: impacts of microbial community composition, land use management, and substrate complexity. Biology and Fertility of Soils 52, 547–559. doi:10.1007/s00374-016-1097-5

Bremer, E., van Houtum, W., van Kessel, C., 1991. Carbon dioxide evolution from wheat and lentil residues as affected by grinding, added nitrogen, and the absence of soil. Biology and Fertility of Soils 11, 221–227. doi:10.1007/BF00335771

Brisson, N., Gary, C., Justes, E., Roche, R., Mary, B., Ripoche, D., Zimmer, D., Sierra, J., Bertuzzi, P., Burger, P., Bussière, F., Cabidoche, Y.., Cellier, P., Debaeke, P., Gaudillère, J.., Hénault, C., Maraux, F., Seguin, B., Sinoquet, H., 2003. An overview of the crop model stics. European Journal of Agronomy 18, 309–332. doi:10.1016/S1161-0301(02)00110-7

Camenzind, T., Grenz, K.P., Lehmann, J., Rillig, M.C., 2021. Soil fungal mycelia have unexpectedly flexible stoichiometric C:N and C:P ratios. Ecology Letters 24, 208–218. doi:10.1111/ele.13632

Chen, J., Xiao, W., Zheng, C., Zhu, B., 2020. Nitrogen addition has contrasting effects on particulate and mineral-associated soil organic carbon in a subtropical forest. Soil Biology and Biochemistry 142, 107708. doi:10.1016/j.soilbio.2020.107708

Cleveland, C.C., Liptzin, D., 2007. C:N:P stoichiometry in soil: is there a '"Redfield ratio"' for the microbial biomass? Biogeochemistry 85, 235–252. doi:10.1007/s10533-007-9132-0

Clivot, H., Mary, B., Valé, M., Cohan, J., Champolivier, L., Piraux, F., Laurent, F., Justes, E., 2017. Quantifying in situ and modeling net nitrogen mineralization from soil organic matter in arable cropping systems. Soil Biology & Biochemistry 111, 44–59. doi:10.1016/j.soilbio.2017.03.010

Coppens, F., Garnier, P., De Gryze, S., Merckx, R., Recous, S., 2006. Soil moisture, carbon and nitrogen dynamics following incorporation and surface application of labelled crop residues in soil columns. European Journal of Soil Science 57, 894–905. doi:10.1111/j.1365-2389.2006.00783.x

Coppens, F., Garnier, P., Findeling, A., Merckx, R., Recous, S., 2007. Decomposition of mulched versus incorporated crop residues: Modelling with PASTIS clarifies interactions between residue quality and location. Soil Biology and Biochemistry 39, 2339–2350. doi:10.1016/j.soilbio.2007.04.005

Curtin, D., Selles, F., Wang, H., Biederbeck, V.O., Campbell, C.A., 1998. Carbon Dioxide Emissions and Transformation of Soil Carbon and Nitrogen during Wheat Straw Decomposition. Soil Science Society of America Journal 62, 1035–1041. doi:10.2136/sssaj1998.03615995006200040026x

Cyle, K.T., Hill, N., Young, K., Jenkins, T., Hancock, D., Schroeder, P.A., Thompson, A., 2016. Substrate quality influences organic matter accumulation in the soil silt and clay fraction. Soil Biology and Biochemistry 103, 138–148. doi:10.1016/j.soilbio.2016.08.014

Datta, A., Jat, H.S., Yadav, A.K., Choudhary, M., Sharma, P.C., Rai, M., Singh, L.K., Majumder, S.P., Choudhary, V., Jat, M.L., 2019. Carbon mineralization in soil as influenced by crop residue type and placement in an Alfisols of Northwest India. Carbon

Management 10, 37–50. doi:10.1080/17583004.2018.1544830

Delgado-Baquerizo, M., García-Palacios, P., Milla, R., Gallardo, A., Maestre, F.T., 2015. Soil characteristics determine soil carbon and nitrogen availability during leaf litter decomposition regardless of litter quality. Soil Biology and Biochemistry 81, 134–142. doi:10.1016/j.soilbio.2014.11.009

Dietrich, G., Recous, S., Pinheiro, P.L., Weiler, D.A., Schu, A.L., Rambo, M.R.L., Giacomini, S.J., 2019. Gradient of decomposition in sugarcane mulches of various thicknesses. Soil & Tillage Research 192, 66–75. doi:10.1016/j.still.2019.04.022

Fanin, N., Fromin, N., Buatois, B., Hättenschwiler, S., 2013. An experimental test of the hypothesis of non-homeostatic consumer stoichiometry in a plant litter – microbe system. Ecology Letters 16, 764–772. doi:10.1111/ele.12108

Findeling, A., Garnier, P., Coppens, F., Lafolie, F., Recous, S., 2007. Modelling water, carbon and nitrogen dynamics in soil covered with decomposing mulch. European Journal of Soil Science 58, 196–206. doi:10.1111/j.1365-2389.2006.00826.x

Frey, S.D., Elliott, E.T., Paustian, K., Peterson, G.A., 2000. Fungal translocation as a mechanism for soil nitrogen inputs to surface residue decomposition in a no-tillage agroecosystem. Soil Biology and Biochemistry 32, 689–698. doi:10.1016/S0038-0717(99)00205-9

Gaillard, V., Chenu, C., Recous, S., Richard, G., 1999. Carbon, nitrogen and microbial gradients induced by plant residues decomposing in soil. European Journal of Soil Science 50, 567–578. doi:10.1046/j.1365-2389.1999.00266.x

Geng, J., Fang, H., Cheng, S., Pei, J., 2021. Effects of N deposition on the quality and quantity of soil organic matter in a boreal forest: Contrasting roles of ammonium and nitrate. Catena 198, 104996. 104996. doi:10.1016/j.catena.2020.104996

George, E., Häussler, K.-U., Vetterlein, D., Gorgus, E., Marschner, H., 1992. Water and nutrient translocation by hyphae of Glomus mosseae. Canadian Journal of Botany 70, 2130–2137. doi:10.1139/b92-265

Giacomini, S.J., Recous, S., Mary, B., Aita, C., 2007. Simulating the effects of N availability, straw particle size and location in soil on C and N mineralization. Plant and Soil 301, 289–301. doi:10.1007/s11104-007-9448-5

Hadas, A., Kautsky, L., Goek, M., Erman Kara, E., 2004. Rates of decomposition of plant residues and available nitrogen in soil, related to residue composition through simulation of carbon and nitrogen turnover. Soil Biology and Biochemistry 36, 255–266. doi:10.1016/j.soilbio.2003.09.012

Harguindeguy, N.P., Blundo, C.M., Gurvich, D.E., Díaz, S., Cuevas, E., 2008. More than the sum of its parts? Assessing litter heterogeneity effects on the decomposition of litter mixtures through leaf chemistry. Plant and Soil 303, 151–159. doi:10.1007/s11104-007-9495-y

Henriksen, T., Brelan, 1999a. Evaluation of criteria for describing crop residue degradability in a model of carbon and nitrogen turnover in soil. Soil Biology and Biochemistry 31, 1135–1149. doi:10.1016/S0038-0717(99)00031-0

Henriksen, T.M., Breland, T.A., 1999b. Nitrogen availability effects on carbon

mineralization, fungal and bacterial growth, and enzyme activities during decomposition of wheat straw in soil. Soil Biology and Biochemistry 31, 1121–1134. doi:10.1016/S0038-0717(99)00030-9

Iqbal, A., Aslam, S., Alavoine, G., Benoit, P., Garnier, P., Recous, S., 2015. Rain regime and soil type affect the C and N dynamics in soil columns that are covered with mixed-species mulches. Plant and Soil 393, 319–334. doi:10.1007/s11104-015-2501-x

Iqbal, A., Garnier, P., Lashermes, G., Recous, S., 2014. A new equation to simulate the contact between soil and maize residues of different sizes during their decomposition. Biology and Fertility of Soils 50, 645–655. doi:10.1007/s00374-013-0876-5

Jung, J.Y., Lal, R., Ussiri, D.A.N., 2011. Changes in CO2, 13C abundance, inorganic nitrogen, β-glucosidase, and oxidative enzyme activities of soil during the decomposition of switchgrass root carbon as affected by inorganic nitrogen additions. Biology and Fertility of Soils 47, 801–813. doi:10.1007/s00374-011-0583-z

Justes, E., Mary, B., Nicolardot, B., 2009. Quantifying and modelling C and N mineralization kinetics of catch crop residues in soil: parameterization of the residue decomposition module of STICS model for mature and non mature residues. Plant and Soil 325, 171–185. doi:10.1007/s11104-009-9966-4

Keeney, D.R., Nelson, D.W., 1982. Nitrogen in organic forms. In: Page, A.L. (Ed.), Methods of Soil Analysis, Part 2. Agronomy Monograph, second ed. ASA and SSSA, Madison, WI, pp. 643-698.

Li, C., Frolking, S., Frolking, T.. A., 1992. A Model of Nitrous Oxide Evolution From Soil Driven by Rainfall Events: 1 . Model Structure and Sensitivity. Journal of Geophysical Research 97, 9759–9776.

Li, L.-J., Han, X.-Z., You, M.-Y., Yuan, Y.-R., Ding, X.-L., Qiao, Y.-F., 2013. Carbon and nitrogen mineralization patterns of two contrasting crop residues in a Mollisol: Effects of residue type and placement in soils. European Journal of Soil Biology 54, 1–6. doi:10.1016/j.ejsobi.2012.11.002

Li, Y., Wu, J., Liu, S., Shen, J., Huang, D., Su, Y., Wei, W., Syers, J.K., 2012. Is the C:N:P stoichiometry in soil and soil microbial biomass related to the landscape and land use in southern subtropical China? Global Biogeochemical Cycles 26, 1–14. doi:10.1029/2012GB004399

Liang, C., Amelung, W., Lehmann, J., Kästner, M., 2019. Quantitative assessment of microbial necromass contribution to soil organic matter. Global Change Biology 25, 3578–3590. doi:10.1111/gcb.14781

Liang, X., Yuan, J., Yang, E., Meng, J., 2017. Responses of soil organic carbon decomposition and microbial community to the addition of plant residues with different C:N ratio. European Journal of Soil Biology 82, 50–55. doi:10.1016/j.ejsobi.2017.08.005

Manzoni, S., Chakrawal, A., Spohn, M., Lindahl, B.D., 2021. Modeling Microbial Adaptations to Nutrient Limitation During Litter Decomposition. Frontiers in Forests and Global Change 4, 1–23. doi:10.3389/ffgc.2021.686945

Mary, B., Recous, S., Darwis, D., Robin, D., 1996. Interactions between decomposition of plant residues and nitrogen cycling in soil. Plant and Soil 181, 71–82. doi:10.1007/BF00011294

Molina, J.A.E., Clapp, C.E., Shaffer, M.J., Chichester, F.W., Larson, W.E., 1983. NCSOIL, A Model of Nitrogen and Carbon Transformations in Soil: Description, Calibration, and Behavior. Soil Science Society of America Journal 47, 85–91.

Mooshammer, M., Wanek, W., Zechmeister-boltenstern, S., Richter, A., 2014. Stoichiometric imbalances between terrestrial decomposer communities and their resources: mechanisms and implications of microbial adaptations to their resources. Frontiers in Microbiology 5, 1–10. doi:10.3389/fmicb.2014.00022

Mulvaney, M.J., Balkcom, K.S., Wood, C.W., Jordan, D., 2017. Peanut Residue Carbon and Nitrogen Mineralization under Simulated Conventional and Conservation Tillage. Agronomy Journal 109, 696–705. doi:10.2134/agronj2016.04.0190

Nicolardot, B., Bouziri, L., Bastian, F., Ranjard, L., 2007. A microcosm experiment to evaluate the influence of location and quality of plant residues on residue decomposition and genetic structure of soil microbial communities. Soil Biology and Biochemistry 39, 1631–1644. doi:10.1016/j.soilbio.2007.01.012

Nicolardot, B., Recous, S., Mary, B., 2001. Simulation of C and N mineralisation during crop residue decomposition: A simple dynamic model based on the C:N ratio of the residues. Plant and Soil 228, 83–103. doi:10.1023/A:1004813801728

Oliveira, M., Rebac, D., Coutinho, J., Ferreira, L., Trindade, H., 2020. Nitrogen mineralization of legume residues: interactions between species, temperature and placement in soil. Spanish Journal of Agricultural Research 18, 1–11. doi:10.5424/sjar/2020181-15174

Recous, S., Robin, D., Darwis, D., Mary, B., 1995. Soil inorganic N availability: Effect on maize residue decomposition. Soil Biology and Biochemistry 27, 1529–1538. doi:10.1016/0038-0717(95)00096-W

Redin, M., Guénon, R., Recous, S., Schmatz, R., Freitas, L.L. De, Aita, C., Giacomini, S.J., 2014a. Carbon mineralization in soil of roots from twenty crop species, as affected by their chemical composition and botanical family. Plant Soil 378, 205–214. doi:10.1007/s11104-013-2021-5

Redin, M., Recous, S., Aita, C., Dietrich, G., Caitan, A., Hytalo, W., Schmatz, R., Jos, S., 2014b. How the chemical composition and heterogeneity of crop residue mixtures decomposing at the soil surface affects C and N mineralization. Soil Biology & Biochemistry 78, 65–75. doi:10.1016/j.soilbio.2014.07.014

Sall, S., Bertrand, I., Chotte, J.L., Recous, S., 2007. Separate effects of the biochemical quality and N content of crop residues on C and N dynamics in soil. Biology and Fertility of Soils 43, 797–804. doi:10.1007/s00374-007-0169-y

Schomberg, H.H., Steiner, J.L., Unger, P.W., 1994. Decomposition and Nitrogen Dynamics of Crop Residues: Residue Quality and Water Effects. Soil Science Society of America Journal 58, 372–381. doi:10.2136/sssaj1994.03615995005800020019x

Sinsabaugh, R.L., Manzoni, S., Moorhead, D.L., Richter, A., 2013. Carbon use efficiency of microbial communities: stoichiometry, methodology and modelling. Ecology Letters 16, 930–939. doi:10.1111/ele.12113

Sukitprapanon, T.-S., Jantamenchai, M., Tulaphitak, D., Vityakon, P., 2020. Nutrient composition of diverse organic residues and their long-term effects on available nutrients

in a tropical sandy soil. Heliyon 6, e05601. doi:10.1016/j.heliyon.2020.e05601

Trinsoutrot, I., Recous, S., Bentz, B., Linères, M., Chèneby, D., Nicolardot, B., 2000. Biochemical Quality of Crop Residues and Carbon and Nitrogen Mineralization Kinetics under Nonlimiting Nitrogen Conditions. Soil Science Society of America Journal 64, 918–926. doi:10.2136/sssaj2000.643918x

Van Soest, P.J., 1963. Use of Detergents in the Analysis of Fibrous Feeds. I. Preparation of Fiber Residues of Low Nitrogen Content. J. Assoc. Off. Anal. Chem. 46, 825–835.

Wang, C., Wang, X., Pei, G., Xia, Z., Peng, B., Sun, L., Wang, J., Gao, D., Chen, S., Liu, D., Dai, W., Jiang, P., Fang, Y., Liang, C., Nanping, W., Bai, E., 2020. Stabilization of microbial residues in soil organic matter after two years of decomposition. Soil Biology and Biochemistry 141, 107687. doi:10.1016/j.soilbio.2019.107687

Wang, W.J., Baldock, J.A., Dalal, R.C., Moody, P.W., 2004. Decomposition dynamics of plant materials in relation to nitrogen availability and biochemistry determined by NMR and wet-chemical analysis. Soil Biology and Biochemistry 36, 2045–2058. doi:10.1016/j.soilbio.2004.05.023

Yansheng, C., Fengliang, Z., Zhongyi, Z., Tongbin, Z., Huayun, X., 2020. Biotic and abiotic nitrogen immobilization in soil incorporated with crop residue. Soil and Tillage Research 202, 104664. doi:10.1016/j.still.2020.104664

Zechmeister-Boltenstern, S., Keiblinger, K.M., Mooshammer, M., Peñuelas, J., Richter, A., Sardans, J., Wanek, W., 2015. The application of ecological stoichiometry to plant–microbial–soil organic matter transformations. Ecological Monographs 85, 133–155. doi:10.1890/14-0777.1

Figure captions

Fig. 1. Cumulative apparent mineralization of C (a, b) and N (c, d) during the decomposition of 10 crop residues in the soil. Crop residues were either incorporated (I) or left on the soil surface (S). The initial mineral N content was 9 mg N kg^{-1} dry soil (9 N) or 77 mg N kg^{-1} dry soil (77 N). These two factors resulted in 4 different treatments.

Fig. 2. Cumulative apparent C mineralization (a, b, c) and net N mineralization (d, e, f) and the relationship between N and C mineralization (g, h, i) for three crop residues (wheat, vetch, oilseed rape) in four treatments (I-77N, I-9N, S-77N, S-9N) during decomposition in soil at 25°C for 120 days. Bars represent the standard deviation values (n=3).

Fig. 3. Observed and simulated apparent C mineralization during the decomposition of wheat (a, b, c, d), vetch (e, f, g, h) and oilseed rape (i, j, k, l) residues incorporated or at the soil surface and with high or low initial soil mineral N content (77 or 9 mg N kg^{-1} dry soil) (symbols). Lines represent the values simulated with STICS default parameters

(dashed lines) and optimized parameters in *scenario 2* (solid lines). Bars represent the standard deviations (*n*=3).

Fig. 4. Observed and simulated apparent N mineralization during the decomposition of wheat (a, b, c, d), vetch (e, f, g, h) and oilseed rape (i, j, k, l) residues incorporated or at the soil surface and with high or low initial soil mineral N content (77 or 9 mg N kg^{-1} soil) (symbols). Lines represent the values simulated with STICS default parameters (dashed lines) and optimized parameters in *scenario 2* (solid lines). Bars represent the standard deviations (*n*=3).

Fig. 5. Model parameters *k* (day^{-1}), λ (day^{-1}), *h* and *CNbio* obtained by individual fitting procedures (scenario 2: *k, λ, h, CNbio* and *CNhum*) vs. total N availability (kg N t^{-1} added C) for the dataset of 40 incubations (10 residues, surface vs. incorporated and high vs. low N availability). Lines represent the nonlinear regression fit. The symbol ** indicates that the Pearson coefficient r is significant at the 1% level.

Figures

Figure 1.
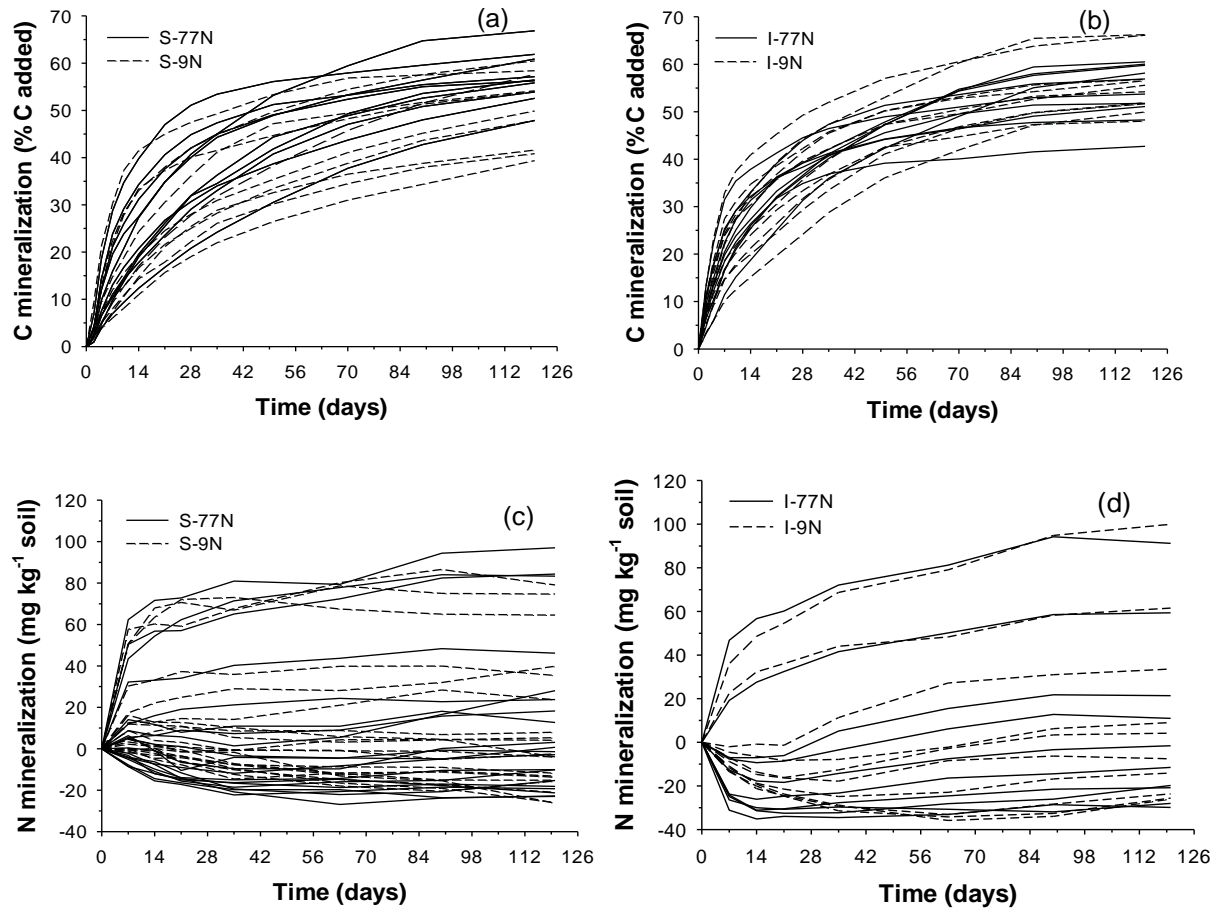
Figure 2.
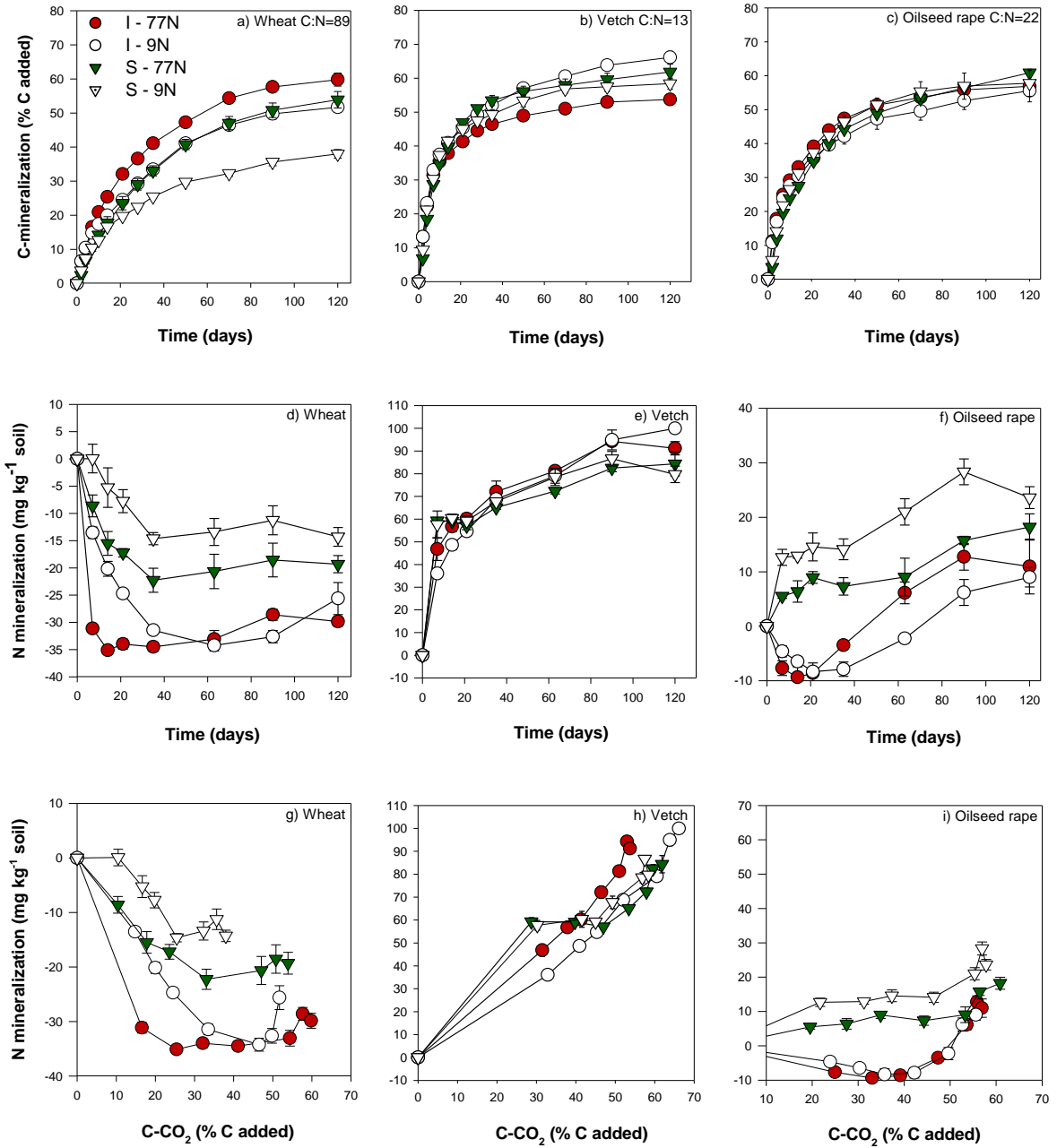
Figure 3.
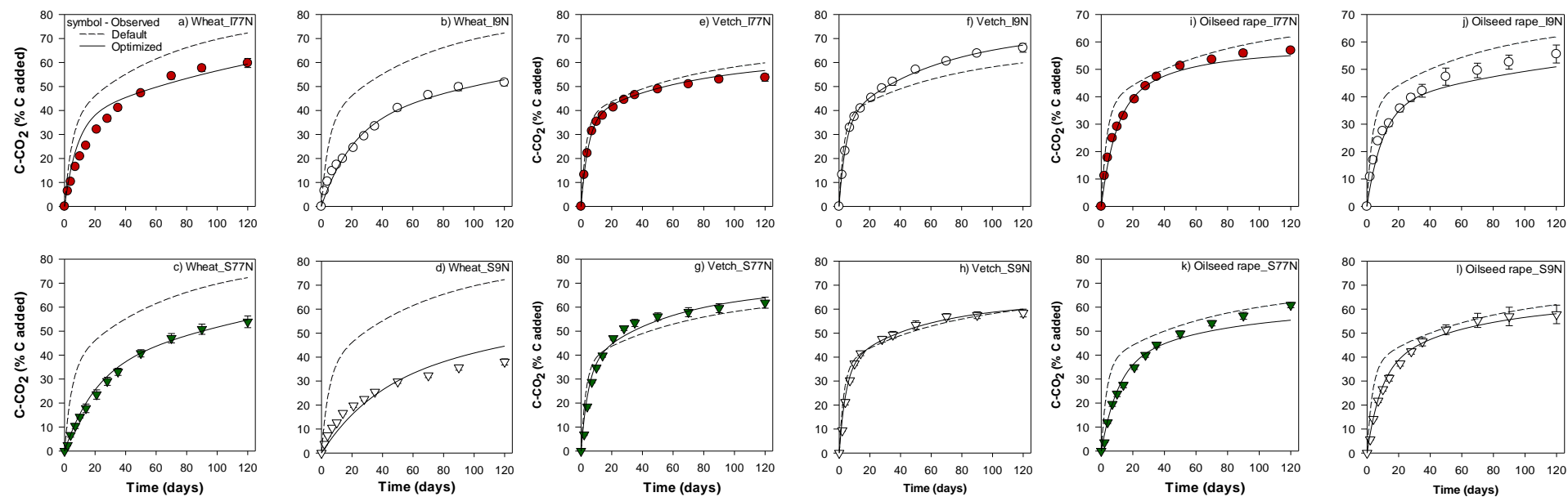
Figure 4.
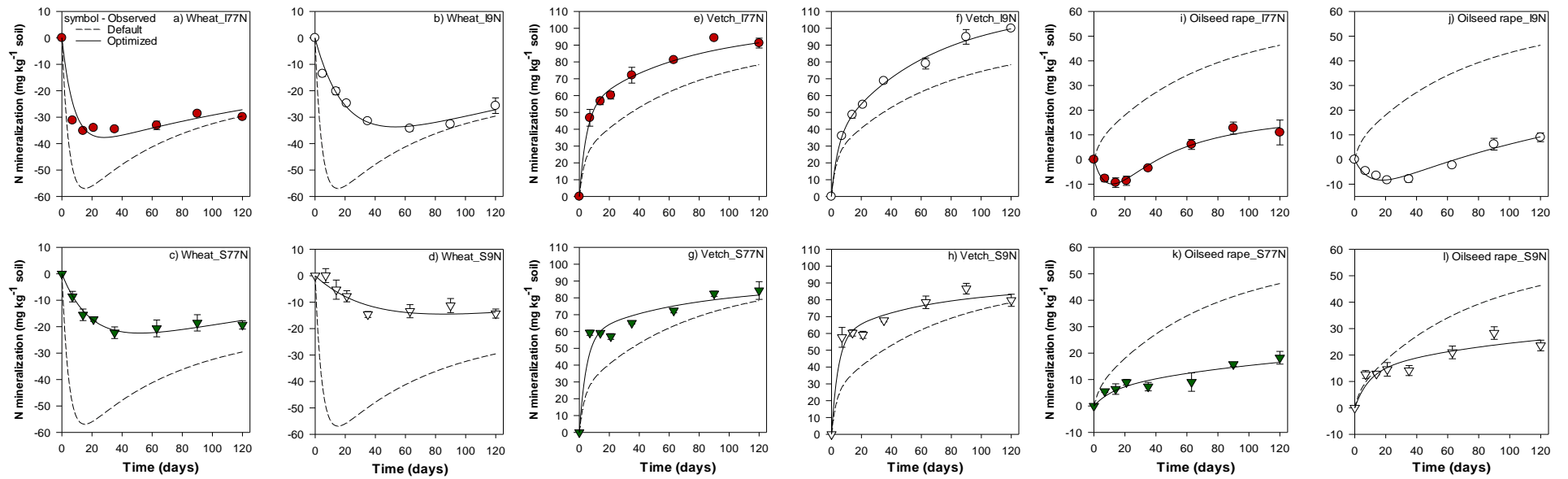
Figure 5.
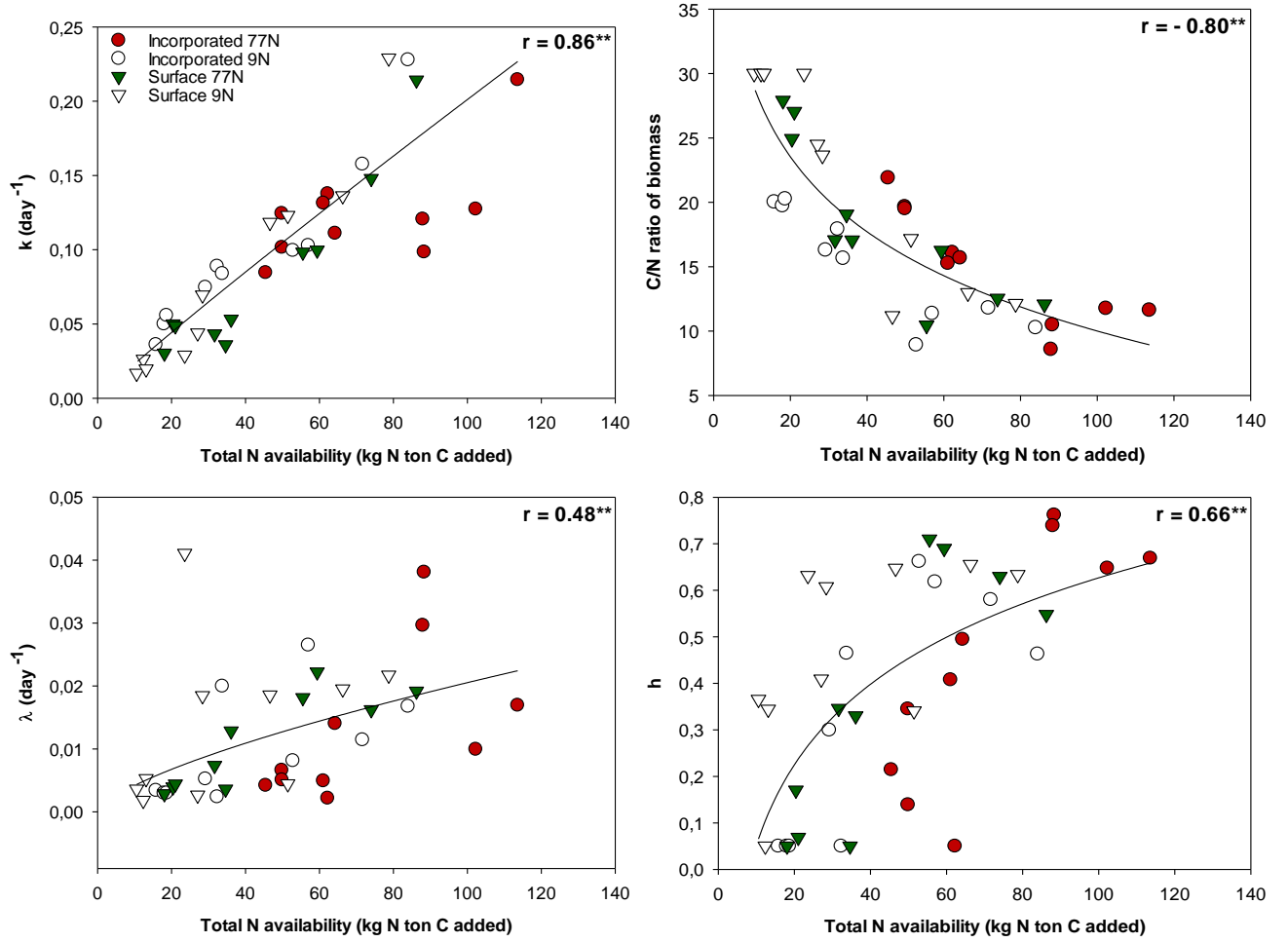
Tables

Table 1. Crop residues used, proportion of their leaves and stems in the mixture (% total of DM) and their initial chemical composition (g kg^{-1} DM).

Latin name	Common name	Agricultural use	% leaf[a]	% stem[a]	SOL[b]	HEM[b]	CEL[b]	LIG[b]	Total C[b]	Total N[b]	C:N ratio
Brassica napus oleifera	Oilseed rape	Main crop	28 ± 3.6	72 ± 2.8	394 ± 8.4	152 ± 4.1	359 ± 14.1	95 ± 2.5	421 ± 6.5	19.1 ± 2.3	22
Glycine max	Soybean	Main crop	38 ± 3.2	62 ± 2.1	349 ± 8.5	122 ± 3.4	386 ± 2.2	143 ± 1.4	450 ± 6.2	11.7 ± 3.4	38
Helianthus annuus	Sunflower	Main crop	39 ± 4.2	61 ± 5.1	322 ± 2.5	79 ± 3.7	485 ± 7.8	114 ± 0.5	428 ± 7.9	9.6 ± 2.8	45
Hordeum vulgare	Barley	Main crop	50 ± 3.3	50 ± 2.0	271 ± 3.5	260 ± 6.6	407 ± 8.7	62 ± 4.5	441 ± 0.7	5.3 ± 0.8	83
Triticum aestivum	Wheat	Main crop	42 ± 4.1	58 ± 3.3	326 ± 11.2	257 ± 10.2	356 ± 3.5	61 ± 6.3	437 ± 0.8	4.9 ± 4.5	89
Zea mays	Maize	Main crop	26 ± 3.6	74 ± 3.9	141 ± 6.3	323 ± 9.5	469 ± 10.1	67 ± 0.7	452 ± 2.4	4.3 ± 5.5	105
Avena strigosa	Black oat	Cover crop	48 ± 2.0	52 ± 2.7	290 ± 5.4	246 ± 8.2	417 ± 12.1	47 ± 0.3	447 ± 4.3	12.2 ± 4.3	37
Crotalaria spectabilis	Showy rattlebox	Cover crop	30 ± 3.1	70 ± 3.1	417 ± 2.6	90 ± 2.4	408 ± 8.9	85 ± 1.9	445 ± 5.1	22.4 ± 4.2	20
Stizolobium niveum	Gray mucuna	Cover crop	42 ± 3.6	58 ± 2.9	464 ± 7.9	119 ± 13.2	318 ± 6.6	99 ± 3.6	451 ± 3.3	29.4 ± 1.1	15
Vicia sativa	Vetch	Cover Crop	62 ± 1.8	38 ± 3.5	571 ± 3.9	88 ± 3.7	272 ± 2.3	69 ± 1.1	453 ± 1.6	35.2 ± 6.1	13

[a] Proportion of leaves and stems in the total dry matter of shoots determined at flowering for cover crops nad harvest main crops.

[b]SOL : Soluble fraction (Van Soest); HEM: Hemicellulose; CEL: Cellulose; LIG: Lignin; C: Total carbon; N: Total nitrogen; Csw: Water-soluble carbon; Nsw: Water-soluble nitrogen; C:N ratio is the ratio between Total C and Total N. Means (*n*=3) ± standard deviation (S.D.).

Table 2. Statistical analysis (RMSE) of default parameter values and of parameters after optimization using four scenarios with the STICS decomposition module.

Optimization Scenarios	Parameters optimized	RMSE (C)[a] % added C	RMSE (N)[a] mg N kg^{-1}soil
Default	-	13.05	18.81
1	*k, λ, CNbio* and *CNhum*	3.00	2.28
2	*k, λ, CNbio, CNhum and h*	2.40	2.00
3	*k, λ, CNbio, CNhum, h and Y*	2.03	1.83

[a]mean of the 40 incubations dataset.

Table S1. Observed percentage of residue C mineralization and kinetic coefficients calculated from a simple exponential decay function after 120 days at 25ºC incubation of crop residues in soil.

Species	Surface						Incorporated					
	9N			77N			9N			77N		
	C min[a]	C_0[b]	b[c]	C min	C_0	b	C min	C_0	b	C min	C_0	b
	%	%	day^{-1}	%	%	day^{-1}	%	%	day^{-1}	%	%	day^{-1}
Soybean	49.9 a	47.8	0.033	52.6 a	50.2	0.035	48.0 ab	46.5	0.051	42.7 b	40.7	0.078
Maize	39.4 c	41.1	0.022	47.9 b	54.3	0.017	50.0 b	53.1	0.023	58.2 a	60.0	0.026
Sunflower	57.7 a	60.7	0.022	56.5 a	58.8	0.026	54.2 a	53.6	0.045	51.8 a	50.6	0.056
Gray mucuna	60.5 a	56.0	0.059	57.2 a	54.3	0.069	56.6 a	51.8	0.084	51.1 b	45.9	0.094
Showy rattlebox	53.9 ab	49.2	0.072	56.3 a	53.8	0.059	56.8 a	53.6	0.066	48.3 b	45.8	0.085
Black oat	54.2 c	53.2	0.042	66.9 a	66.6	0.035	66.3 a	63.2	0.048	60.5 b	57.2	0.048
Vetch	58.4 bc	54.6	0.104	61.9 ab	58.4	0.085	66.2 a	59.4	0.092	53.7 c	49.4	0.126
Wheat	47.9 c	47.5	0.028	53.9 b	55.8	0.027	51.7 bc	51.4	0.034	59.8 a	58.6	0.038
Oilseed rape	57.8 a	55.0	0.068	60.9 a	57.1	0.046	55.6 a	50.4	0.070	56.9 a	53.8	0.073
Barley	41.6 c	41.8	0.032	55.9 ab	56.7	0.029	51.9 b	51.2	0.037	60.0 a	59.0	0.039
MSD[d]	7.2			5.0			5.1			5.7		

[a] The % of added C mineralized measured from residues plant after 120 days.
[b] Potentially mineralizable C pool.
[c] Mineralization constant rate.
[d] Minimum significant difference between crop residues for a given treatment according to Tukey test ($p < 0.05$).
C min values with different letters for a given crop residue are significantly different ($p < 0.05$) between treatments according to Tukey test.

Table S2. Parameters obtained by STICS parameters optimization in *scenario 4*, quality of fit (RMSE) and N availability estimated using 24% of total mineral soil N for surface residues.

Residue	Treatment	Total N availability (kg N ton C added)	k day^{-1}	λ day^{-1}	*CNbio*	*CNhum*	h	RMSE (C) % added C	RMSE (N) mg N kg^{-1}
Soybean	I	62.2	0.138	0.002	16.1	12.0	0.050	5.30	2.87
	I	32.3	0.089	0.002	17.9	12.0	0.050	2.44	2.14
	S	34.6	0.036	0.004	19.1	12.0	0.050	3.31	3.23
	S	27.0	0.044	0.003	23.8	8.0	0.409	1.11	2.07
Maize	I	45.5	0.085	0.004	21.9	12.0	0.214	5.27	3.89
	I	15.8	0.036	0.003	20.0	12.0	0.050	1.45	1.57
	S	18.1	0.030	0.003	27.9	12.0	0.050	1.83	1.66
	S	10.6	0.017	0.004	30.0	8.0	0.366	2.45	1.90
Sunflower	I	61.0	0.131	0.005	15.3	12.0	0.408	3.03	2.00
	I	29.2	0.075	0.005	16.3	9.8	0.300	2.04	0.72
	S	31.6	0.043	0.007	17.1	10.5	0.346	1.19	1.01
	S	23.5	0.029	0.041	30.0	12.0	0.632	2.26	1.38
Gray mucuna	I	102.3	0.127	0.010	11.8	12.0	0.648	1.81	1.74
	I	71.7	0.158	0.011	11.8	10.6	0.580	1.11	1.19
	S	74.0	0.148	0.016	12.5	8.4	0.630	2.17	3.42
	S	66.3	0.136	0.020	13.0	8.0	0.655	2.40	2.25
Showy rattlebox	I	88.3	0.098	0.038	10.5	12.0	0.762	3.64	1.29
	I	57.0	0.103	0.026	11.4	12.0	0.618	3.01	1.91
	S	59.4	0.100	0.022	16.2	11.2	0.690	0.87	0.76
	S	51.4	0.123	0.004	17.2	8.0	0.341	1.41	1.31
Black oat	I	64.2	0.111	0.014	15.7	12.0	0.495	2.65	0.86
	I	33.7	0.084	0.020	15.7	12.0	0.465	2.18	1.55
	S	36.1	0.053	0.013	17.1	8.0	0.330	3.55	1.01
	S	28.4	0.069	0.018	23.7	12.0	0.607	2.60	1.70
Vetch	I	113.6	0.214	0.017	11.6	12.0	0.669	1.10	3.08
	I	84.0	0.228	0.017	10.3	10.0	0.463	0.62	1.73
	S	86.2	0.214	0.019	12.1	8.3	0.548	2.81	5.54
	S	78.7	0.229	0.022	12.1	9.7	0.634	1.69	4.77
Wheat	I	49.8	0.124	0.007	19.7	12.0	0.345	4.59	3.09
	I	17.9	0.050	0.003	19.7	9.3	0.050	1.92	1.13
	S	20.4	0.050	0.004	24.9	12.0	0.170	1.42	1.20
	S	12.3	0.026	0.002	30.0	12.0	0.050	3.48	2.09
Oilseed rape	I	88.0	0.121	0.030	8.6	8.0	0.739	1.75	1.33
	I	52.8	0.100	0.008	8.9	8.0	0.662	3.21	1.32
	S	55.5	0.098	0.018	10.4	8.0	0.710	2.70	1.88
	S	46.6	0.118	0.019	11.2	8.0	0.647	1.48	2.75
Barley	I	49.8	0.102	0.005	19.5	12.0	0.139	3.14	1.89
	I	18.6	0.056	0.003	20.3	9.0	0.050	1.17	1.05
	S	21.0	0.049	0.004	27.0	12.0	0.069	1.14	1.62
	S	13.1	0.020	0.005	30.0	12.0	0.344	4.77	2.27

1 I and S are incorporated and surface residue, respectively.
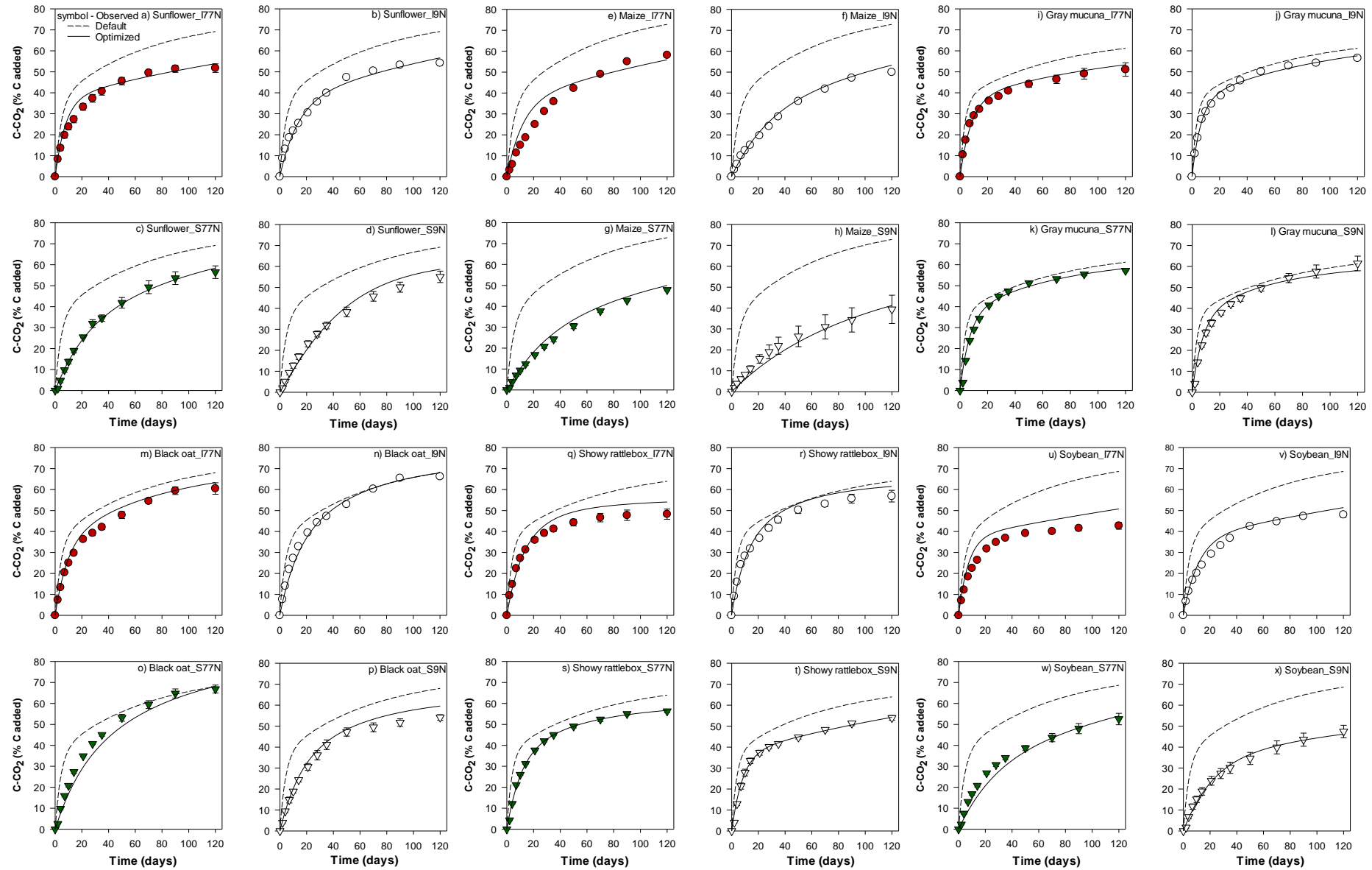
Fig. S1. Observed and simulated apparent mineralization of C during the decomposition of sunflower (a, b, c, d), maize (e, f, g, h), gray mucuna (i, j, k, l), black oat (m, n, o, p), showy rattlebox (q, r, s, t) and soybean (u, v, w, x) residues, incorporated or at soil surface and with high or low initial soil mineral N content (77 or 9 mg N kg^{-1} dry soil) (symbols). Lines represent the values simulated with STICS default parameters (dashed lines) and optimized parameters in *scenario 2* (solid lines). Bars are standard deviations (*n*=3).
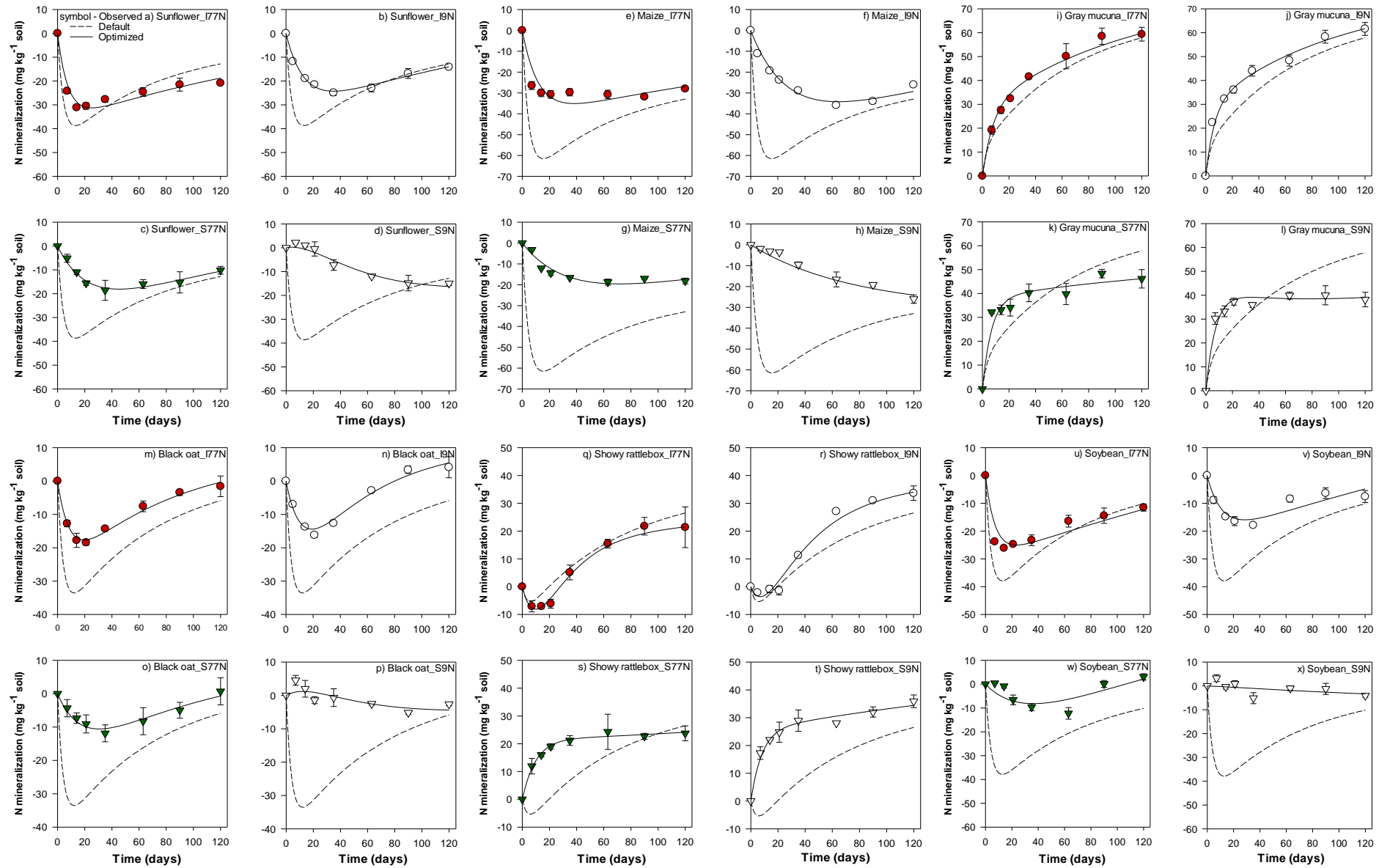
Fig. S2. Observed and simulated apparent mineralization of N during the decomposition of sunflower (a, b, c, d), maize (e, f, g, h), gray mucuna (i, j, k, l), black oat (m, n, o, p), showy rattlebox (q, r, s, t) and soybean (u, v, w, x) residues, incorporated or at soil surface and with high or low initial soil mineral N content (77 or 9 mg N kg^{-1} soil) (symbols). Lines represent the values simulated with STICS default parameters (dashed lines) and optimized parameters in *scenario 2* (solid lines). Bars are standard deviations (*n*=3).
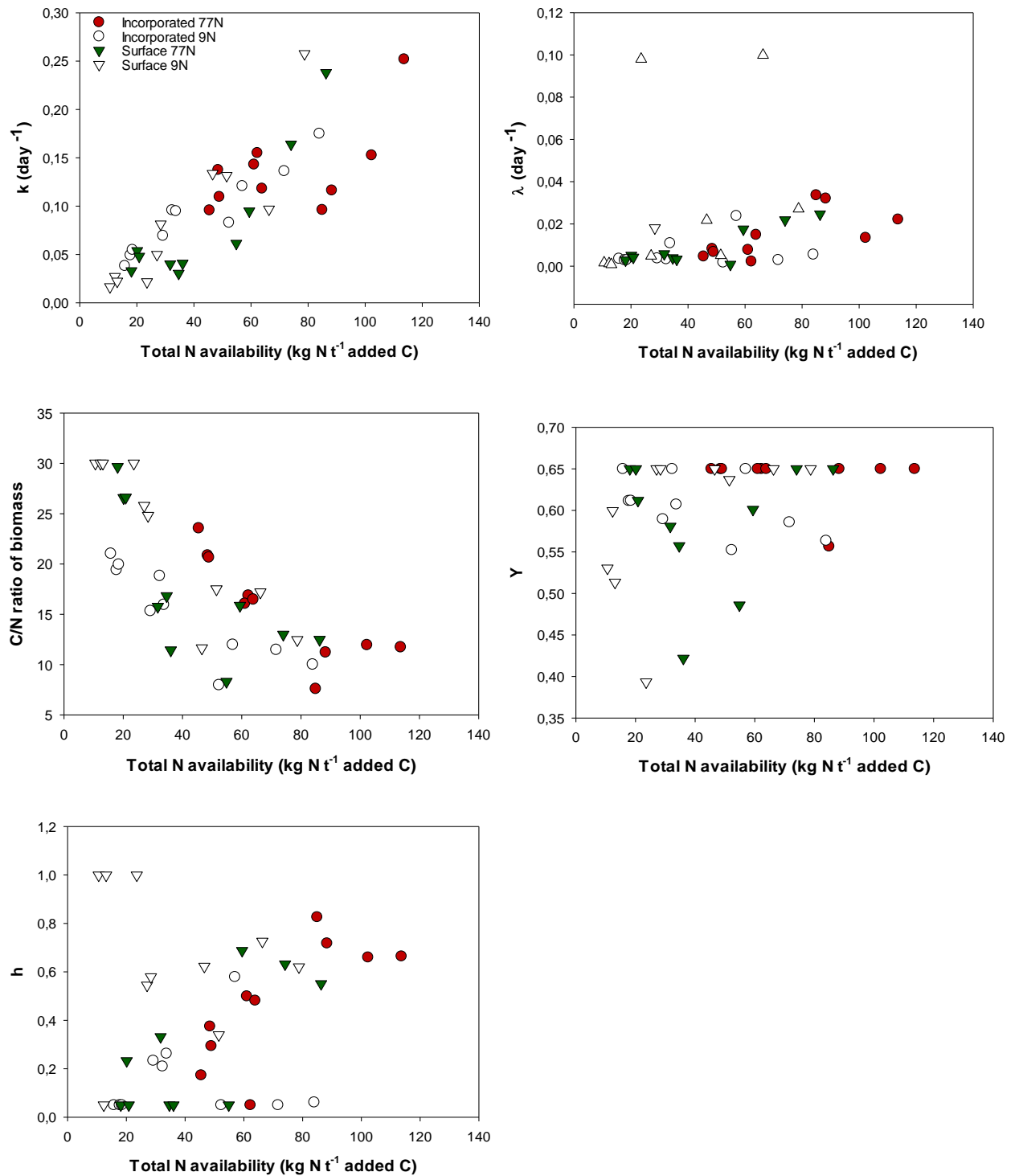
Fig. S3. Model parameters in *scenario 3*, *k* (day[-1]), λ (day[-1]), *CNbio*, *h* and *Y* obtained by individual fitting procedure, (*k, λ, CNbio, Y* and *h*) vs. total N availability (kg N t[-1] added C) for the dataset of 40 incubations (10 crops residues, surface vs. incorporated and high vs. low N availability).
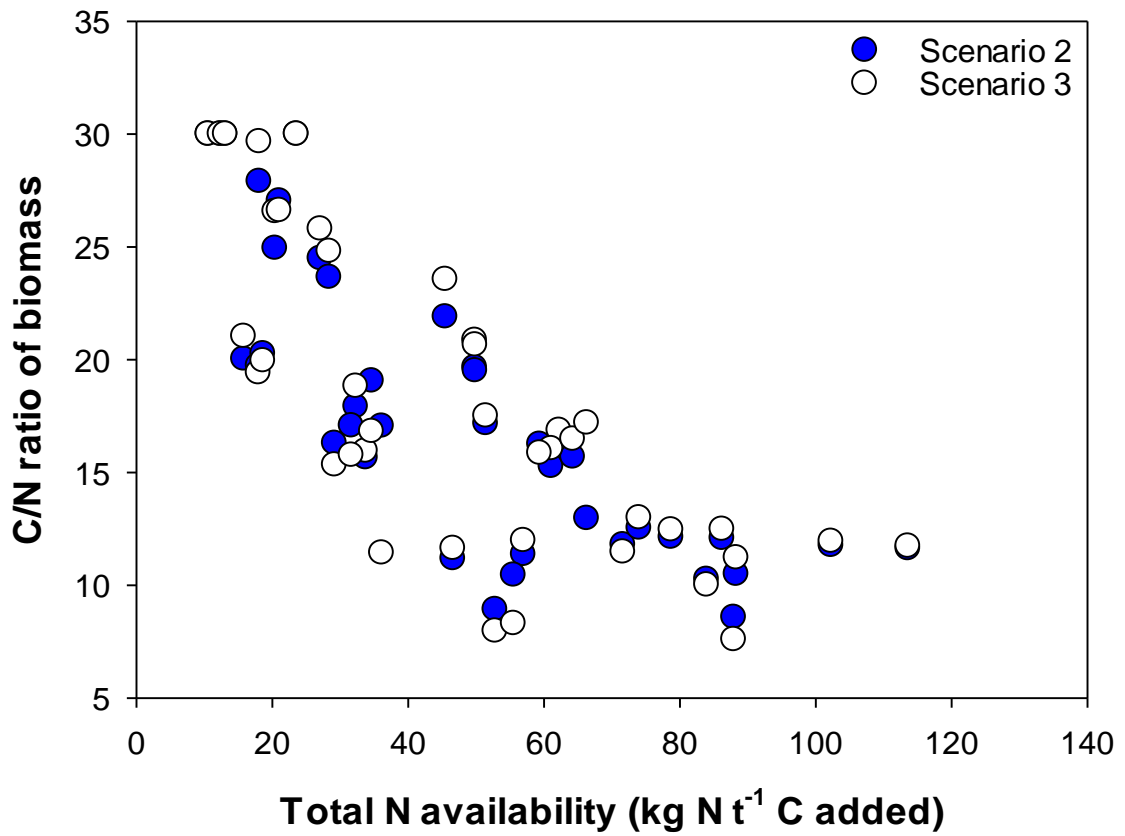
Fig. S4. *CNbio* values after optimization procedure for scenario 2 (*k, λ, CNbio, CNhum* and *h*) and scenario 3 (*k, λ, CNbio, CNhum, h* and *Y*) vs. total N availability (kg N t^{-1} added C) for the dataset of 40 incubations (surface vs. incorporated and high vs. low N availability).

3 ARTIGO II – MODELLING DECOMPOSITION AND NITROUS OXIDE EMISSIONS OF VETCH AND WHEAT MULCHES OF VARYING THICKNESS[2]

3.1 ABSTRACT

Mulch decomposition in no-tillage systems leads to changes in C and N dynamics and N_2O fluxes and its description is essential to reduce their negative impacts on agroecosystems. We test then improve the ability of the STICS model to simulate C and N dynamics and N_2O fluxes during mulch decomposition. We used a published dataset combining two residue with distinct chemical characteristics (vetch, *Vicia sativa* L., and wheat *Triticum aestivum* L.) and four rates of mulch addition (0, 3, 6 and 9 Mg DM ha^{-1}) decomposing over one year in agricultural and pedoclimatic conditions of southern Brazil. The mulch decomposition dynamic was improved when the whole mulch mass was considered decomposable, whatever the initial mass. This change resulted in a better fit for the remaining C in the mulch for both residues (vetch and wheat) and mulch mass evaluated (0, 3, 6 and 9 Mg DM ha^{-1}). However, for the mulch N dynamics, this adjusts resulted in improvements only for vetch residues, with N immobilization observed to wheat residues. N_2O emissions were improved, defining a new function to determine denitrification potential calculated according to the CO_2 emissions (one from soil humus and one from residue) as a proxy of easy C availability to decomposers. We also added the residue C:N ratio to better describe the differences between the vetch and wheat residues. With the use of this function, the model reproduced well the magnitude (called hot moments) and temporal variability for the two residues and four mass addition, mainly for vetch residues, with was observed large fluxes after residue addition. Additionally, the improvement of N_2O fluxes was made taking into account the effect of residue addition on N_2O precursors. The use of the new function to determine denitrification potential according CO_2 fluxes and residue C:N ratio need to be evaluated to verify its accuracy and possibility to use in different agrosystems and pedoclimatic conditions.

Key words: nitrous oxide emissions, STICS model, residue decomposition, mulch

3.2 INTRODUCTION

Conservation tillage has been largely adopted worldwide with influences on many agroecosystems services, increasing carbon (C) storage, soil moisture retention and nutrient cycling (Arcand et al., 2016; Kong and Six , 2010). These systems are recognized by their diversity of species used in crop rotation, inducing a large range in the amounts and nature (chemical composition) of crop residues left on the soil surface that form a mulch (Sithole et al., 2016). The presence of mulches can result in modifications of N_2O emitted due to changes in the variables that affect the main processes related to the production of this powerful greenhouse gas (GHG) in the soil (Fracetto et al., 2017; Pinheiro et al., 2019; Schmatz et al., 2020). However, the accurate estimate of N_2O emission remains problematic, due to its high temporal and spatial variability and difficulty for extrapolation over time, and the contribution of numerical models is essential (Hénault et al., 2005; Plazza-Bonilla et al., 2017). The accurate prediction of mulch C and N dynamics is also crucial to describe N_2O fluxes by agroecosystems models, where they control the availability of the main precursors of this process (Fracetto et al., 2017).

The N_2O emissions result of the nitrification and denitrification processes (Butterbach-Bahl et al., 2013; Mei et al., 2018), that are strongly affected by environmental conditions (temperature and humidity) and soil characteristics (NH_4 and NO_3 contents, pH, soil texture and soluble C) (Charles et al., 2017). The surface residues can affect directly N_2O emissions during their decomposition by increasing soil N and labile C availability to soil microbial biomass (Chen et al., 2013), and indirectly by regulate soil water status and temperature (Coppens et al., 2007). Particularly, denitrification occurs in anoxic conditions and respond by the higher N_2O emissions (Li et al., 2016), where easily available C plays an important role in fueling denitrification for short periods ('hot moments') (Surey et al., 2020). In general, simplified models determines the value of the denitrification potential according to C availability (soil property or computed from organic C dynamics) or the first-order decay rate constant (Heinen, 2006). However, a positive correlation between soil CO_2 and N_2O fluxes were observed in many studies after residue addition (Chen et al., 2013; Baggs et al., 2003; Schmatz et al., 2020), and suggest that the N_2O production can be related to the increase in the microbial activity stimulated by residue addition and its characteristics (amounts and chemical characteristics) (Schmatz et al., 2020).

Several models simulate explicitly the processes involving the mulch decomposition dynamics (STICS, Brisson et al., 2003; PASTIS, Findeling et al., 2007; APSIM, Thorburn et al., 2001). These models simulate mulch decomposition occurring in a decomposable layer in

contact with the soil, while a layer of overlying residues remaining non-decomposable. This formalization was developed based on studies that observed a reduction of decomposition with increasing mulch mass (Steiner et al., 1999; Stott et al., 1990). Recently studies have proposed a different approach of mulch decomposition, where the mulch decomposition is proportional to the initial mass of residue (Acosta et al., 2014; Dietrich et al., 2017; Dietrich et al., 2019; Halde and Entz, 2016; Williams et al., 2018), i.e., the decomposition rate (*k)* was not affected by the residue mass added. Dietrich et al. (2019) showed that decomposition was faster in the mulch layer at the soil-residue interface than in mulch top layers, a decomposition gradient related to a vertical gradient of moisture within the mulch (Dietrich et al., 2019). However, these recent findings on mulch decomposition are not yet integrated into models and need to be further evaluated to simulate mulch decomposition dynamics accurately.

STICS is a soil-crop dynamic model characterized by genericity, robustness and operationality that integrates and simulate mulch decomposition dynamics and N_2O emissions. STICS has been proved able to simulate crop production, N and water dynamics in a large range of situations (Coucheney et al., 2015; Sierra et al., 2010). However, STICS has been rarely tested for its ability to simulate mulch decomposition in fields (Beaudoin et al., 2008) and its ability to predict N_2O emission in no-tilled system (Plaza-Bonilla et al., 2018). Therefore, the aim of this study was to test then improve the ability of the STICS model to simulate C and N dynamics during mulch decomposition and the CO_2 and N_2O emitted. For this, we used a published dataset combining two residue (vetch and wheat.) with distinct chemical characteristics and four rates of mulch addition (0, 3, 6 and 9 Mg DM ha^{-1}) decomposing over one year in agricultural and pedoclimatic conditions of southern Brazil. In the present study we i) evaluated and improved the STICS model ability to simulate the decomposition and N_2O fluxes of crop residues left at the soil surface; ii) evaluated the actual mulch two-layer module performance for prediction of the decomposition of mulches of increasing thickness; ii) hypothesized and tested the use of CO_2 fluxes as a proxy of C availability determining denitrification potential and subsequent variations in the N_2O emissions.

3.3 MATERIALS AND METHODS

3.3.1 STICS model description

STICS (Simulateur mulTIdisciplinaire pour les Cultures Standard) is a daily time-step soil-crop dynamic model that simulates C, N and water cycles. The upper boundary of the system is the atmosphere, characterized by standard weather variables (radiation, temperature, rainfall,

reference evapotranspiration, wind and humidity) and the lower boundary result of the soil/sub soil interface. The soil is described as a sequence of horizontal layers, each one characterized in terms of its water content, mineral and organic N contents (Brisson et al., 2003). In this study, we focused on describe the decomposition dynamics of two residues with distinct chemical composition (C:N ratio of 12 vs. 83) and mass added on soil surface (3, 6 and 9 Mg DM ha^{-1}) and the associated N_2O emissions.

The main formalism of interest were focusing on the residue decomposition and N_2O modules, which does not imply the need for a crop component in the model. However, the possibility of use the proposed formalisms in real situations makes the choice of the STICS model coherent, which has been widely evaluated to describe crop development (Coucheney et al, 2015). In STICS, residue decomposition dynamics are simulated using a simple dynamic model, where the rate of residue decomposition (DCRES, in kg C ha^{-1} day^{-1}) follow first-order kinetics against the amount of decomposable C (CRES) and depends on their nature (KRES), on soil temperature (FTH), water content (FH) and the available nitrogen in the vicinity of residues (FN). The model described by Nicolardot et al. (2001) present three organic compartments: the crop residues (*R*), the decomposer microbial biomass (*B*) and the humified organic matter (*H*). The C and N fluxes are governed for seven parameters: two rate parameters (*k* and *λ*), two partitioning coefficients (*Y* and *h*) and three C:N ratios (crop residue (*CNres*), microbial biomass (*CNbio*) and the newly formed humified organic matter (*CNhum*)). Except the C:N ratio of residues, the default values are obtained from hyperbolic relationships according to the *CNres*: decomposition rate constant of the residues (*k*), the biomass C:N ratio (*CNbio*) and humification rate (*h*); or were fixed values: decay rate of microbial biomass (*λ*) and the assimilation yield of residue-C by the microbial biomass (*Y*). The model simulates plant mulch decomposition according a double compartment model in a similar way to APSIM-residue (Thorburn et al., 2001).

3.3.1.1 Mulch submodule

The STICS model (v6.9 and later) simulates mulch decomposition (C and N balance) and the physical modifications in the soil surface (water balance) in the presence of surface residues (QMULCH). Mulch presence results in modifications of soil temperature and humidity induced for a physical effect that modify soil evaporation by a physical barrier to convective and diffusive fluxes between the soil and atmosphere. Mulch intercept rainwater and stores it, and the water that is not intercepted is transmitted to the soil. As described in the PASTIS model (Findeling et al., 2007), the decomposition of the mulch is assumed to occur according to one

two layers function/model through the inclusion of a contact factor, as shown in the conceptual diagram of mulch decomposition (Fig. 1). One of the layer is in contact with the soil, defined as the decomposable part, and a non-decomposable layer, located above. When the first layer in contact with the soil is decomposed, the second layer located above replenish it from the non-decomposable part regulated by an empirical factor. The decomposable layer of the mulch (*qmulchdec*) is defined in Mg DM ha^{-1} and varies with the type of the mulch simulated (entire plant, fresh or decomposed, stalks). The default value of *qmulchdec* at the model is 1 Mg DM ha^{-1}. The decomposition submodule, as described above simulates the decomposition of the mulch layer in contact with the soil. The decomposition parameters used in mulch residues are different from those used in decomposition parameters of the mixed residues, which decomposition rates (*k*) per unit mass of residue lower with larger initial residue masses, resulting of the inaccessibility of the soil microorganisms to upper mulch layers and its drier conditions. During decomposition, a limited topsoil layer is assumed to contribute to the mulch decomposition according to the influence of the zymogenous biomass, restricted by the maximum length of the fungal hyphae.

3.3.1.2 *Nitrous oxide emissions submodule*

The STICS model simulates nitrification, denitrification and the associated N$_2$O emissions, represented as a fixed or variable proportion from these processes. The nitrification process is assumed to occur in the biologically active soil layer (*profhum*), described as a first order process resulted of one potential rate according NH$_4^+$ fraction available nitrified in one day (*fnx*) with default value of 0.80, and regulation factors: availability of substrate (NH$_4^+$) and environmental conditions (soil temperature, soil water content and soil pH). The temperature effect is described for a linear model, increasing until an optimum rate of 30°C (*tnitopt*) and then decreasing (*tnitopt2*). The water filled pore space (WFPS) has a double effect in the nitrification process, where nitrification increases elevating soil water content until field capacity is reached, then decreases when the oxygen extinction lead to a non-favorable nitrification condition. The effect of the pH in the nitrification is linear between the pH minimal (*pHminnit* = 4.0) and the pH maximal (*pHmaxnit* = 7.2) for nitrification, where the nitrification is maximal. The proportion of nitrified N emitted as N$_2$O if constant is 0.16% (*rationit*), however, the default option in STICS the fraction of the N nitrified emitted as N$_2$O varies according to soil WFPS.

Denitrification results of a potential rate (*vpotdenit*) and the relating factors: availability of nitrate (NO$_3^-$), and environmental conditions (temperature and soil water filled pore space).

The *vpotdenit* is expressed as a constant potential defined in kg N ha^{-1} day^{-1} over the depth *profdenit* (20 cm), which a value of 2.0 kg N ha^{-1}day^{-1} in the default parametrization of STICS model. The denitrification rate increases with nitrate concentration (*fNO3*) and is described by a Michaelis-Menten function. The temperature (*f$_T$*) is represented by a Gaussian function and increase the process until the optimum rate at 47 °C. In view of the fact that denitrification is an anaerobic process, soil water content is very important, as described in the model proposed by Hénault et al. (2005), denitrification starts when the WFPS reaches 0.62 (*wfpsc*) by default value, and increase exponentially with the WFPS. The soil pH has an effect on the potential of reduction of N$_2$O to N$_2$ (*pHminden and pHmaxden*).

3.3.2 Field dataset

The experimental dataset used in this work were obtained and published by Schmatz et al. (2020). The main properties of the present dataset are the field experiment condition that is a proximal of the real conditions and support its future application. Additionally, the fact that were no plant growing during the experimental evaluations avoid the necessity of describe complexes processes related to N availability and water dynamics and allows to cover a large range of mulch thickness and two contrasted C:N ratio residues. Briefly, the field experiment was carried out at the Federal University of Santa Maria (29°42'54" S, 53°42'23" W), state of Rio Grande do Sul, Brazil. The site has an elevation of 90 m, a mean annual rainfall of 1660 mm and a mean annual air temperature of 19.3 °C. The climate is classified as humid subtropical (type Cfa2 in Köppen's classification). The soil is classified as Typic Paleudalf (Soil Survey Staff, 2010) with 110 g kg^{-1} clay, 260 g kg^{-1} silt and 630 g kg^{-1} sand in the 0-10 cm layer. The study comprised the evaluation over a year (November 2016 to November 2017) of the decomposition of two crop residues having a contrasted chemical quality (both the C:N ratio and the biochemical composition) of vetch (*Vicia sativa* L., C:N = 12) and wheat (*Triticum aestivum* L., C:N = 83) added on soil surface with no plant growing. The treatments were composed of a control treatment (no residue addition) and the two residues added on soil surface (vetch and wheat) with three different mulch masses (3, 6 and 9 Mg DM applied per ha), resulting in six treatments plus one control (bare soil). Vetch shoots were cut at flowering time and wheat residues were collected at crop maturity and cut into 20 cm (vetch) and 5-20 cm in length (wheat) before the start of the study. The detailed description of the study can be found in Schmatz et al., 2020.

Soil water content (SWC) was measured using FDR (frequency domain reflectometry) sensors placed into two soil profile depths, at 2.5 cm (0-5 cm) and 7.5 cm (5-10 cm), and the

readings were recovered each every 10 min. Soil temperature (°C) was measured with T-type sensors installed at the same soil depth and time reading describe for SWC sensors. Inorganic N content (NH_4^+ and NO_3^-) were extracted from the 0 to 10 cm soil layer and quantified using an automated colorimeter (SAN plus, Skalar, Breda, Netherlands). The decomposition of the mulch was assessed using open wooden frames (40 cm length, 40 cm width and 8 cm height) with an equivalent crop residue DM added in each litter box of 3, 6 and 9 Mg DM ha^{-1}. Residue matter was collected ten times during the one-year experimental period and analyzed by destructive sampling of the wooden frames. The total C and total N in the residue were measured using an elemental analyzer (Flash EA 1112; Thermo Electron Corporation, Milan, Italy). N_2O and CO_2 fluxes were measured using insulated, fan-mixed, non-flow-through, non-steady-state chambers (Rochette and Bertrant, 2008) from 26 November 2016 to 21 November 2017 during 62 air-sampling events and analyzed using gas chromatography (GC-2014, Shimadzu Corp., Kyoto, Japan). The kinetics of mulch decomposition and the gas emissions have been discussed by Schmatz et al. (2020).

3.3.3 Input data and STICS model calibration using bare soil

The inputs required by the STICS model concerns crop management and climate variables. The climate data (radiation, temperature, rainfall, reference evapotranspiration, wind and humidity) were obtained from an automatic meteorological station located 1.6 km away from the experimental site. The soil characteristics required to STICS simulated processes (bulk density, initial soil organic carbon, soil C:N ratio, soil water contents at field capacity and wilting point) were measured values of soil collect in 2016 (Schmatz et al., 2020). The characteristics of the soil and the experimental study used in the STICS model are shown in the Table 1. The model (STICS version 9.1) was not previously calibrated for the present study site. To the calibration of the model, initially the control treatment (bare soil) was used to describe the variables: soil water content, soil temperature, soil mineral N, soil organic matter (using mineral N and CO_2 emissions) mineralization and N_2O emissions in conditions of no residue addition. The calibration step aimed to describe these variables accurately as possible before describing the different mulches treatments.

3.3.4 Steps of simulations with the mulch

3.3.4.1 *Standard parameters of decomposition*

Using the parameters obtained at calibration step using bare soil data (control treatment), the default parameterization of the STICS mulch submodule decomposition (*qmulchdec* = 1 Mg DM ha^{-1}) and the actual formalism of N$_2$O emissions (*vpotdenit* = 0.1) were tested against two contrasting quality residues (C:N ratio of 12 *vs.* 83) and mulch thickness (3, 6 and 9 Mg DM ha^{-1}). The test and evaluation give access to interpret model performance and provide improvements to describe decomposition and N$_2$O emissions of distinct mulch thickness and residue quality.

3.3.4.2 *Adjusting decomposition parameters*

In STICS, the proportion of the mulch in contact of the soil passible of decomposition is 1 Mg DM ha^{-1} (*qmulchdec*) at default parameterization. To improve mulch decomposition performance, our hypothesis was based in recent studies that have been describing mulch decomposition as proportional to the initial residue mass added on soil surface. To represent these proportional mulch decomposition dynamics observed with distinct residue addition on soil surface, the parameter *qmulchdec* were tested with increasing values (3, 6, 9 and >9 Mg DM ha^{-1}), which aim to represent the proportional mulch decomposition with residue increasing mass addition. At this step, the improvement were made keeping the formalism of N$_2$O emissions to verify the effect of the improvements of C and N mulch dynamics on the simulated N$_2$O fluxes.

3.3.4.3 *Introducing a new denitrification potential varying according to carbon availability*

The main hypothesis of the present work is that denitrification should not be considered as a constant, but should depend on how easily C is available to denitrifiers. Initially, the STICS model was tested for different residue quality and quantity for the study conditions with no adjustments on the model patterns related to the model subroutine of N$_2$O emissions, keeping the previous calibration to bare soil (control treatment) and the improvement of the mulch decomposition dynamics. At this step, the denitrification potential rate (*vpodenit*) was calculated as a constant rate. The test and improvement of the N$_2$O emissions were made assuming that CO$_2$ emissions from decomposition (the one from the humus and/or the one from residue) could be considered as a good proxy of C availability. Since there is no variable in STICS, which corresponds exactly to C availability.

The denitrification potential proposition tested resulted of the sum of the one of the bare soil and a component proportional to the CO$_2$ emissions of the decomposing residues, and that the coefficient of proportionality is also proportional to the N:C ratio of the residue to take into

account the variation in the chemical characteristics of residues. The denitrification potential was described as:

$$Dp = a\ CO2_{soil} + b\ CO2_{residue}\ N{:}C\_residue$$

where *Dp* represent the denitrification potential (kg ha⁻¹cm⁻¹day⁻¹); *CO2soil* is the CO_2 flux from soil (kg ha⁻¹day⁻¹) and *CO2soil* from residue decomposition (kg ha⁻¹day⁻¹); *N:C_residue* represent the N:C ratio of the decomposing residue; *a* and *b* are constant values (a = 25e-5 cm⁻¹ and b = 0.075 cm⁻¹). These hypotheses were incorporated into their respective submodules and evaluate against the same treatments to verify the model performance. For both calibration and improvement steps, the method consisted in minimizing the sum of squared errors between the observed and simulated values.

3.3.5 Evaluation of STICS model performance

The evaluation of the accuracy and model performance against the measured data was assessed using five statistical criteria demonstrated by Smith et al. (1997): the root mean square error (*RMSE*), relative error (*E%*), the mean difference (*M*), sample correlation coefficient (*r*) and the *t* statistic to verify significant differences between observed and simulated values in *M*. The equations are calculated as:

$$RMSE = \sqrt{\frac{1}{n}\sum_{i=1}^{n}(Si - Oi)^2}$$

$$E(\%) = \frac{100}{n}\sum_{i=1}^{n}\frac{(Oi - Si)^2}{Oi}$$

$$M = \sum_{i=1}^{n}\frac{(Oi - Si)}{n}$$

$$r = \frac{\sum_{i=1}^{n}(Oi - \bar{O})(Si - \dot{S})}{\sqrt{[\sum_{i-1}^{n}(Oi - \bar{O})^2]\ [\sum_{i-1}^{n}(Si - \dot{S})^2]}}$$

$$t = \frac{M \; x \; \sqrt{n}}{\sqrt{\sum_{i=1}^{n}(Oi - Si) - (\sum_{i=1}^{n}(Oi - Si))^2/(n - 1)}}$$

where n represent the number of observations, Si and Oi are the simulated and observed values, respectively; $\bar{O}$ is the mean values of observed data and $\dot{S}$ is the mean of simulated values. *RMSE* provides the total difference between the simulated and measured data. The relative error (*E%)* determine the bias in the total difference between simulations and measurements. The nature of the bias is evaluated using the mean difference (*M*) between measured and simulated values. Mean difference gives an indication of the bias in the simulation, but errors are not proportioned to the size of measurements. Correlation coefficient (*r*) is used to assess how well the shape of simulation follow the same pattern as observed values. The *t* statistic is used to show a significance difference of simulated vs. measured values in *M*.

3.4 RESULTS

3.4.1 STICS model calibration on control soil

The calibration of the STICS model was made using the control treatment to reproduce the study observed variables: SWC, temperature and soil mineral N, and CO_2 and N_2O emissions. Statistics of the model calibration with the control treatment are given in Table 2. Initially, soil water dynamics were not well simulated, with in particular a strong drying of the soil to very low values (data not show). The estimation of the residual content from soil clay content was changed according Dexter et al. (2012). With this change, the model prediction of the SWC was satisfactory, with no differences between the predicted and observed soil water content. The correlation coefficients for the measured vs. predicted values were 0.72 and 0.55 for 0-5 and 5-10 cm layers, respectively. Despite the significant correlation found, the primary differences between the patterns of measured and predicted soil water contents appeared following rainfall events, where the soil water content exceeded the soil field capacity (Fig. 2a). However, generally speaking, the model overestimated the soil water contents by 5.2 % and 3.3 % for 0-5 and 5-10 cm soil layer, respectively. The model also simulated well the soil temperature for the 0-5 cm (r = 0.83; RMSE = 2.52; E(%) = 7.2 and M = 1.67) and 5-10 cm (r = 0.76; RMSE = 2.61; E(%) = 6.85 and M = 1.59) layers. In conditions of high temperature, the

model tended to underestimate the values, a pattern observed for both soil layers (0-5 and 5-10 cm) (Fig. 2c, d).

Soil NH_4^+-N was not well simulated after STICS model calibration (Fig. 2e). The correlation between measured and predicted values was not significant (r = -0.31) and STICS underestimated it (E(%) = 28.0 and M = 1.86). Soil NO_3^--N was fairly well simulated throughout the year, as shown by a significant correlation coefficient between measured vs. predicted values (r = 0.66) (Table 2). However the model failed at predicting the high NO_3^--N content observed in the 0-10cm soil layer at the beginning of the study (Fig. 2f), and on average the model overestimated NO_3^--N contents by 10.0% (Table 2).

Observed and simulated daily CO_2 emissions agreed well for most of the experimental period (Fig 2h). The potential mineralization rates (*gmin1*) was increased from 0.0007 to 0.0020, to better simulate the CO_2 outputs. The simulated total CO_2 emission was 2.08 Mg C ha^{-1} compared with the measured total CO_2 of 2.41 Mg C ha^{-1}. Daily measured and simulated N_2O emissions are shown in the Fig. 2g. The denitrification potential was also strongly reduced (*vpodenit* from 2 to 0.1) so that N_2O emissions in order of magnitude were correct on the bare soil treatment. The correlation between predicted and measured emissions was significant (r = 0.31). For this treatment, the sampling period did not present peaks of N_2O emission, and the measured N_2O were simulated with a reasonable agreement of measured data (Fig. 2g). The predicted and observed cumulative N_2O-N fluxes were 0.87 and 0.59 kg N ha^{-1}, respectively.

3.4.2 Mulch simulations

3.4.2.1 *Default parameterization of mulch decomposition module*

Using the soil-calibrated parameters obtained in the previously step, STICS systematically overestimated the mulch remaining C for increasing mulch mass using this actual mulch decomposition parameterization (Fig. 3). This pattern was observed especially for wheat residues and was lower for vetch residues. The mulch N dynamics followed the same pattern than for mulch C. For all treatments, the model overestimated the N content in the remaining residues, and this was particularly true for the wheat residues (Fig. 4).

3.4.2.2 *Mulch decomposition module improvements*

To improve simulated mulch decomposition dynamics, the rate of decomposition was increased (*bkres* from ~0.41/CN to 0.70/CN) and the parameter *qmulchdec* was systematically raise to verify the model decomposition performance to residue added treatments. The best prediction

of observed values were found when all mulch was considerable decomposable for the three mulch mass evaluated (*qmulchdec* $\geq$ 9 Mg DM ha^{-1}). With these changes, STICS model reproduced satisfactory the C dynamics for all treatments (wheat and vetch at 3, 6 and 9 Mg ha^{-1}) (Fig. 3). The correlation between observed and predicted values was significant for the six treatments evaluated (Table 3).

The use of no limiting decomposable mulch (*qmulchdec* $\geq$ 9 Mg DM ha^{-1}) resulted in improvements of remaining N mulch content only for vetch residues with the three mulch mass treatments (3, 6 and 9 Mg DM ha^{-1}) (Fig. 4a, c, e). The simulated values were reduced and close to observed values of N present in the remaining mulch with a significant correlation (0.89, 0.91 and 0.93 to vetch_3, vetch_6 and vetch_9 treatments, respectively (Table 3). For wheat residues, the change in the mulch decomposable layer resulted in a strong N immobilization, with high N content in the mulch after residue addition, and a strong decrease along the study (Fig.4b, d, f). The correlation between predicted and observed values were not significant to wheat residues treatments (Table 3).

With the mulch module adjustments, the patterns of the CO_2 fluxes from all treatments were well captured and generally in agreement for most of the measured period, with a progressive increase due to the contribution of residue (Supplementary Fig. S3). The model reproduced the increase of the CO_2 fluxes after residue addition and showed a significant correlation between the measured and predicted emissions for all treatments, except Vetch_6 and Vetch_9 (Table 3). However, the model overestimated the cumulative C-CO_2 flux by an average of 19.5% for wheat residue treatments (3, 6 and 9 Mg DM ha^{-1}) (Table 3). For the vetch treatments, STICS predicted cumulative C-CO_2 fluxes were 2.88, 3.75 and 4.60 compared with the observed fluxes of 3.07, 3.75 and 4.84 to 3, 6 and 9 Mg DM ha^{-1} treatments. For the wheat residues, STICS predicted cumulative C-CO_2 fluxes of 3.20, 4.25 and 5.42 Mg C-CO_2 emitted compared with the observed fluxes of 3.13, 3.33 and 3.70 to 3, 6 and 9 Mg DM ha^{-1} residue added (Supplementary Table S2).

The SWC were well simulated by the STICS model in conditions of different residue quality after the mulch decomposition improvement, reproducing reasonably the trend of higher soil moisture for wheat than vetch residues (Supplementary Table S1). As observed at calibration step, differences between measured and predicted soil water contents appeared after rainfall events, where the soil water content exceed the soil field capacity. These differences are particularly stronger for wheat residues with high residue mass addition (3<6<9 Mg DM ha^{-1}). The temperature variation was satisfactory reproduced for all treatments by STICS (Supplementary Table S1).

Predicted soil NH_4^+-N was overestimated for vetch residues and underestimated for wheat residues (Supplementary Fig. S1 and Table 3). STICS model did not reproduced well NH_4^+-N, as previously observed in calibration step with bare soil (Supplementary Fig. S1). Soil NO_3^--N contents were well reproduced by the model with significant correlation only for vetch residues (Table 3). For these treatments, STICS predicted the NO_3^--N increase observed particularly after residue addition (Supplementary Fig. S2). The wheat residues showed a lower non-significant correlation between predicted and measure data (Table 3).

3.4.3 Changes to the denitrification module

Predicted and measured daily N_2O emissions are shown in Fig. 5. Initially, the simulations were carried out using the constant denitrification potential obtained at calibration step with bare soil (*vpodenit* = 0.1) and keeping the initial formalisms of the model to describe mulch decomposition (double layers). Using this constant value of denitrification potential, STICS underestimated the N_2O emitted from all mulch treatments. The model also did not reproduce the N_2O emissions peaks observed in response to rainfall events and to residue addition at several measurement times. When using a constant denitrification potential, it was neither possible to represent variations between different C treatments nor the dynamics of emissions over time, independent the mulch dynamics prediction accuracy (Fig. 5). The improvements in the mulch C and N dynamics with no limitation to residue decomposition did not result in improvements of N_2O fluxes, keeping the same pattern observed in the previous step (Fig. 5).

The use of the proposed function to determine denitrification potential tested the hypothesis that denitrification potential is not a constant value, but changes according the availability of C to denitrifiers. At the same time, we evaluated the use of CO_2 emissions from organic matter decomposition (from the humus in the control and from residue in the wheat and vetch treatments) as a proxy of carbon availability. Described as a component proportional to the CO_2 emissions of the decomposing residues, and that the coefficient of proportionality is also proportional to the N:C ratio of the residue.

The test of this simple model allowed simulating the correct order of magnitude of emissions for the different treatments including the bare soil, and helped to improve dynamics of emissions, higher at the beginning of the experiment and reducing after (Fig. 5). Especially, the model capture the timing and magnitude of high peaks of N_2O emissions measured for all treatments induced by residue application or precipitation (Fig. 5). Wheat residues treatments were also well reproduced and with a significant correlation (Table 3). Using this dynamic model of denitrification potential allows with only one set of parameters to reproduce the very

large of emission rate between bare soil (control), vetch and wheat residues and mulch rates (0, 3, 6 and 9 Mg DM ha^{-1}). The model was able to describe maximum emissions ranging from ~0.015 kg ha^{-1} for the control, 0.06-0.10 kg ha^{-1} for wheat, 0.3-0.8 kg ha^{-1} for vetch, covering the minimum and maximum fluxes observed. The cumulative fluxes were also well reproduced for all treatments, except Vetch_9. For the vetch treatments, STICS predicted cumulative N$_2$O-N fluxes of 3.12, 5.60 and 8.14 kg N ha^{-1} compared with the observed fluxes of 2.86, 5.21 and 4.84 kg N ha^{-1} to 3, 6 and 9 Mg DM ha^{-1} treatments (Supplementary Material Table 2). The prediction of wheat treatments, resulted in cumulative N$_2$O-N fluxes of 1.50, 2.28 and 3.01 kg N ha^{-1} emitted compared with the observed fluxes of 1.47, 2.18 and 2.09 kg N ha^{-1} to 3, 6 and 9 t DM ha^{-1} residue addition treatments (Supplementary Material Table 2).

3.5 DISCUSSION

3.5.1 Performance of STICS model using bare soil

The correct simulation of mulch decomposition and the associated N$_2$O emissions depends on the accuracy of the model to predict the variables that controls these processes (soil mineral N, soil water content (SWC), temperature). Using the bare soil treatment, STICS model described soil temperature with low bias, in accordance with the other studies that evaluated this variable (Jégo et al., 2014; Plaza-Bonilla et al., 2017). SWC was also fairly well predicted, despite the necessity of smaller adjustments, the model showed a good correlation. In general, soil water content is well simulated by the STICS model, whereas soil mineral N was simulated with less efficiency, particularly NH$_4$-N contents, and this is attributed to the complexity of the high interactions and biological processes involved in the soil, and measurement uncertainty (Coucheney et al., 2015). The cumulative and daily CO$_2$ and N$_2$O fluxes were well captured and agree with early findings with STICS model showing that STICS reproduce well these variables (Plaza-Bonilla et al., 2017).

3.5.2 Simulation of C and N dynamics of vetch and wheat residues with increasing mulch mass

The main differences between decomposition of surface and incorporated residues reflect in slower decomposition of surface crop residues, attributed to reduced mineral N availability to decomposers with the limited soil-residue contact (Chaves et al., submitted; Coppens et al., 2007). STICS simulates mulch decomposition as some other models (PASTIS Findeling et al., 2007; APSIM Thorburn et al., 2001) that take into account the possible role of N limitation with surface-applied residues. Mulch decomposition in STICS is described in two layers, with one

in direct contact with the soil (decomposable layer), and one layer located above the first one, non-decomposable but replenishing the decomposable layer as its decomposes. The model limitation factors in the decomposition, besides of soil-residue contact, are temperature, moisture and N availability. Using default STICS formalism, the mulch decomposition overestimated the C and N contents in the remaining mulch, for both residues (vetch and wheat) with increasing mulch thickness (3<6<9 Mg DM ha^{-1}). These results were expected, because the present dataset is one of the recent studies that have observed that the initial mulch mass has no effect on decomposition rate of the mulch. This pattern (mass loss proportional to the initial mass) was also observed with sugarcane mulch in the range 4 to 12 Mg DM ha^{-1} (Dietrich et al., 2017), hairy vetch, pea, oilseed radish, sunflower, flax and barley in the range 5 to 10 Mg DM ha^{-1} (Halde and Entz, 2016), and rye residues in the range 0 to 15 Mg DM ha^{-1} (Williams et al., 2018).

To improve the simulation of the mulch decomposition dynamics, we hypothesized that considering all mulch to be in contact with the soil and subject to decomposition might be a plausible representation of the fact that decomposition is proportional to the initial mass in the range of mulch masses (3, 6 and 9 Mg DM ha^{-1}) observed in the present dataset. With this hypothesis, the whole residue mass is in contact with the soil, i.e., there is no physical limitation to microbial decomposers to access soil N resources. We also tested the allocation of various proportions of the initial mulch masses to the decomposable layer to verify the model response. Thereby, the best prediction of mulch decomposition was found when the total mulch mass was considered in contact with the soil. This change in the *qmulchdec* parameter (size of the mulch mass in contact with the soil, here set at ≥9 Mg DM ha^{-1}), resulted in a better fit between simulated and observed mulch C dynamics for vetch and wheat residues for the three mulch mass (3, 6 and 9 Mg DM ha^{-1}). Simulating that the whole mulch is decomposing does not reflect however that there is a gradient in decomposition within the mulch mass and a compensatory effect. According to Dietrich et al. (2019), evaluating the decomposition of sugar cane residues added on soil surface with different mulch mass (4, 8 and 12 Mg ha^{-1}), the water dynamics within the mulch was determining a decomposition gradient in the mulch, also dependent of the mulch thickness. Although the assumption that the entire residue mass is in contact with the soil and decomposable, allows for a good simulation of the carbon dynamics of the thickest mulches obtained with mass 6 and 9 Mg DM ha^{-1}, STICS neglects possible gradients with mulches of high mass and thickness.

Mulch N dynamics were better predicted for vetch residues than wheat residues after model adjustments. For vetch residues, the modification of the *qmulchdec* parameter value did

not result in large change in the mulch N dynamics, with a good agreement between predicted and observed values. The high N contents of vetch residues (low C:N ratio) reduce the importance of the soil-residue contact effect on residue decomposition, where the main source of N to microbial decomposers is the residue itself, reducing the N requirements from soil, as observed by Abiven and Recous (2007), Coppens et al., (2007) and Chaves et al., (submitted). This was not observed for wheat mulches and we hypothesize that the low soluble fraction and N contents (high C:N ratio) resulted in a stronger effect of the higher soil-residue contact on the N dynamics, observed as a strong N immobilization from soil. This effect is associated to high C inputs from residues and no limitation to soil mineral N sources by decomposers, increasing the mulch N content above its initial content (Coppens et al., 2006).

Likewise, the leaching of soluble C and N fractions from residue mulch by rain is observed in other studies (Schreiber, 1999; Thiébeau et al., 2021) and can play an important role in the dynamics of mulch C and N dynamics, especially for immature residues having high soluble C and N contents, as vetch residues (Redin et al., 2014). Particularly, this pattern can be important in regions of high precipitations, as south of Brazil, where the mean annual rainfall is about 1666 mm (mean annual rainfall for the present dataset). The C and N leaching under high rain intensities can modify on the short term labile C and mineral N in the top soil layer that are the main precursors of N_2O emissions, in addition to possible losses of mineral N by leaching to deeper soil layers of the soil. STICS model does not simulate losses of soluble compounds from surface-applied residues under precipitations, and STICS also does not consider the chemical composition of crop residues, aside from their C:N ratio, which influence key-parameters of the decomposition module. In STICS, these soluble C and N fractions remain into the residues whatever the rain regime, which explain the lack of fit between observed and simulated C and N in the early phase, particularly for vetch, together with the underestimation of the mineral N in soil under the vetch mulches. The necessity of a better characterization of the residue quality in the model is one option to characterize labile fractions, despite the model be characterized by its simplicity and robustness (Nicolardot et al., 2001), together with the need to represent the transport of soluble C and N from mulch to soil with rainfall.

3.5.3 N_2O emissions as affected by mulch mass and quality: a new function to represent denitrification potential

The soil N_2O emissions result of the two main processes; nitrification and denitrification (Butterbach-Ball et al., 2013). Nitrification is an aerobic process and dependent on NH_4 concentration, soil temperature, soil moisture and the soil pH (Butterbach-Ball et al., 2013).

Denitrification is the main source of the N_2O emissions from soil (Li et al., 2016), and occurs in anoxic conditions, regulated by the soil available NO_3, SWC, temperature and C sources (Butterbach-Ball et al., 2013). STICS model use a potential rate of the N_2O fluxes, governed by the potential of denitrification, which represent the maximal possible amount of NO_3 reduced to N_2O per day (Henault et al., 2005). In this model, the total denitrification potential rate (kg N ha^{-1} day^{-1}) is assumed to be a constant value, as used by many models to determine the denitrification rate (Heinen, 2006). Using this formalism, the N_2O fluxes were fairly well simulated with the bare soil treatment. When the model, calibrated with the bare soil treatment, was tested against the mulch treatments, STICS underestimated the N_2O fluxes for all mulch treatments and did not represent the high N_2O peaks (so-called hot moments), suggesting that the constant value for denitrification potential, calibrated on bare soil, could not describe the variations in N_2O emissions observed with decomposing residues. As largely reported (Li et al., 2016; Miller et al., 2008), higher N_2O emissions are observed after residue addition, with a stronger effect of low C:N ratio residues (mostly residues from immature crops, as cover crops), which labile C and N plays an important role for soil denitrifiers (Lashermes et al., submitted). Plaza-Bonilla et al. (2017) related low simulated N_2O fluxes during the evaluation of Faba bean growing in Mediterranean conditions using STICS model.

To improve the model and describe the high N_2O emissions observed with mulch treatments, our hypothesis was that in favorable conditions to denitrification, the available C compounds to denitrifying organisms could be simulated taking into account the soil CO_2 fluxes. Surey et al. (2020) evaluated the effect of water-soluble C in plant residues and N_2O and CO_2 emissions, and found a direct relationship between $(N_2O + N_2)$-N/CO_2-C ratio and soluble C contents. The soluble C content depends on the overall residue chemical composition, and is closely related to its C:N ratio or N content (Chaves et al., submitted) with the lower the C:N, the highest the soluble concentration. This is confirmed in this study with the vetch residues having lower C:N ratio than wheat residue and higher N_2O emission. The correlation between the CO_2 emissions and N_2O emissions were shown by e.g., Xu et al. (2008) and observed mainly at the initial residue decomposition stages (Lashermes et al., submitted), where soluble fraction are high available and could lead to produce high N_2O emissions ("hot moments") as in the present dataset. Despite the STICS model does not have a variable to describe C availability, the CO_2 fluxes could be used as a proxy of the availability of labile C to denitrifying microorganisms.

With the new denitrification potential function, STICS reproduced much better the peaks of N_2O observed at the beginning of residue decomposition. The use of the C:N ratio in

the function, lead to better take into account the differences in N_2O fluxes between vetch and wheat residues, which suggests that C:N ratio (12 and 83 for vetch and wheat residues, respectively) was indirectly reflecting well the differences in residue chemical characteristics, between wheat and vetch. The reason for a better description of N_2O fluxes taking into account the C:N ratio of the residues is not clear, but this could reflect indirectly a higher residue C or N availability with vetch residue, or a change in the soluble C composition according to residue type. The magnitude of the N_2O peaks and the temporal dynamics of fluxes were particularly well reproduced after the implementation of this new function. Cumulative emissions were well reproduced too, except with the treatment with vetch residues at 9 Mg DM ha^{-1}. For this latter situation, Schmatz et al. (2020) discussed the decrease in N_2O emitted observed with the 9 Mg DM compared to 6 Mg DM, particularly the possible increase in the N_2O to N_2 reduction rate with high soluble C and N availability. With the present formalism of the N_2O module, STICS cannot simulate such change in the N_2O reduction rate.

3.6 CONCLUSION

The test of the STICS model on mulch decomposition and N_2O modules, against data involving two residues (vetch and wheat) with different mulch mass (0, 3, 6 and 9 Mg DM ha^{-1}), inducing different thicknesses, allowed to propose significant improvements in the formalism and parametrization of these modules, to better reflect C and N dynamics in no-tilled cropping system. First, our results showed that whatever the range of mass and thickness (in the range of agricultural practice, from 0 to 9 Mg DM ha^{-1}), the model better described mulch C dynamics when the whole mulch mass was considered decomposing, whatever the initial mass. These results calls into question the present representation of mulch (a decomposable layer fed by a non-decomposable layer). Despite this improvement of the prediction of C mulch dynamics, the dynamics of N in the mulch were not well simulated for wheat mulch, with increasing mulch N attributed to microbial N immobilization, not described by STICS. This work also demonstrate the importance of simulating mulch C and N transport under rain, particularly for agricultural and climatic contexts with no tilled systems and high precipitation regime. Lastly the improvement of the denitrification potential function of STICS taking into account specific impact of residues additions on C and microbial dynamics and subsequently N_2O emitted, taking into account CO_2 emissions and the C:N ratio of residues, lead to a much better prediction of the N_2O fluxes. These results are very promising to simulating accurately N_2O emission associated to residue decomposition. However, the limits of use of this function based in CO_2 emissions as a proxy of C availability to determine denitrification potential need to be

evaluated in other systems involving the simulation of a wide diversity of pedoclimatic and contrasted agronomic scenarios to verify its accuracy and possibility of extrapolation.

3.7 REFERNCES

Abiven, S., Recous, S., 2007. Mineralisation of crop residues on the soil surface or incorporated in the soil under controlled conditions. Biol. Fertil. Soils 43, 849–852. https://doi.org/10.1007/s00374-007-0165-2

Acosta, J.A. de A., Amado, T.J.C., Da, S.L.S., Santi, A., Weber, M.A., 2014. Decomposição da fitomassa de plantas de cobertura e liberação de nitrogênio em função da quantidade de resíduos aportada ao solo sob sistema plantio direto. Ciência Rural.

Arcand, M.M., Helgason, B.L., Lemke, R.L., 2016. Microbial crop residue decomposition dynamics in organic and conventionally managed soils. Appl. Soil Ecol. 107, 347–359. https://doi.org/10.1016/j.apsoil.2016.07.001

Baggs, E.M., Stevenson, M., Pihlatie, M., Regar, A., Cook, H., Cadisch, G., 2003. Nitrous oxide emissions following application of residues and fertiliser under zero and conventional tillage. Plant Soil 254, 361–370. https://doi.org/10.1023/A:1025593121839

Beaudoin, N., Launay, M., Sauboua, E., Ponsardin, G., Mary, B., 2008. Evaluation of the soil crop model STICS over 8 years against the "on farm" database of Bruyères catchment. Eur. J. Agron. 29, 46–57. https://doi.org/10.1016/j.eja.2008.03.001

Brisson, N., Gary, C., Justes, E., Roche, R., Mary, B., Ripoche, D., Zimmer, D., Sierra, J.,

Bertuzzi, P., Burger, P., Bussière, F., Cabidoche, Y.., Cellier, P., Debaeke, P., Gaudillère, J.., Hénault, C., Maraux, F., Seguin, B., Sinoquet, H., 2003. An overview of the crop model stics. Eur. J. Agron. 18, 309–332. https://doi.org/10.1016/S1161-0301(02)00110-7

Butterbach-bahl, K., Baggs, E.M., Dannenmann, M., Kiese, R., Zechmeister-boltenstern, S., 2013. Nitrous oxide emissions from soils : how well do we understand the processes and their controls? Philos. Trans. R. Soc. 368, 20130122.

Charles, A., Rochette, P., Whalen, J.K., Angers, D.A., Chantigny, M.H., Bertrand, N., 2017. Global nitrous oxide emission factors from agricultural soils after addition of organic amendments: A meta-analysis. Agric. Ecosyst. Environ. 236, 88–98. https://doi.org/10.1016/j.agee.2016.11.021

Chaves, B., Redin, M., Giacomini, S. J., Schmatz, R., Léonard, Joël., Ferchaud, F., Recous, S. Submitted. Combination of residue quality, residue placement and soil mineral N content drives C and N dynamics by modifying the N access to microbial decomposers. Soil Biol. Biochem.

Chen, H., Li, X., Hu, F., Shi, W., 2013. Soil nitrous oxide emissions following crop residue addition: A meta-analysis. Glob. Chang. Biol. 19, 2956–2964. https://doi.org/10.1111/gcb.12274

Coppens, F., Garnier, P., De Gryze, S., Merckx, R., Recous, S., 2006. Soil moisture, carbon and nitrogen dynamics following incorporation and surface application of labelled crop residues in soil columns. Eur. J. Soil Sci. 57, 894–905. https://doi.org/10.1111/j.1365-2389.2006.00783.x

Coppens, F., Garnier, P., Findeling, A., Merckx, R., Recous, S., 2007. Decomposition of mulched versus incorporated crop residues: Modelling with PASTIS clarifies interactions between residue quality and location. Soil Biol. Biochem. 39, 2339–2350. https://doi.org/10.1016/j.soilbio.2007.04.005

Coucheney, E., Buis, S., Launay, M., Constantin, J., Mary, B., Cortázar-Atauri, I.G. de, Ripoche, D., Beaudoin, N., Ruget, F., Andrianarisoa, K.S., Le bas, C., Justes, E., Léonard, J., 2015. Accuracy , robustness and behavior of the STICS soil e crop model for plant , water and nitrogen outputs : Evaluation over a wide range of agro-environmental conditions in France. Environ. Model. Softw. 64, 177–190. https://doi.org/10.1016/j.envsoft.2014.11.024

Dexter, A.R., Czyz, E.A., Richard, G., 2012. Equilibrium, non-equilibrium and residual water: Consequences for soil water retention. Geoderma 177–178, 63–71. https://doi.org/10.1016/j.geoderma.2012.01.029

Dietrich, G., Recous, S., Pinheiro, P.L., Weiler, D.A., Luiza, A., Roberto, M., Rambo, L., José, S., 2019. Gradient of decomposition in sugarcane mulches of various thicknesses. Soil Tillage Res. 192, 66–75. https://doi.org/10.1016/j.still.2019.04.022

Dietrich, G., Sauvadet, M., Recous, S., Redin, M., Pfeifer, I.C., Garlet, C.M., Bazzo, H., Giacomini, S.J., 2017. Sugarcane mulch C and N dynamics during decomposition under different rates of trash removal. Agric. Ecosyst. Environ. 243, 123–131. https://doi.org/10.1016/j.agee.2017.04.013

Findeling, A., Garnier, P., Coppens, F., Lafolie, F., Recous, S., 2007. Modelling water, carbon and nitrogen dynamics in soil covered with decomposing mulch. Eur. J. Soil Sci. 58, 196–206. https://doi.org/10.1111/j.1365-2389.2006.00826.x

Fracetto, F.J.C., Fracetto, G.G.M., Bertini, S.C.B., Cerri, C.C., Feigl, B.J., Siqueira Neto, M., 2017. Effect of agricultural management on N2O emissions in the Brazilian sugarcane yield. Soil Biol. Biochem. 109, 205–213. https://doi.org/10.1016/j.soilbio.2017.02.004

Halde, C., Entz, M.H., 2016. Plant species and mulch application rate affected decomposition of cover crop mulches used in organic rotational no-till systems. Can. J. Plant Sci. 96, 59–71.

Heinen, M., 2006. Simplified denitrification models : Overview and properties. Geoderma 133, 444–463. https://doi.org/10.1016/j.geoderma.2005.06.010

Hénault, C., Bizouard, F., Laville, B., Gabeielle, B., Nicoullaud, B., Germon, J.C., Cellier, P., 2005. Predicting in situ soil N2O emission using NOE algorithm and soil database. Global Biogeochem. Cycles 11, 115–127. https://doi.org/10.1111/j.1365-2486.2004.00879.x

Jégo, G., Chantigny, M., Pattey, E., Bélanger, G., Rochette, P., Vanasse, A., Goyer, C., 2014. Improved snow-cover model for multi-annual simulations with the STICS crop model under cold, humid continental climates. Agric. For. Meteorol. 195–196, 38–51. https://doi.org/10.1016/j.agrformet.2014.05.002

Kong, A.Y.Y., Six, J., 2010. Tracing Root vs. Residue Carbon into Soils from Conventional

and Alternative Cropping Systems. Soil Sci. Soc. Am. J. 74, 1201–1210. https://doi.org/10.2136/sssaj2009.0346

Lashermes, G., Recous, S., Alavoine, G., Janz, B., Butterbach-Bahl, K., Ernfors, M., Laville, P., Submitted. The N2O emission from decomposing crop residues is strongly linked to their initial soluble fraction and early mineralization dynamics.

Li, X., Sørensen, P., Olesen, J.E., Petersen, S.O., 2016. Evidence for denitrification as main source of N2O emission from residue-amended soil. Soil Biol. Biochem. 92, 153–160. https://doi.org/10.1016/j.soilbio.2015.10.008

Mei, K., Wang, Z., Huang, H., Zhang, C., Shang, X., Dahlgren, R.A., Zhang, M., Xia, F., 2018. Stimulation of N2O emission by conservation tillage management in agricultural lands: A meta-analysis. Soil Tillage Res. 182, 86–93. https://doi.org/10.1016/j.still.2018.05.006

Miller, M.N., Zebarth, B.J., Dandie, C.E., Burton, D.L., Goyer, C., Trevors, J.T., 2008. Crop residue influence on denitrification, N2O emissions and denitrifier community abundance in soil. Soil Biol. Biochem. 40, 2553–2562. https://doi.org/10.1016/j.soilbio.2008.06.024

Nicolardot, B., Recous, S., Mary, B., 2001. Simulation of C and N mineralisation during crop residue decomposition: A simple dynamic model based on the C:N ratio of the residues. Plant Soil 228, 83–103. https://doi.org/10.1023/A:1004813801728

Pinheiro, P.L., Recous, S., Dietrich, G., Weiler, D.A., Schu, A.L., Bazzo, H.L.S., Giacomini, S.J., 2019. N2O emission increases with mulch mass in a fertilized sugarcane cropping system. Biol. Fertil. Soils 55, 511–523. https://doi.org/10.1007/s00374-019-01366-7

Plaza-Bonilla, D., Álvaro-Fuentes, J., Bareche, J., Pareja-Sánchez, E., Justes, É., Cantero-Martínez, C., 2018. No-tillage reduces long-term yield-scaled soil nitrous oxide emissions in rainfed Mediterranean agroecosystems: A field and modelling approach. Agric. Ecosyst. Environ. 262, 36–47. https://doi.org/10.1016/j.agee.2018.04.007

Plaza-bonilla, D., Léonard, J., Peyrard, C., Mary, B., Justes, É., 2017. Precipitation gradient and crop management affect N2O emissions : Simulation of mitigation strategies in rainfed Mediterranean conditions. Agric. Ecosyst. Environ. 238, 89–103. https://doi.org/10.1016/j.agee.2016.06.003

Redin, M., Recous, S., Aita, C., Dietrich, G., Skolaude, A.C., Ludke, W.H., Schmatz, R., Giacomini, S.J., 2014. How the chemical composition and heterogeneity of crop residue mixtures decomposing at the soil surface affects C and N mineralization. Soil Biol. Biochem. 78, 65–75. https://doi.org/10.1016/j.soilbio.2014.07.014

Schmatz, R., Recous, S., Adams, D., Elias, G., Luiza, A., Lago, R., José, S., 2020. Geoderma How the mass and quality of wheat and vetch mulches affect drivers of soil N2O emissions. Geoderma 372, 114395. https://doi.org/10.1016/j.geoderma.2020.114395

Schreiber, J.D., 1999. Nutrient Leaching from Corn Residues under Simulated Rainfall. J. Environ. Qual. 28, 1864–1870. https://doi.org/10.2134/jeq1999.00472425002800060024x

Sierra, J., Brisson, N., Ripoche, D., Déqué, M., 2010. Modelling the impact of thermal adaptation of soil microorganisms and crop system on the dynamics of organic matter in a tropical soil under a climate change scenario. Ecol. Modell. 221, 2850–2858. https://doi.org/10.1016/j.ecolmodel.2010.08.031

Sithole, N.J., Magwaza, L.S., Mafongoya, P.L., 2016. Conservation agriculture and its impact on soil quality and maize yield: A South African perspective. Soil Tillage Res. 162, 55–67. https://doi.org/10.1016/j.still.2016.04.014

Smith, P., Smith, J.U., Powlson, D.S., Mcgill, W.B., Arah, J.R.M., Chertov, O.G., Coleman, K., Franko, U., Frolking, S., Jenkinson, D.S., Jensen, L.S., Kelly, R.H., Klein-gunnewiek, H., Komarov, A.S., Li, C., Molina, J.A.E.J., Mueller, T., Parton, W.J., Thornley, J.H.M., Whitmore, A.P., 1997. A comparison of the performance of nine soil organic matter models using datasets from seven long-term experiments. Geoderma 81, 153–225.

Soil Survey Staff, 2010. Keys to soil taxonomy. United States Department of Agriculture-Natural Reseources Conservation Service, Washington, DC.

Steiner, J.L., Schomberg, H.H., Unger, P.W., Cresap, J., 1999. Crop Residue Decomposition in No-Tillage Small-Grain Fields. Soil Sci. Soc. Am. J. 63, 1817–1824.

Stott, D.E., Stroo, H.F., Elliott, L.F., Papendick, R.I., Unger, P.W., 1990. Wheat Residue Loss from Fields under No-till Management. Soil Sci. Soc. Am. J. 54, 92–98.

Surey, R., Schimpf, C.M., Sauheitl, L., Mueller, C.W., Rummel, P.S., Dittert, K., Kaiser, K., Jürgen, B., Mikutta, R., 2020. Potential denitrification stimulated by water-soluble organic carbon from plant residues during initial decomposition. Soil Biol. Biochem. 147, 107841. https://doi.org/10.1016/j.soilbio.2020.107841

Thiébeau, P., Girardin, C., Recous, S., 2021. Water interception and release of soluble carbon by mulches of plant residues under contrasting rain intensities. Soil Tillage Res. 208, 104882. https://doi.org/10.1016/j.still.2020.104882

Thorburn, P.J., Probert, M.E., Robertson, F.A., 2001. Modelling decomposition of sugar cane surface residues with APSIM-Residue. F. Crop. Res. 70, 223–232.

Williams, A., Wells, M.S., Dickey, D.A., Hu, S., Maul, J., Raskin, D.T., Reberg-horton, S.C., Mirsky, S.B., 2018. Establishing the relationship of soil nitrogen immobilization to cereal rye residues in a mulched system. Plant Soil 426, 95–107. https://doi.org/10.1007/s11104-018-3566-0

Xu, X., Tian, H., Hui, D., 2008. Convergence in the relationship of CO2 and N2O exchanges between soil and atmosphere within terrestrial ecosystems. Glob. Chang. Biol. 14, 1651–1660. https://doi.org/10.1111/j.1365-2486.2008.01595.x

Figure captions

Figure 1. Conceptual representation of mulch decomposition processes with the two compartment patterns.

Figure 2. Control treatment (bare soil without mulches) measured (symbols) and simulated soil water content (a, b) (0-5 and 5-10 cm), soil temperature (c, d) (0-5 and 5-10 cm), soil mineral nitrogen (NO_3 and NH_4) in the 0-10 cm depth (e, f), $C-CO_2$ and $N-N_2O$ emissions (g, h) after model calibration (lines), (Error bars for measured values are $\pm$ standard error).

Figure 3. Measured (symbols) and estimated mulch C (default and improved) from vetch (a, c, e) and wheat residues (b, d, f), with 3 Mg ha^{-1} (a, b), 6 Mg ha^{-1} (c, d), and 9 Mg ha^{-1} (e, f) (lines). Lines represent the values simulated with STICS default parameters (dashed line) and improved (solid line), (Error bars for measured values are $\pm$ standard error).

Figure 4. Measured (symbols) and estimated mulch N (default and improved) from vetch (a, c, e) and wheat (b, d, f) residues, with 3 Mg ha^{-1} (a, b), 6 Mg ha^{-1} (c, d), and 9 Mg ha^{-1} (e, f) (lines). Lines represent the values simulated with STICS default parameters (dashed line) and improved (solid line), (Error bars for measured values are $\pm$ standard error).

Figure 5. Measured (symbols) and estimated nitrous oxide emissions (default mulch parameters, improved mulch parameters and improved $N-N_2O$ fluxes) from vetch (a, c, e) and wheat (b, d, f) residues, with 3 Mg ha^{-1} (a, b), 6 Mg ha^{-1} (c, d), and 9 Mg ha^{-1} (e, f) (lines). Lines represent the values simulated with STICS default mulch parameters (dotted line), improved mulch (dashed line) and N_2O fluxes improved (solid line), (Error bars for measured values are $\pm$ standard error).

Table 1. Soil characteristics used in STICS model.

	Depth (cm)	Units	Values
Soil pH	0-10	-	4.8
Clay content	0-10	g kg $^{-1}$	110
Organic N	0-10	g kg $^{-1}$	0.9
Organic C	0-10	g kg $^{-1}$	9.6
Soil C:N ratio	0-10	-	10.67
Bulk density	0-5	g cm^{-3}	1.48
	5-10		1.71
	10-20		1.74
	20-65		1.67
	65-100		1.51
Field capacity	0-5	% dry weight	18.0
	5-10		14.0
	10-35		13.4
	35-65		13.1
	65-100		22.1
Wilting point	0-5	% dry weight	10.3
	5-10		11.5
	10-35		6.0
	35-65		5.3
	65-100		11.9

Table 2. Performance of STICS model for control treatment in the calibration step.

Variable	Soil depth (cm)	r	RMSE	E(%)	M	t
Soil water content (% dry weight)	0-5	0.72	2.01	-5.17	-0.73	ns
	5-10	0.55	1.25	-3.35	-0.40	ns
Soil temperature (°C)	0-5	0.83	2.52	7.20	1.67	*
	5-10	0.76	2.61	6.85	1.59	*
Soil nitrate (kg N ha^{-1})	0-10	0.66	9.48	-10.02	-1.56	ns
Soil ammonium (kg N ha^{-1})	0-10	-0.31	3.69	28.02	1.86	*
C-CO$_2$ (kg ha^{-1} day^{-1})	-	0.39	6.05	13.95	1.46	ns
N-N$_2$O (kg ha^{-1} day^{-1})	-	0.31	0.01	-6.27	-0.00	ns

r: Correlation Coefficient; RMSE: Root mean square error of model; E(%): relative error; M: Mean difference; t: Student's t of M; * - Significant; ns – no significant.

Table 3. Statistical criteria after improvement of mulch decomposition and using the new function to determine denitrification potential.

Variable	Soil depth (cm)		Vetch 3	Vetch 6	Vetch 9	Wheat 3	Wheat 6	Wheat 9
Soil nitrate (kg ha^{-1})	0-10	r	0.82	0.73	0.82	0.38	0.30	0.37
		$RMSE$	8.55	13.66	21.80	7.43	6.67	6.65
		$E(\%)$	-24.18	-30.19	-70.42	-35.65	-25.58	-27.51
		M	-4.31	-6.28	-13.37	-4.32	-3.30	-3.46
		t	ns	ns	ns	ns	ns	ns
Soil ammonium (kg ha^{-1})	0-10	r	-0.02	0.30	0.53	-0.06	-0.31	-0.12
		$RMSE$	4.85	7.48	9.81	4.17	3.93	4.44
		$E(\%)$	-3.15	-24.88	-32.55	31.39	32.04	37.58
		M	-0.23	-2.09	-3.15	2.10	2.16	2.63
		t	ns	ns	ns	*	*	*
C mulch (kg ha^{-1})	-	r	0.99	0.99	0.99	1.00	0.99	0.97
		$RMSE$	100.76	141.99	230.33	57.07	170.25	385.36
		$E(\%)$	-22.79	-10.69	-6.73	1.75	1.82	-4.40
		M	-77.86	-79.12	-75.49	12.63	27.46	-101.41
		t	ns	ns	ns	ns	ns	ns
N mulch (kg ha^{-1})	-	r	0.89	0.91	0.93	0.25	0.48	0.45
		$RMSE$	22.41	39.47	50.01	7.27	12.94	19.74
		$E(\%)$	-86.62	-68.67	-52.20	-58.38	-57.96	-60.53
		M	-16.98	-29.10	-35.84	-5.06	-10.22	-15.39
		t	ns	ns	ns	ns	ns	ns
C-CO$_2$ (kg ha^{-1}day^{-1})	-	r	0.33	0.25	0.22	0.46	0.46	0.44
		$RMSE$	15.41	28.44	43.15	8.93	16.76	14.92
		$E(\%)$	3.78	-1.90	0.65	-3.41	-25.11	-29.90
		M	0.77	-0.54	0.27	-0.49	-4.70	-6.35
		t	ns	ns	ns	ns	ns	ns
N-N$_2$O (kg ha^{-1}day^{-1})	-	r	0.56	0.78	0.74	0.62	0.67	0.62
		$RMSE$	0.06	0.07	0.10	0.01	0.02	0.02
		$E(\%)$	-11.38	-8.26	-45.43	-12.58	-15.05	-51.51
		M	-0.00	-0.01	-0.03	-0.00	-0.00	-0.01
		t	ns	ns	ns	ns	ns	ns

R: Correlation Coefficient; RMSE: Root mean square error of model; E(%): relative error; M: Mean difference; t: Student's t of M; * - Significant; ns – no significant.
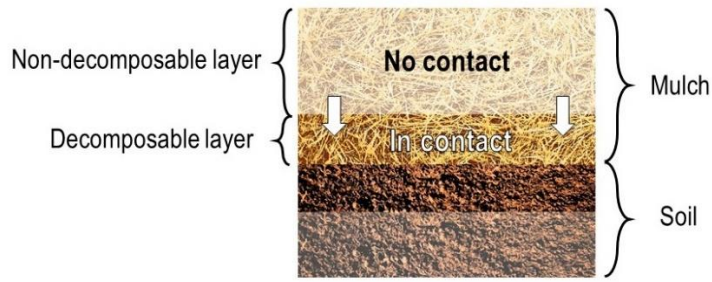
Fig 1.
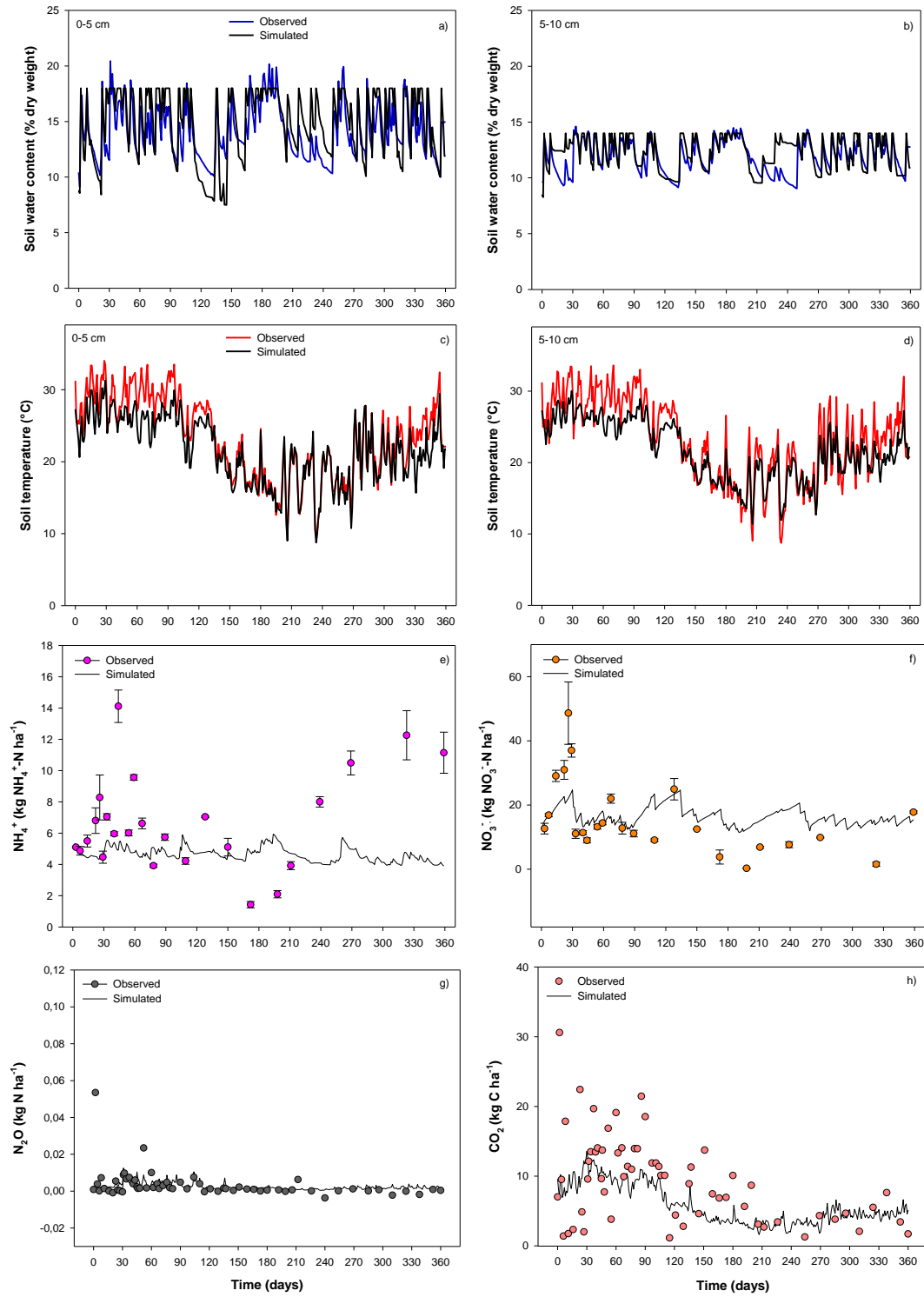
Fig 2.
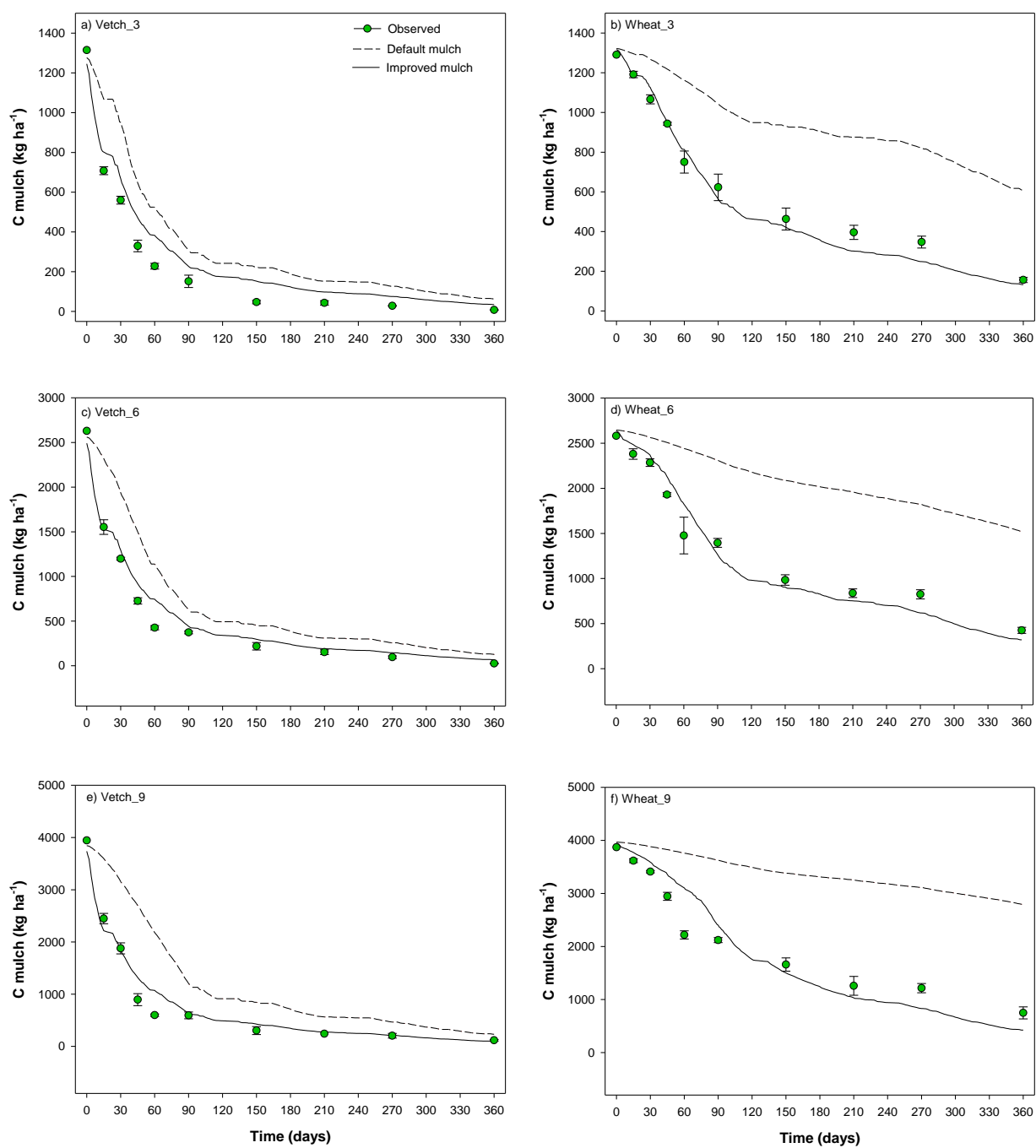
Fig 3.
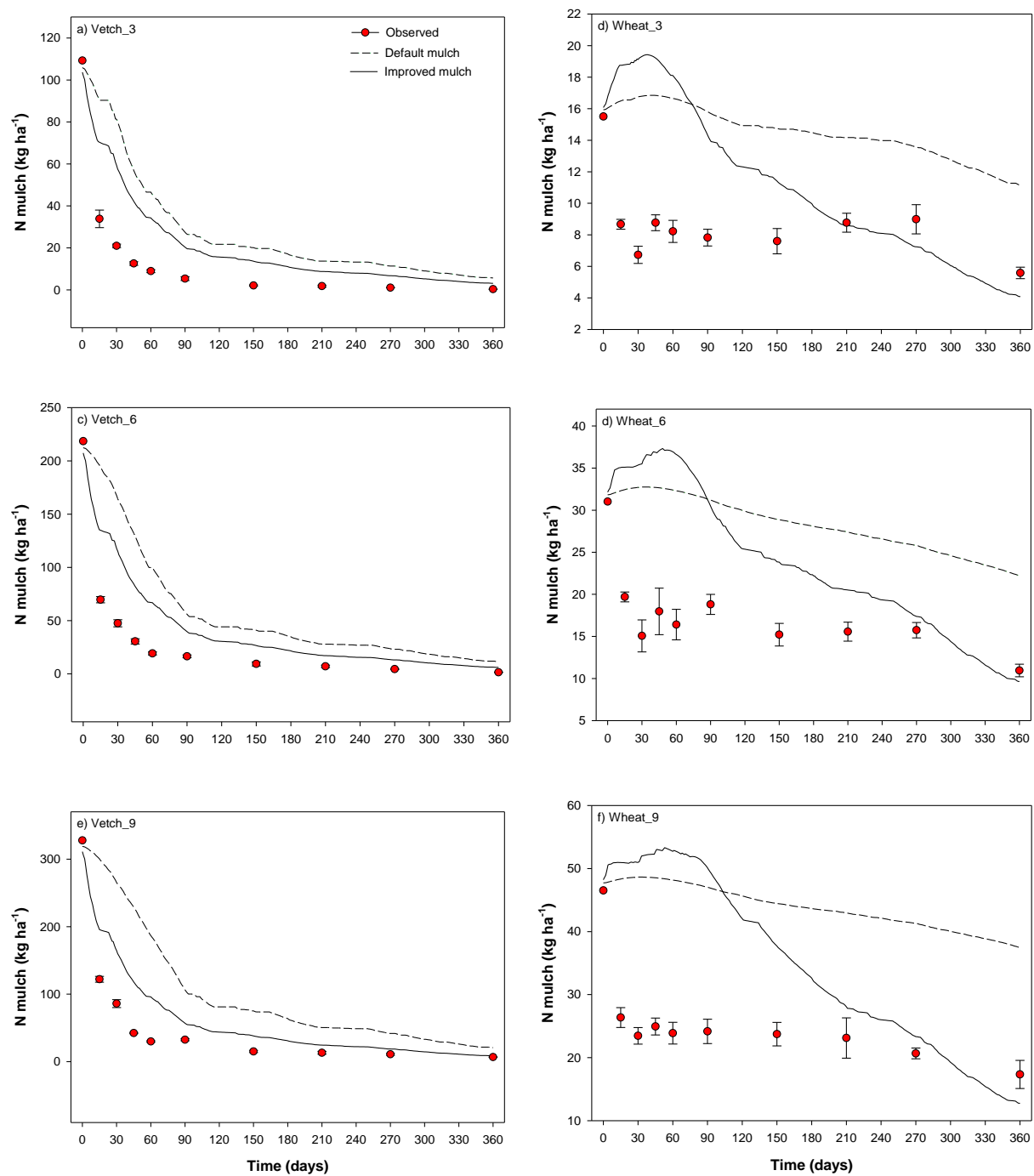
Fig 4.
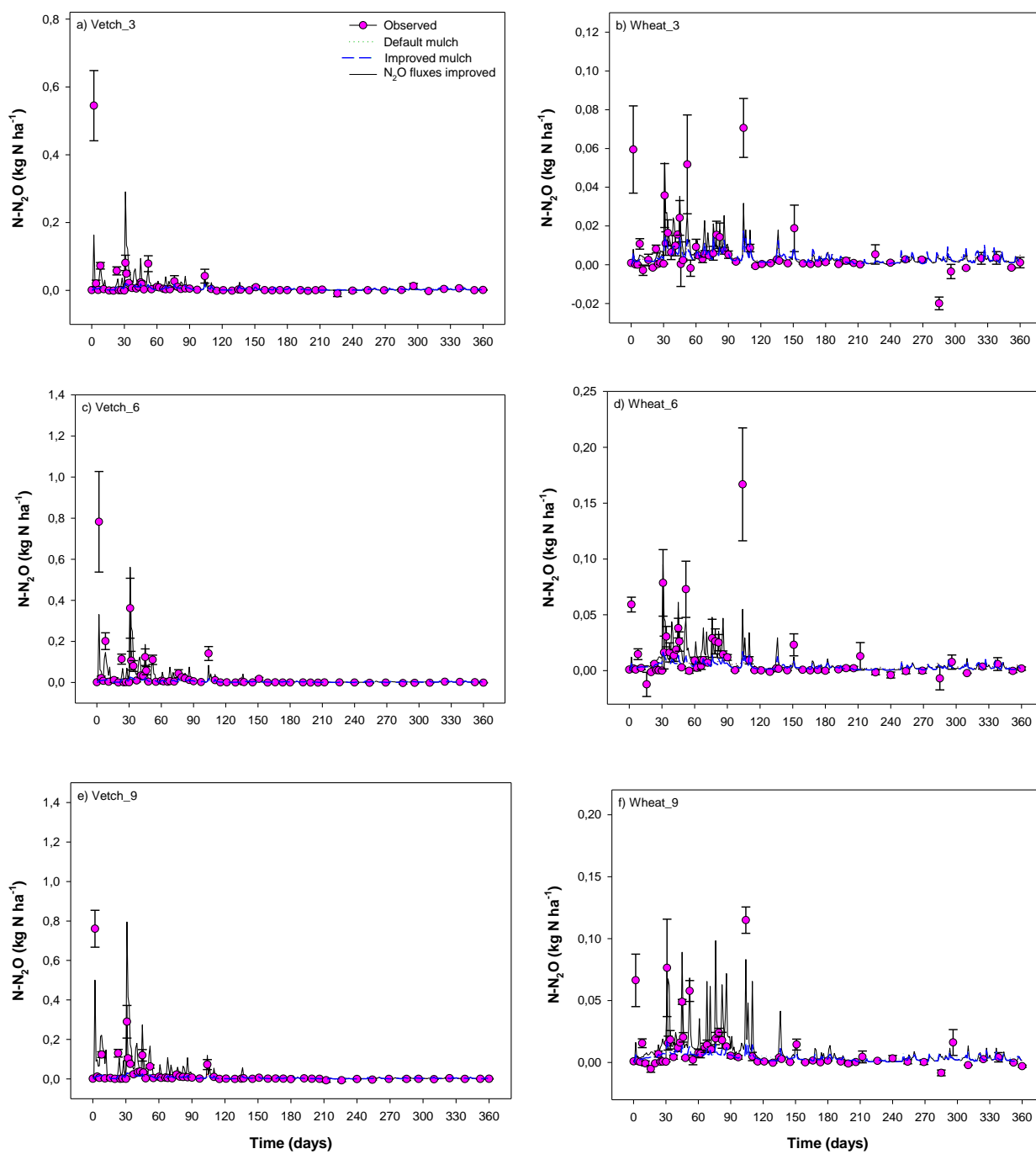
Fig 5.

Supplementary files

Table S1. Soil moisture and temperature statistical criteria at the evaluation step.

Variable	Soil depth (cm)	Treatment	*r*	*RMSE*	*E(%)*	*M*	*t*
		Vetch 3	0.84	1.76	-1.93	-0.28	ns
		Vetch 6	0.75	2.10	3.46	0.53	*
	0-5	Vetch 9	0.73	2.06	2.60	0.40	*
		Wheat 3	0.82	2.55	-14.89	-1.97	ns
		Wheat 6	0.61	2.81	-5.02	-0.74	ns
Soil water		Wheat 9	0.75	1.71	3.86	0.64	*
content							
(% dry weight)		Vetch 3	0.81	1.09	3.99	0.50	*
		Vetch 6	0.80	1.11	4.68	0.59	*
	5-10	Vetch 9	0.77	1.57	9.46	1.26	*
		Wheat 3	0.65	1.26	1.13	0.14	*
		Wheat 6	0.69	1.07	0 .56	0.07	ns
		Wheat 9	0.68	1.05	0.40	0.05	ns
		Vetch 3	0.78	2.10	5.45	1.24	*
		Vetch 6	0.73	1.89	4.38	0.99	*
	0-5	Vetch 9	0.71	1.89	4.41	0.99	*
		Wheat 3	0.76	2.02	5.70	1.30	*
		Wheat 6	0.74	1.59	2.86	0.64	*
Soil		Wheat 9	0.77	1.48	3.50	0.79	*
temperature							
(°C)		Vetch 3	0.71	2.15	6.12	1.40	*
		Vetch 6	0.67	1.84	4.41	0.99	*
	5-10	Vetch 9	0.66	1.85	4.51	1.02	*
		Wheat 3	0.69	1.88	4.72	1.07	*
		Wheat 6	0.69	1.50	3.11	0.70	*
		Wheat 9	0.71	1.57	3.30	0.75	*

r: Correlation Coefficient; RMSE: Root mean square error of model; E(%): relative error; M: Mean difference; t: Student's t of M; * - Significant; ns – no significant.

Table S2. C-CO$_2$ and N-N$_2$O accumulated simulated and observed emissions for the two residues (vetch and wheat) and three mulch mass (3, 6 and 9 Mg DM ha^{-1}) plus control treatment.

Variable	Treatment	Observed	Simulated
C-CO$_2$ accumulated (kg C ha^{-1})	Control	2474.01	2081.27
	Vetch_3	3067.52	2882.94
	Vetch_6	3754.64	3749.99
	Vetch_9	4839.97	4598.72
	Wheat_3	3131.58	3172.51
	Wheat_6	3326.92	4252.91
	Wheat_9	3702.00	5425.52
N-N$_2$O accumulated (kg N ha^{-1})	Control	0.59	0.87
	Vetch_3	2.86	3.12
	Vetch_6	5.21	5.60
	Vetch_9	4.11	8.14
	Wheat_3	1.46	1.50
	Wheat_6	2.17	2.28
	Wheat_9	2.09	3.01

Fig. S1 Measured (symbols) and estimated NH_4^+- N with improved parameters for vetch (a, c, e) and wheat (b, d, f) residues, with 3 Mg ha^{-1} (a, b), 6 Mg ha^{-1} (c, d), and 9 Mg ha^{-1} (e, f) (lines), (Error bars for measured values are $\pm$ standard error).
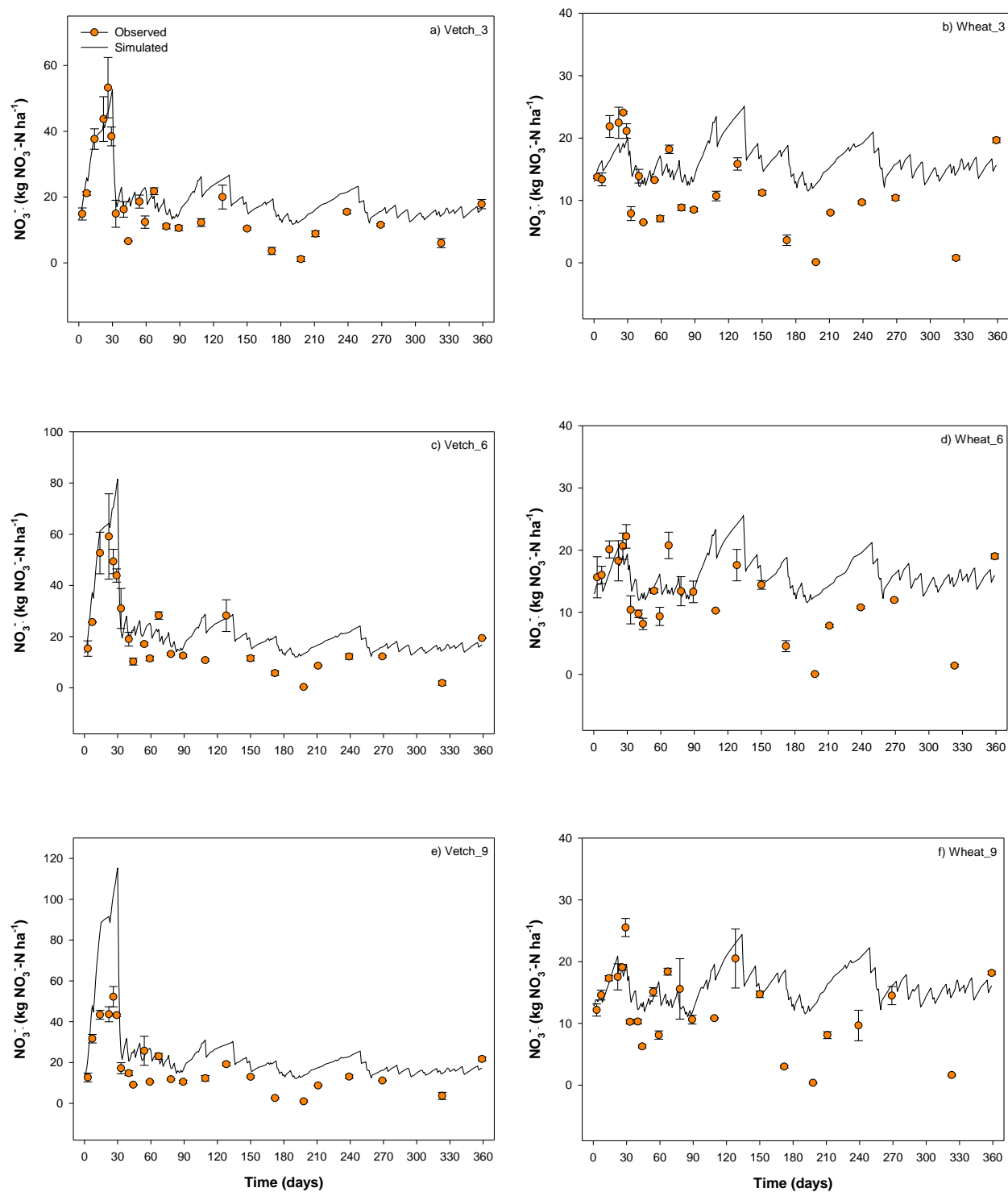
Fig. S2 Measured (symbols) and estimated NO_3^-- N with improved parameters for vetch (a, c, e) and wheat (b, d, f) residues, with 3 Mg ha^{-1} (a, b), 6 Mg ha^{-1} (c, d), and 9 Mg ha^{-1} (e, f) (lines), (Error bars for measured values are $\pm$ standard error).
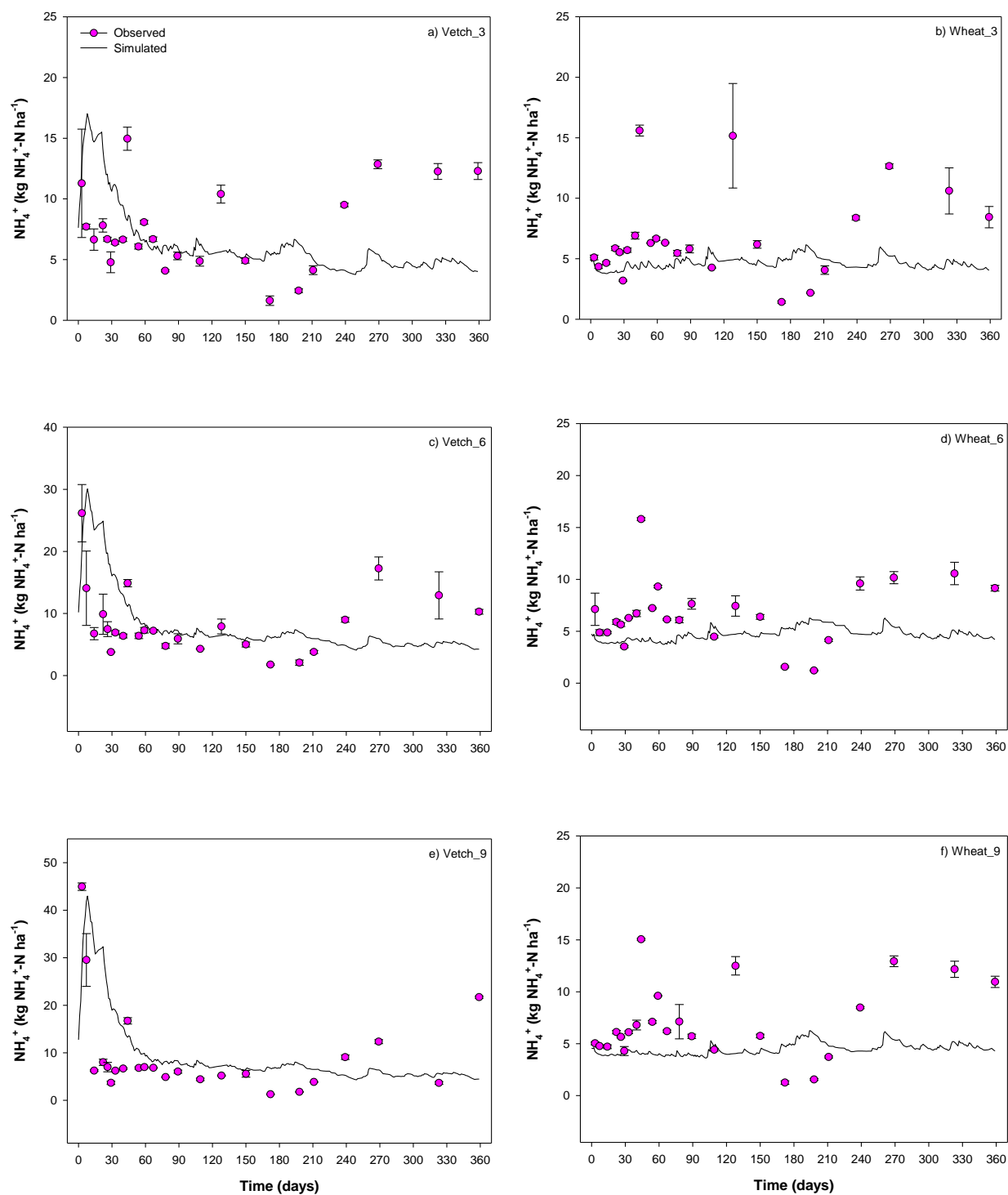
Fig. S3 Measured (symbols) and estimated C-CO$_2$ with improved parameters for vetch (a, c, e) and wheat (b, d, f) residues, with 3 Mg ha^{-1} (a, b), 6 Mg ha^{-1} (c, d), and 9 Mg ha^{-1} (e, f) (lines), (Error bars for measured values are $\pm$ standard error).
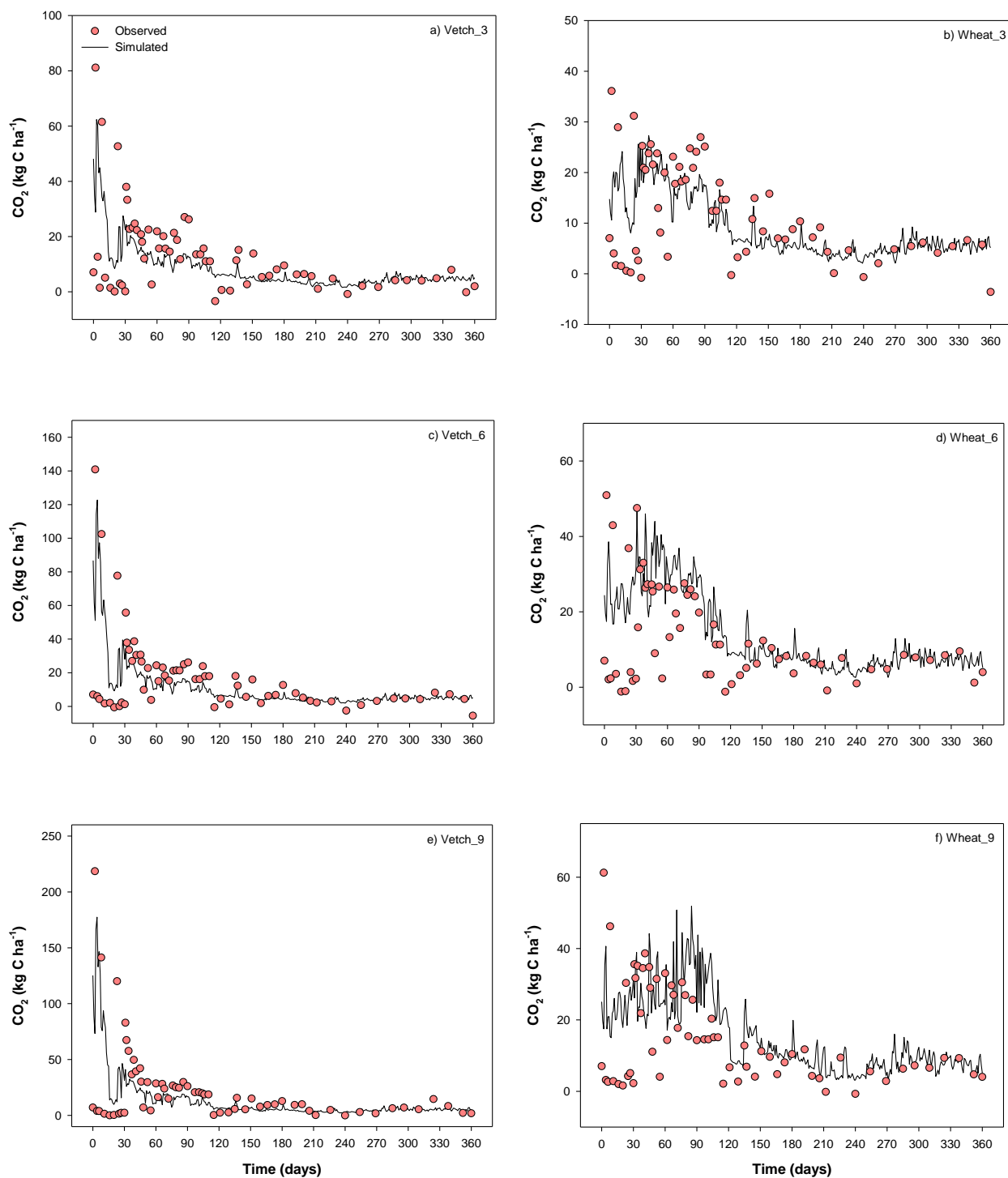
4 DISCUSSÃO GERAL

O presente estudo evidencia a importância do uso de modelos de simulação (submodelo decomposição de STICS) na interpretação da relação entre a composição química, localização dos resíduos culturais e disponibilidade de N no solo, estabelecendo uma variável simples que descreve as alterações nas dinâmicas de mineralização do C e N no solo, denominada de disponibilidade total de N (Artigo I). Da mesma forma, o modelo STICS se mostrou uma importante ferramenta na descrição dos processos de decomposição e emissão de N_2O de resíduos culturais com distinta composição química e quantidade adicionados em superfície em condições de campo (Artigo II).

A interação da composição química de 10 resíduos culturais (C:N de 13 a 105), localização (superfície e incorporado) e teor inicial de N do solo (9 e 77 mg kg^{-1} de solo) mostrou governar as dinâmicas do C e N durante a decomposição de resíduos no solo. Estas condições permitiram explorar uma elevada gama de disponibilidade de N e a resposta da biomassa decompositora usando o submodelo de decomposição de STICS (BRISSON et al., 2003). O submodelo de decomposição (NICOLARDOT; RECOUS; MARY, 2001) foi utilizado na interpretação destes resultados através da otimização de diferentes parâmetros relacionados a biomassa microbiana do solo, visando compreender as alterações que ocorrem com a diminuição da disponibilidade de N para os decompositores. O submodelo descreveu as alterações na dinâmica de mineralização do C e N a partir das modificações de cinco parâmetros do modelo (*CNbio, CNhum , k, h* e *λ*). A redução da disponibilidade de N resultou no aumento da relação C:N da biomassa microbiana (*CNbio*), e redução da taxa de decomposição do resíduo (*k*), da decomposição da biomassa microbiana (*λ*) e humificação (*h*). A redução de *k* e *λ* foi menor para resíduos de alta qualidade comparado com resíduos de baixa qualidade, refletindo o efeito da composição química do resíduo na disponibilidade de N (TRINSOUTROT et al., 2000). O aumento de *h* com a maior disponibilidade de N demonstra a importância da biomassa microbiana como precursora na formação da matéria orgânica do solo (WANG et al., 2020). Por outro lado, o aumento da *CNbio* sugere uma adaptação da biomassa microbiana, possivelmente com uma maior proporção da população fúngica em condições de baixa disponibilidade de N (FREY et al., 2000).

Dentre os cinco parâmetros otimizados, *CNbio, k, h e λ* foram significativamente correlacionados com a disponibilidade total de N, definida como a soma dos conteúdos de N do resíduo e solo, e permitiram calcular o conteúdo de N do solo disponível para a decomposição de resíduos em superfície, estimada em 24%. Desta forma, a disponibilidade

total de N foi definida para os resíduos incorporados como o conteúdo de N do resíduo (100%) e o conteúdo de N do solo (100%), e para resíduos em superfície, 100% do N presente no resíduo e 24% do N presente no solo. Esta abordagem permitiu definir a disponibilidade total de N para os 40 tratamentos avaliados (10 resíduos x 2 localizações x 2 conteúdos de N inicial no solo), a qual variou de 10.6 kg ha^{-1} até 113.7 kg ha^{-1} para resíduos de milho em superfície (9 mg N kg^{-1} solo) e ervilhaca incorporados (77 mg N kg^{-1} solo), respectivamente.

No segundo estudo, STICS foi utilizado na simulação da decomposição e emissão de N_2O de dois resíduos culturais com distinta qualidade (ervilhaca e trigo) e quantidades (3, 6 e 9 Mg ha^{-1}). No modelo STICS a decomposição do mulch ocorre em duas camadas, uma em contato com o solo, onde os resíduos são decomponíveis, e a segunda camada localizada acima, que permanece inalterada e alimenta a primeira camada. No modelo, a camada passível de decomposição é definida em 1 Mg ha^{-1} de resíduo (standard). O atual formalismo do modelo visa representar a redução do contato solo/resíduo com o aumento do mulch, reduzindo o acesso da população microbiana aos recursos do solo (COPPENS et al., 2007). Com essa parametrização, o contato solo/resíduo limitou a decomposição do mulch, e resultou na superestimação da quantidade de C e N remanescente no mulch com o aumento da quantidade adicionada (3<6<9 Mg MS ha^{-1}), confirmando nossa hipótese.

A taxa de decomposição semelhante para distintas quantidades de resíduos adicionados ocorre em função da dinâmica da água no mulch, que forma um gradiente de decomposição no interior do mulch, conforme descrito por DIETRICH et al. (2019) e observada no presente estudo. Logo, para obter uma aproximação das taxas de decomposição semelhantes entre quantidades distintas de resíduos adicionados na superfície do solo, o parâmetro *qmulchdec*, que representa a massa de resíduo decomponível, foi alterado para descrever com maior eficiência as dinâmicas de decomposição observadas. Com a definição de todo o mulch decomponível para as três quantidades avaliadas (*qmulchdec* $\geq$9 Mg ha^{-1}), as simulações das dinâmicas do C no mulch foram melhoradas, representando o padrão de decomposição observado para os resíduos de trigo e ervilhaca. Contudo, a melhora nas simulações da dinâmica do N do mulch foi observada apenas para resíduos de ervilhaca, onde o contato solo/resíduo tem menor efeito na taxa de decomposição. Neste caso, a principal fonte de N para os decompositores é oriundo do resíduo, e não do solo, efeito observado para resíduos de alta qualidade (baixa C:N) (BREMER; VAN HOUTUM; VAN KESSEL, 1991; CHAVES et al., 2021, no prelo). Logo, os tratamentos contendo resíduos de trigo resultaram na simulação de elevada imobilização de N após a adição dos resíduos ao solo. A lixiviação das frações de C e N lábeis do mulch também podem reduzir drasticamente os conteúdos do C e N em condições

de elevada pluviosidade, levando a uma superestimação dos conteúdos pelo modelo, uma vez que o mesmo não simula estas frações.

STICS foi utilizado para descrever as emissões de N_2O associadas a decomposição de resíduos de trigo e ervilhaca com diferentes quantidades em SPD. Em STICS, os fluxos de N_2O são oriundos dos processos microbianos de nitrificação e desnitrificação (PLAZA-BONILLA et al., 2017). As elevadas emissões de N_2O são observadas principalmente após a adição de resíduos ao solo (CHARLES et al., 2017; FRACETTO et al., 2017), e são relacionadas principalmente ao processo microbiano de desnitrificação, o qual ocorre em condições de espaço poroso saturado por água acima de 60% e é fortemente influenciado pelo conteúdo de C disponível (LI et al., 2016; KRAUSE et al., 2017). Em STICS, as emissões de N_2O oriundas do processo de desnitrificação são simuladas de acordo com uma taxa potencial constante (potencial de desnitrificação) e fatores relacionados: umidade, temperatura e disponibilidade de NO_3^- no solo (HÉNAULT et al., 2005). Utilizando estes formalismos, o modelo foi capaz de descrever os fluxos de N_2O do tratamento controle na etapa de calibração do modelo. Neste tratamento, os fluxos de N_2O observados foram baixos, não apresentando picos de emissão durante o período avaliado. Contudo, o modelo não representou os fluxos de N_2O para os tratamentos contendo resíduo, subestimando as emissões para os dois resíduos (trigo e ervilhaca) e quantidades distintas (3, 6 e 9 Mg ha^{-1}).

Para descrever os fluxos de N_2O observados com a adição de resíduos de trigo e ervilhaca e quantidades distintas, o potencial de desnitrificação deveria ser estimado de acordo com a disponibilidade de C e não um valor constante. Contudo, devido ao modelo STICS não apresentar uma variável que descreva os conteúdos de C lábil disponível para os desnitrificadores, a hipótese deste trabalho se baseou na possibilidade de utilizar os fluxos de CO_2 como um indicador das variações da disponibilidade de C no solo. Para isto, foi formulada uma nova função para determinação do potencial de desnitrificação, usando uma proporção dos fluxos de CO_2 (do solo e resíduo) como indicadores do C lábil disponível. Ao mesmo tempo, o uso da relação C:N dos resíduos mostrou uma maior aproximação entre os fluxos de N_2O simulados e observados para os resíduos de trigo e ervilhaca. A implementação desta nova função para determinar o potencial de desnitrificação de acordo com a dinâmica de decomposição dos resíduos adicionados permitiu ao modelo STICS simular satisfatoriamente os fluxos de N_2O. Para todas as condições avaliadas (2 resíduos x 3 quantidades + controle) o modelo descreveu as variações temporais e os picos de emissão de N_2O observados após adição dos resíduos ao solo.

5 CONCLUSÕES GERAIS

A interação entre o conteúdo de N mineral do solo, qualidade e localização do resíduo cultural (superfície vs incorporado) controla a dinâmica do C e N, modificando o acesso da população decompositora as fontes de N, definida como disponibilidade total de N. A utilização do submodelo de decomposição de STICS permitiu explorar os resultados destas interações e compreender os efeitos da disponibilidade total de N nas características da biomassa microbiana do solo. A redução da disponibilidade total de N resultou no decréscimo da taxa de decomposição dos resíduos e da biomassa microbiana do solo, além da redução na taxa de humificação, e levou ao aumento da relação C:N da biomassa microbiana. A utilização da disponibilidade total de N para predizer a dinâmica de mineralização do C e N em condições limitantes de N (sistemas agrícolas) parece promissora e necessita ser testada em condições de campo.

O modelo de decomposição do mulch de dupla camada adotado no modelo STICS não foi capaz de descrever as dinâmicas de decomposição dos resíduos culturais de ervilhaca e trigo com quantidades distintas (3, 6 e 9 t MS ha^{-1}) adicionados na superfície do solo. Particularmente, para os resíduos de trigo, o modelo superestimou sistematicamente a quantidade de C remanescente no mulch seguindo o padrão 3<6<9 t MS ha^{-1}. A melhoria nas simulações das dinâmicas da decomposição foi obtida ao estabelecer todo o mulch decomponível, independentemente das quantidades adicionadas. Contudo, esta alteração resultou na redução da qualidade na descrição das dinâmicas do N nos resíduos de trigo, resultando em uma elevada imobilização de N.

A utilização dos fluxos de CO_2 como uma aproximação da disponibilidade de C lábil para a população de desnitrificadores do solo permitiu melhorar as simulações das dinâmicas de emissão de N_2O do solo para todos os tratamentos avaliados. A definição de uma nova função para a determinação do potencial de desnitrificação descrita como uma proporção da mineralização de C do solo e dos resíduos culturais, conjuntamente a C:N dos resíduos culturais, permitiu descrever as variações temporais e magnitude dos fluxos de N_2O nos tratamentos avaliados. Esta abordagem se mostra promissora na simulação dos fluxos de N_2O após a adição de resíduos culturais no solo em sistemas agrícolas e necessita ser avaliada em diferentes condições climáticas.

6 REFERÊNCIAS

ABIVEN, S. et al. Mineralisation of C and N from root, stem and leaf residues in soil and role of their biochemical quality. **Biology and Fertility of Soils**, v. 42, n. 2, p. 119–128, 28 nov. 2005.

ABIVEN, S.; RECOUS, S. Mineralisation of crop residues on the soil surface or incorporated in the soil under controlled conditions. **Biology and Fertility of Soils**, v. 43, n. 6, p. 849–852, 4 jul. 2007.

ACOSTA, J. A. DE A. et al. Decomposição da fitomassa de plantas de cobertura e liberação de nitrogênio em função da quantidade de resíduos aportada ao solo sob sistema plantio direto. **Ciência Rural**, 2014.

BERNOUX, M. et al. Cropping Systems, Carbon Sequestration and Erosion in Brazil : A Review. **Agronomy for Sustainable Developtment**, v. 26, p. 1–8, 2009.

BREMER, E.; VAN HOUTUM, W.; VAN KESSEL, C. Carbon dioxide evolution from wheat and lentil residues as affected by grinding, added nitrogen, and the absence of soil. **Biology and Fertility of Soils**, v. 11, n. 3, p. 221–227, 1991.

BRISSON, N. et al. An overview of the crop model stics. **European Journal of Agronomy**, v. 18, n. 3–4, p. 309–332, 2003.

BUTTERBACH-BAHL, K. et al. Nitrous oxide emissions from soils: how well do we understand the processes and their controls? **Philosophical Transactions of the Royal Society**, v. 368, n. 1621, p. 20130122, 2013.

CHARLES, A. et al. Global nitrous oxide emission factors from agricultural soils after addition of organic amendments: A meta-analysis. **Agriculture, Ecosystems and Environment**, v. 236, p. 88–98, 2017.

CHAVES, B et al. 2021 Combination of residue quality, residue placement and soil mineral N content drives C and N dynamics by modifying the N acces to microbial decomposers. **Soil Biology and Biochemistry,** no prelo.

CHELLAPPA, J. et al. Soil organic carbon , aggregate stability and biochemical activity under tilled and no-tilled agroecosystems. **Journal of Agriculture and Food Research**, v. 4, p. 100139, 2021.

CHEN, H. et al. Soil nitrous oxide emissions following crop residue addition: A meta-analysis. **Global Change Biology**, v. 19, p. 2956–2964, 2013.

COPPENS, F. et al. Decomposition of mulched versus incorporated crop residues: Modelling with PASTIS clarifies interactions between residue quality and location. **Soil Biology and Biochemistry**, v. 39, n. 9, p. 2339–2350, 2007.

DIETRICH, G. et al. Sugarcane mulch C and N dynamics during decomposition under different rates of trash removal. **Agriculture, Ecosystems and Environment**, v. 243, p. 123–131, 2017.

DIETRICH, G. et al. Gradient of decomposition in sugarcane mulches of various thicknesses. **Soil & Tillage Research**, v. 192, p. 66–75, 2019.

FINDELING, A. et al. Modelling water, carbon and nitrogen dynamics in soil covered with decomposing mulch. **European Journal of Soil Science**, v. 58, n. 1, p. 196–206, 2007.

FRACETTO, F. J. C. et al. Effect of agricultural management on N2O emissions in the Brazilian sugarcane yield. **Soil Biology and Biochemistry**, v. 109, p. 205–213, 2017.

FREY, S. D. et al. Fungal translocation as a mechanism for soil nitrogen inputs to surface residue decomposition in a no-tillage agroecosystem. **Soil Biology and Biochemistry**, v. 32, n. 5, p. 689–698, maio 2000.

GALE, W. J.; CAMBARDELLA, C. A. Carbon Dynamics of Surface Residue– and Root-derived Organic Matter under Simulated No-till. **Soil Science Society of America Journal**, v. 64, n. 1, p. 190, 2000.

GOMES, Juliana et al. Soil nitrous oxide emissions in long-term cover crops-based rotations under subtropical climate. **Soil and Tillage Research**, v. 106, n. 1, p. 36-44, 2009.

HALDE, C.; ENTZ, M. H. Plant species and mulch application rate affected decomposition of cover crop mulches used in organic rotational no-till systems. **Canadian Journal of Plant Science**, v. 96, p. 59–71, 2016.

HEINEN, M. Simplified denitrification models: Overview and properties. **Geoderma**, v. 133, p. 444–463, 2006.

HÉNAULT, C. et al. Predicting in situ soil N2O emission using NOE algorithm and soil database. **Global Biogeochemical Cycles**, v. 11, p. 115–127, 2005.

HÉNAULT, C.; GERMON, J. . NEMIS , a predictive model of denitrication on the field scale. **European Journal of Soil Science**, v. 51, p. 257–270, 2000.

HENRIKSEN, T. M.; BRELAND, T. A. Carbon mineralization, fungal and bacterial growth, and enzyme activities as affected by contact between crop residues and soil. **Biology and Fertility of Soils**, v. 35, p. 41–48, 2002.

IPCC. **Climate Change 2014: Synthesis Report.** Contribution of Working Groups I, II, III to the Fifth Assessment Report of the Intergovernmental Panel on Climate Change.

JENSEN, L. S. et al. Influence of biochemical quality on C and N mineralisation from a broad variety of plant materials in soil. **Plant and Soil**, v. 273, p. 307–326, 2005.

KRAUSE, H. M. et al. Long term farming systems affect soils potential for N2O production and reduction processes under denitrifying conditions. **Soil Biology and Biochemistry**, v. 114, p. 31–41, 2017.

LI, X. et al. Evidence for denitrification as main source of N2O emission from residue-amended soil. **Soil Biology and Biochemistry**, v. 92, p. 153–160, 2016.

NICOLARDOT, B. et al. A microcosm experiment to evaluate the influence of location and quality of plant residues on residue decomposition and genetic structure of soil microbial communities. **Soil Biology and Biochemistry**, v. 39, n. 7, p. 1631–1644, 2007.

NICOLARDOT, B.; RECOUS, S.; MARY, B. Simulation of C and N mineralisation during crop residue decomposition: A simple dynamic model based on the C:N ratio of the residues. **Plant and Soil**, v. 228, n. 1, p. 83–103, 2001.

OLIVEIRA, M. et al. Nitrogen mineralization of legume residues: interactions between species, temperature and placement in soil. **Spanish Journal of Agricultural Research**, v. 18, n. 1, p. 1–11, 2020.

PLAZA-BONILLA, D. et al. Precipitation gradient and crop management affect N2O emissions: Simulation of mitigation strategies in rainfed Mediterranean conditions. **Agriculture, Ecosystems and Environment**, v. 238, p. 89–103, 2017.

QUEMADA, M.; CABRERA, M. L. Carbon and Nitrogen Mineralized from Leaves and Stems of Four Cover Crops. **Soil Science Society of America Journal**, v. 59, n. 2, p. 471–477, 1995.

REDIN, M. et al. How the chemical composition and heterogeneity of crop residue mixtures decomposing at the soil surface affects C and N mineralization. **Soil Biology and Biochemistry**, v. 78, p. 65–75, 2014.

SCHMATZ, R. et al. Crop residue quality and soil type influence the priming effect but not the fate of crop residue C. **Plant and Soil**, p. 229–245, 2017.

SCHMATZ, R. et al. How the mass and quality of wheat and vetch mulches affect drivers of soil N 2 O emissions. **Geoderma**, v. 372, p. 114395, 2020.

SIGNOR, D.; CERRI, C. E. P. Nitrous oxide emissions in agricultural soils : a review. **Pesquisa Agropecuaria Tropical**, v. 43, n. 3, p. 322–338, 2013.

STEINER, J. L. et al. Crop Residue Decomposition in No-Tillage Small-Grain Fields. **Soil Science Society of America Journal**, v. 63, p. 1817–1824, 1999.

STEWART, C. E. et al. Lignin biochemistry and soil N determine crop residue decomposition and soil priming. **Biogeochemistry**, v. 124, p. 335–351, 2015.

STOTT, D. E. et al. Wheat Residue Loss from Fields under No-till Management. **Soil Science Society of America Journal**, v. 54, p. 92–98, 1990.

THORBURN, P. J.; PROBERT, M. E.; ROBERTSON, F. A. Modelling decomposition of sugar cane surface residues with APSIM-Residue. **Field Crops Research**, v. 70, p. 223–232, 2001.

TIECHER, T. et al. Soil fertility and nutrient budget after 23-years of di ff erent soil tillage systems and winter cover crops in a subtropical Oxisol. **Geoderma**, v. 308, p. 78–85, 2017.

TRINSOUTROT, I. et al. Biochemical Quality of Crop Residues and Carbon and Nitrogen Mineralization Kinetics under Nonlimiting Nitrogen Conditions. **Soil Science Society of**

America Journal, v. 64, n. 3, p. 918–926, 2000.

TUURE, J. et al. Plant residue mulch increases measured and modelled soil moisture content in the effective root zone of maize in semi-arid Kenya ¨ s a. **Soil & Tillage Research**, v. 209, p. 104945, 2021.

WANG, C. et al. Stabilization of microbial residues in soil organic matter after two years of decomposition. **Soil Biology and Biochemistry**, v. 141, n. 72, p. 107687, 2020.

WILLIAMS, A. et al. Establishing the relationship of soil nitrogen immobilization to cereal rye residues in a mulched system. **Plant Soil**, v. 426, p. 95–107, 2018.